

**The mechanisms of stress memory responses
and translational regulation during dehydration
and rehydration in the resurrection plant
*Craterostigma plantagineum***

Dissertation

zur

Erlangung des Doktorgrades (Dr. rer. nat.)

der

Mathematisch-Naturwissenschaftlichen Fakultät

der

Rheinischen Friedrich-Wilhelms-Universität Bonn

vorgelegt von

Xun Liu

aus

Sichuan, Volksrepublik China

Bonn, 2020

Angefertigt mit Genehmigung der Mathematisch-Naturwissenschaftlichen
Fakultät der Rheinischen Friedrich-Wilhelms-Universität Bonn

1. Gutachter: Prof. Dr. Dorothea Bartels
2. Gutachter: Prof. Dr. Peter Dörmann

Tag der Promotion: 14.05.2020

Erscheinungsjahr: 2020

CONTENTS

CONTENTS.....	I
ABBREVIATIONS.....	V
SUMMARY	1
CHAPTER 1	5
General introduction	5
1 Introduction of desiccation tolerance.....	5
2 Resurrection plants and the experimental system <i>Craterostigma plantagineum</i>	6
2.1 Resurrection plants.....	6
2.2 The desiccation tolerant plant <i>C. plantagineum</i>	7
3 Plant stress memory, acclimation and priming	8
3.1 The physiological perspective of the drought stress memory.....	8
3.2 Molecular mechanisms and epigenetics of drought stress memory..	10
3.3 Cross memory	12
3.4 Priming of seeds.....	13
4 Polysome profiling and translational regulation.....	15
4.1 Isolation of polysome RNAs.....	15
4.2 Polysome profiling.....	16
4.3 Polysome occupancy.....	16
4.4 Translational regulation	17
5 The changes of cellular membrane under dehydration stress	19
5.1 Cell membranes affected by dehydration stress.....	19
5.2 Phosphatidylcholine involved in membrane integrity	20
5.3 Enzymes involved in phosphatidylcholine synthesis.....	20
6 Objectives of this study.....	23
CHAPTER 2	27
Transcriptional and metabolic changes in the desiccation tolerant plant <i>Craterostigma plantagineum</i> during recurrent exposures to dehydration	
Abstract.....	28
1 Introduction.....	29
2 Materials and methods	32
2.1 Plant growth and stress treatments.....	32
2.2 Relative water content measurement	32
2.3 Assay of electrolyte leakage.....	33
2.4 Determination of chlorophyll content	33
2.5 Quantification of proline content.....	33
2.6 Assay of H ₂ O ₂ content	34
2.7 Lipid peroxidation assay	35
2.8 Determination of superoxide dismutase activity.....	35
2.9 Sugar extraction and analysis.....	35

2.10 RNA isolation and reverse transcription-PCR	36
2.11 Protein analysis	36
2.12 Cluster and correlation analysis	37
2.13 Statistical analysis	37
3 Results.....	38
3.1 Dehydration stress-trained <i>C. plantagineum</i> plants.....	38
3.2 Changes in physiological parameters during repeated dehydration and rehydration in leaves of <i>C. plantagineum</i>	39
3.3 Correlation of electrolyte leakage with other physiological parameters under the repetitive dehydration and rehydration conditions	41
3.4 Transcript accumulation during recurrent stress treatments	41
3.5 Expression patterns of stress-induced proteins	48
3.6 Dehydration-stress memory	48
4 Discussion	51
4.1 Metabolites during dehydration/rehydration.....	51
4.2 Gene expression patterns	52
4.3 Photosynthesis-related processes	53
4.4 Stress memory.....	53
Acknowledgements.....	55
Author contribution statement	55
Supporting data	56
CHAPTER 3	59
Translational regulation during dehydration and rehydration in <i>Craterostigma plantagineum</i> revealed by polysome profiling	
Abstract.....	60
1 Introduction.....	61
2 Materials and methods	63
2.1 Plant material and growth conditions	63
2.2 Relative water content measurement	63
2.3 Total mRNA and polysomal mRNA isolation.....	63
2.4 RNA sequencing analysis	64
2.5 cDNA synthesis and quantitative RT-PCR (RT-qPCR)	64
2.6 Data analysis	65
2.7 Analysis of interaction networks.....	66
2.8 RNA sequence feature analysis.....	66
2.9 Motif analysis.....	67
3 Results.....	68
3.1 RNA profiling reveals translational activation during four stages of dehydration and rehydration cycle in <i>C. plantagineum</i>	68
3.2 Polysomal profiling of <i>C. plantagineum</i> during the dehydration and rehydration cycle.....	68
3.3 Dynamics of genes under translational regulation.....	71
3.4 Sequence features correlate with translational regulation	74
3.5 GO term and pathway enrichment analyses of genes under translational	

regulation in D/M group and R/D group.....	77
3.6 Regulation overview of genes under translational control	80
3.7 Transcription factors in D/M group and R/D group.....	80
4 Discussion	86
Acknowledgements.....	89
Supporting data	90
CHAPTER 4	93
Identification and characterization of CTP:phosphocholine cytidyltransferase CpCCT1 in the resurrection plant <i>Craterostigma plantagineum</i>	
Abstract	94
1 Introduction.....	95
2 Materials and methods	98
2.1 Plant materials and treatments	98
2.2 Gene cloning	98
2.3 Phylogenetic analysis and sequence analysis	98
2.4 RNA isolation and cDNA synthesis	99
2.5 CpCCT1 antibody generation and protein analysis	99
2.6 Protein localization prediction and analysis	100
2.7 Analysis of interaction network	101
2.8 Subcellular fractionation.....	101
2.9 Yeast complementation assay.....	101
2.10 Promoter analysis.....	102
3 Results.....	104
3.1 Quantification of <i>CpCCT1</i> transcripts and molecular phylogeny of <i>CCT</i> genes	104
3.2 Prediction of CpCCT1 functional domains.....	107
3.3 Localization of CpCCT1	110
3.4 Transcript changes of <i>CpCCT1</i> during different treatments	113
3.5 Expression patterns of CpCCT1 protein under different treatments.....	117
3.6 Yeast complementation assay.....	121
3.7 <i>CpCCT1</i> promoter activity in response to dehydration	124
3.8 CpCCT1 interaction network prediction.....	125
4 Discussion	126
Supporting data	132
CHAPTER 5	133
General discussion	133
1 The responses to reiterated dehydration in plants.....	133
2 Regulation of expression of genes related to desiccation tolerance and recovery in <i>C. plantagineum</i>	136
3 The function, regulation and structure of CTP:phosphocholine cytidyltransferase (CCT) in plants	137
REFERENCES	139
ACKNOWLEDGEMENTS.....	161

CONTENTS

ABBREVIATIONS

AAG	Alkyl-acylglycerol
AAPT	Aminoalcoholaminophosphotransferase
ABA	Abscisic acid
ABREs	ABA-responsive elements
ALAD	5-aminolaevulinic acid dehydratase
APX	Ascorbate peroxidase
ARF	Auxin response factor
BHT	Butylated hydroxytoluene
CAT	Catalase
CCT	CTP:phosphocholine cytidyltransferase
CDS	Coding DNA sequence
CEK	Choline/ethanolamine kinase
CHLG	Chlorophyll synthase
CHLM	Mg-protoporphyrin IX methyltransferase
CHO	Carbohydrate
CK	Choline kinase
CPO	Coprogen oxidase
CPT	Cholinephosphotransferase
Cu/Zn-SOD	Copper/zinc superoxide dismutase
DAG	Diacylglycerol

ABBREVIATIONS

DRE	Dehydration responsive element
DREB	Dehydration responsive element binding
DTT	Dithiothreitol
DW	Dry weight
EDR1	Early dehydration responsive 1
EDTA	Ethylenediamine tetraacetic acid
EF1a	Elongation factor 1-alpha
EGTA	Ethylene glycol tetraacetic acid
FW	Fresh weight
GC/MS	Gas chromatography/mass spectrometry
GFP	Green Fluorescent Protein
GSA	Glutamate-1-semialdehyde aminoytansferase
GUS	<i>E. coli</i> β -glucuronidase gene (<i>uidA</i>)
His	Histidine
IAA	Indole-3-acetic acid
LEA	Late embryogenesis abundant
MDA	Malondialdehyde
Mn-SOD	Manganese superoxide dismutase
mRNPs	Messenger ribonucleoparticles
NBT	4-nitro-blue tetrazolium chloride
<i>Nc</i>	Effective codon numbers
NF	Normalized frequency

ABBREVIATIONS

NYE1	Non-yellowing 1
OD	Optical density
PA	Phosphatidic acid
PAL	Phenylalanine ammonia lyase
PaO	Pheophorbide a oxygenase
PBGD	Porphobilinogen deaminase
PCA	Principal component analysis
PC	Phosphatidylcholine
PCho	Phosphocholine
PE	Phosphatidylethanolamine
PECP	Phosphoethanolamine/phosphocholine phosphatase
PEG	Polyethylene glycol
PEMT	Phosphatidylethanolamine methyltransferase
PLMT	Phospholipid methyltransferase
PMT	Phospho-base N-methyltransferase
POD	Peroxidase
PP	Pyrophosphate
PPH	Pheophytinase
PS	Phosphatidylserine
RCCR	Red chlorophyll catabolite reductase
ROS	Reactive oxygen species
RT-qPCR	Real time-quantitative polymerase chain reaction

ABBREVIATIONS

RWC	Relative water content
SDC	Serine decarboxylase
SnRK1	Sucrose nonfermenting 1-related protein kinase 1
SOD	Superoxide dismutase
TAG	Triacylglycerol
TBA	Thiobarbituric acid
Tris	Tris-(hydroxymethyl)-aminomethane
TW	Turgid weight
UTR	Untranslated region

SUMMARY

Dehydration stress is one of the major environmental factors affecting the survival rate and productivity of plants. The resurrection plant *Craterostigma plantagineum* as an extreme desiccation tolerant plant has been used to study the mechanisms of desiccation tolerance. Currently, many dehydration-induced genes and some dehydration-related protective mechanisms have been reported. However, the mechanisms involved in desiccation tolerance and the regulation of the fast recovery process are not fully understood.

In **CHAPTER 2**, the dehydration stress memory has been analyzed in the desiccation tolerant resurrection plant *C. plantagineum*, which had been exposed to four dehydration/rehydration treatment cycles. Expression of four representative stress-related genes gradually increased during four repeated cycles of treatment. This reflects a transcriptional memory and suggests that the selected genes are trainable genes. On the contrary, the chlorophyll synthesis/degradation-related genes are un-trainable, because transcript abundance of these genes did not significantly change during four dehydration cycles and the transcript levels were retained at a similar level during three recovery phases as in the untreated tissues. The transcript level of reactive oxygen species (ROS) pathway-related genes increased during dehydration/rehydration treatment cycles, accompanied by increasing levels of superoxide dismutase (SOD) activity, proline content and sucrose content. Conversely the H₂O₂ content and electrolyte leakage (EL) decreased, which indicates a gain of stress tolerance and also points a stress memory. Interestingly, the analysis of four representative stress-related proteins showed that the activated stress memory can persist over several days. This phenomenon is most likely a general feature of the dehydration stress memory response in resurrection plants.

In **CHAPTER 3**, the total mRNA and polysomal mRNA profiles were investigated through RNA sequencing to identify genes related to desiccation

tolerance and to the fast recovery process during four different stages in dehydration and rehydration in *C. plantagineum*. The polysome occupancy (the ratio between polysomal mRNA abundance and total mRNA abundance of a specific mRNA) between each stage and the next time point was monitored in this work. A significant polysome occupancy change of a specific transcript means that expression of this gene is under translational regulation. We found that genes in two phases (from partial dehydration to desiccation: D/M group, and from desiccation to rehydration: R/D group) had extensive changes of polysome occupancy. The results showed that more mRNAs combine with ribosomes in the desiccation stage than other stages which might contribute to desiccation tolerance. We also analyzed sequence features of genes under translational regulation, including transcript length, GC content, GC3 content, effective number of codons and enriched motifs. In the D/M group and R/D group, the sequence features were significantly different from each other, which indicated different regulation of translation in the two phases. The results revealed by GO term and MapMan pathway analysis showed that genes under translational regulation in the D/M group and R/D group are involved in several pathways, including carbohydrate (CHO) metabolism, signal transduction, kinase activity, transcription factor activity, cell wall, lipid metabolism and hormone metabolism. Among these, several transcription factor families were identified, such as zinc finger, WRKY, NAC and ARF, which are involved in translational regulation during dehydration and rehydration.

In **CHAPTER 4**, we focused on the identification and characterization of CTP:phosphocholine cytidyltransferase CpCCT1 in the resurrection plant *C. plantagineum*. According to the RNA-sequencing results in **CHAPTER 3**, *CpCCT1* is a dehydration-induced gene, which is under translational control from partial dehydration to desiccation. In this work, we cloned the *CpCCT1* cDNA from *C. plantagineum* and compared the putative amino acid sequences with *Arabidopsis thaliana*, the animal homolog *Rattus norvegicus*, and the yeast homolog *Saccharomyces cerevisiae*. The results showed that CpCCT1 has a conserved catalytic

domain and a membrane-binding domain while the N-terminal and C-terminal domains were divergent. The response of *CpCCT1* to different abiotic stresses (including dehydration stress, salt stress, cold stress, mannitol and sorbitol treatments, and exogenous plant hormone application) were investigated in leaf and root tissues of *C. plantagineum*. The expression of *CpCCT1* was increased both on the transcriptional and translational level under dehydration stress, 0.5 M NaCl solution treatment, and exposure to 0.5 M/0.8 M mannitol/sorbitol in leaves and roots, whereas no changes were observed in response to cold stress, exogenous 100 μ M ABA or 1 μ M IAA treatments on the translational level in both leaf and root samples. A yeast complementation assay was performed to elucidate the possible function of *CpCCT1*. However, no significant functional complementation was observed in all the treatments (including different concentration of NaCl, KCl, mannitol, and 3-amino-1,2,4-triazole (3-AT), and different pH values). The inapparent result might be caused by the divergent sequence between *ScCCT* and *CpCCT1*. We also analyzed the promoter activity of *CpCCT1* in response to dehydration both in *C. plantagineum* and *A. thaliana*. The relative lower *CpCCT1* promoter activity, together with the highest transcripts level in partially dehydrated samples and the highest protein level in desiccated samples revealed that the expression of *CpCCT1* was mainly under translational regulation during dehydration stress, which coincides with the initial RT-qPCR results (**CHAPTER 3**). The characteristics and functional study of *CpCCT1* in this work can be a general feature of CCT in resurrection plants.

SUMMARY

CHAPTER 1

General introduction

1 Introduction of desiccation tolerance

The extreme climate and weather events are getting serious, which is effected by global warming (Jiang et al. 2018). The frequently changing precipitation capacity and uneven rainfall distribution very likely lead to more irregular and multiple abiotic stresses, such as heat stress, dehydration stress, cold stress or the combination of stresses (Wang et al. 2014; Niinemets et al. 2017). Dehydration stress as one of the most important environmental factors can affect the growth situation, the survival rate and the productivity of plants (Todaka et al. 2017).

Many plants can survive from dehydration to different extents. Drought tolerance regarded as the tolerance to moderate dehydration (water loss around 20-30%) is different from desiccation tolerance which is used to describe the tolerance of further dehydration (water loss up to 90%) and the ability of successfully rehydration after re-watering (Gaff 1971; Hoekstra et al. 2001). It is reported that the desiccation tolerance trait is widely distributed in the plant kingdom, but differences exist between species (Bewley and Krochko 1982; Oliver and Bewley 1996). From the phylogenetic and ecological aspects, desiccation tolerance is considered as a very ancient feature of land plants, which was lost during the evolution of the vascular plants (Proctor et al. 2007; Farrant and Moore 2011). However, desiccation tolerance is still retained in plant structures such as pollen, seeds and spores, and re-established in the vegetative tissues of a few angiosperm plants termed as resurrection plants (Bartels 2005; Farrant and Moore 2011).

The mechanisms of desiccation tolerance in seeds are correlated to their maturation programs regulated by seed development (Farrant and Moore 2011).

Furthermore, the desiccation tolerance in plant vegetative tissues is considered as a complex phenotype affected by multigenic and multifaceted regulatory mechanisms (Moore et al. 2009; Oliver et al. 2010; Gechev et al. 2012). The accumulation of protective proteins and specific carbohydrates, the adaptive changes of morphology, the remodeling of cell wall and membrane lipids contribute to acquisition of vegetative desiccation tolerance (Gechev et al. 2013; Giarola et al. 2017; Yobi et al. 2017).

2 Resurrection plants and the experimental system *Craterostigma plantagineum*

2.1 Resurrection plants

Resurrection plants, as a small group of angiosperm plants, contain around 300 species (including herbaceous plants, shrubs and trees), which are found in desert and dry areas, in more temperate areas, and even in the tropical rainforests areas (Bartels 2005; Phillips et al. 2008; Porembski 2011; Challabathula et al. 2012). Resurrection plants possess a remarkable ability to tolerate extreme air dryness or desiccation (relative leaf water content less than 5%) and survive from an inactive state after rehydration (Bartels 2005; Gechev et al. 2013). In contrast, most angiosperm plants are desiccation sensitive, especially in their vegetative tissues (Bartels 2005). Therefore, resurrection plants can be a potential source for improving the dehydration tolerance of crop plants through analyzing physiological and molecular mechanisms.

Since most resurrection plants are polyploid and have large genomes, it is speculated that the genome polyploidy might be advantageous for the acquisition of desiccation tolerance during evolution, but up to now there is no evidence showing up (Otto 2007; Siljak-Yakovlev et al. 2008; Rodriguez et al. 2010). In order to understand the molecular basis under the desiccation tolerance, several species of resurrection plants have been extensively studied, including *Boea hygrometrica* (dicot), *C. plantagineum* (dicot), *C. wilmsii* (dicot), *Myrothamnus flabellifolia* (dicot), *Sporobolus stapfianus* (monocot), *Xerophyta humilis* (monocot), *X. viscosa* (monocot),

Tortula ruralis (moss), *Selaginella tamariscina* (clubmoss), and *S. lepidophylla* (clubmoss) (Ingram and Bartels 1996; Alpert and Oliver 2002; Moore et al. 2009; Cushman and Oliver 2011; Oliver et al. 2011a, b). Resurrection plants can protect cells from damage during desiccation through a constitutive system, which can perceive and respond to slowly moisture loss (Ingram and Bartels 1996; Oliver et al. 2000). The resurrection plants are mainly separated into two groups: poikilochlorophyllous and homoiochlorophyllous, according to the different ability of chlorophyll degrading or retaining (Sherwin and Farrant 1998; Bartels and Hussain 2011). Among them, *C. plantagineum* belongs to the homoiochlorophyllous group, because the thylakoid and chlorophyll are retained during dehydration (Sherwin and Farrant 1998; Rodriguez et al. 2010).

2.2 The desiccation tolerant plant *C. plantagineum*

The Southern African plant *C. plantagineum* is an extreme desiccation tolerant plant, which is an indispensable member of the *Linderniaceae* family and belongs to the tribus of the *Scrophulariaceae* (Bartels and Salamini 2001; Bartels 2005; Phillips et al. 2008).

As we know, the large genomes owned by most resurrection plants make them difficult to transform and unsuitable for molecular or genetic studies (Challabathula and Bartels 2013). However, *C. plantagineum* has the advantage that it displays desiccation tolerance both in vegetative tissues and in undifferentiated callus which makes it a model resurrection plant for the analysis of molecular mechanisms (Rodriguez et al. 2010). The desiccation tolerance in *C. plantagineum* callus is not intrinsic. Callus needs a pretreatment with the exogenous plant hormone abscisic acid (ABA) to acquire the tolerance (Bartels et al. 1990). The dehydration process in *C. plantagineum* is characterized by inducing numerous dehydration-related genes and proteins, while during the rehydration process the amount of induced genes and proteins are rapidly decreased (Bernacchia et al. 1996; Bartels 2005). This response

process is different to other plants, such as *T. ruralis*, in which the majority of gene expression changes take place during the first hours after re-watering (Wood and Oliver 1999).

3 Plant stress memory, acclimation and priming

Due to the more frequent climatic changes and extreme conditions occurring recently plants are likely to be exposed to multiple abiotic stresses during their whole life span, instead of single stress events (Li and Liu 2016). In order to survive from stress and to adapt to the harsh environment, plants have to find suitable ways to respond to recurrent stresses. It has been observed that pre-exposure to a mild biotic or abiotic stress can prepare plants for subsequent severe stress exposures (Walter et al. 2011; Ramírez et al. 2015). This phenomenon is referred to as “plant priming”, which is considered as a potential way to improve stress tolerance, and it is related to “plant stress memory” (Bruce et al. 2007). The expression “plant priming” is generally used in the context of biotic stresses and chemical agent application for the first exposure, while the similar process is termed “hardening” or “acclimation” when it comes to abiotic stress (Sinclair and Roberts 2005; Chen et al. 2012a; Hilker et al. 2016; Savvides et al. 2016). The concept of stress memory represents an intrinsic response to a repeated stress event (Avramova 2015). Many efforts have been made to explore the mechanisms of stress memory in different plant species which have encountered diverse stresses (Ramírez et al. 2015; Walter et al. 2011; Wang et al. 2014, 2015; Shukla et al. 2015; Sun et al. 2018). The results show that stress memory is involved in modifications at different levels, including morphological, physiological, transcriptional, translational, and epigenetic level (Kinoshita and Seki 2014; Sun et al. 2018).

3.1 The physiological perspective of the drought stress memory

To optimize the growth and reproduction in frequently changing environments, plants may adjust their physiology rapidly to give rise to structural and physiological

adaptation (Fleta-Soriano and Munné-Bosch 2016). Previous research showed that many plant species display a drought stress memory on the physiological and biochemical level, such as ROS homeostasis, photosynthetic rate alteration, biomass or grain yield changes, variations of phytohormone contents etc.

In long term stress memory experiments, the yield of the crop plant potato was investigated using primed or non-primed tubers (Ramírez et al. 2015). The results showed that the potato tubers which were produced under drought conditions had a higher tuber yield than the ones produced in well watered conditions, when the potatoes had been grown in similar conditions of watering (Ramírez et al. 2015). The biomass of *Arrhenatherum elatius* plants which had been pre-exposed twice to drought stress was higher than that of these plants only encountered a single drought stress (Walter et al. 2011). Wheat plants were used to explore the possible effect of drought stress memory during plant development (Wang et al. 2014). The ascorbate peroxidase activity and photosynthesis rate of primed (before anthesis) wheat plants were higher whereas the content of malondialdehyde was lower than that of the non-primed wheat plants, which contributed to higher grain yield during a severe drought event encountered during the grain filling stage (Wang et al. 2014).

In *A. thaliana* plants, which underwent a previous drought stress treatment the stomata were still partially closed during the well-watered recovery period, which is beneficial for water conservation when exposed to a subsequent drought stress (Virilouvet and Fromm 2015). A repetitive dehydration/rehydration system was developed by Ding et al. (2012) to determine whether *A. thaliana* plants retain a drought stress memory. A significant lower water loss rate was observed in the second, third and fourth dehydration stress compared to the first stress (Ding et al. 2012). Similarly to the results from *A. thaliana* (Ding et al. 2012), trained (pre-exposed to dehydration stress) maize plants showed higher relative leaf water content (RWC) than the non-trained plants when exposed to a subsequent dehydration episode (Ding et al. 2014). A drought stress memory was also found in *Aptenia cordifolia* plants

which encountered repeated stresses (Fleta-Soriano et al. 2015). The *A. cordifolia* plants exposed twice to drought stress had increased lipid hydroperoxide levels and increased chlorophyll a/b ratios in comparison with the reference group (Fleta-Soriano et al. 2015).

Abscisic acid (ABA) as an essential phytohormone in plants can respond to drought stress through a complex equilibrium of synthesis, degradation or conjugation (Kim 2012; Finkelstein 2013). A study of *A. cordifolia* plants finds that ABA levels increased in leaves which encountered two subsequent drought stress episodes compared to plants which were only exposed once (Fleta-Soriano et al. 2015). Neves et al. (2017) observed that citrus plants which underwent multiple dehydration stress exposures also had higher ABA levels compared to the single stressed plants. Research on spring wheat (*Triticum aestivum* L. cv. Vinjett) showed that the wheat plants pre-exposed to moderate water deficit had higher concentrations of ABA compared to non-primed plants, which resulted in higher grain yields at the end (Wang et al. 2015).

3.2 Molecular mechanisms and epigenetics of drought stress memory

Evidences for a drought stress memory on the transcriptional level suggest that the regulatory mechanisms in response to a single stress stimulation are different from reiterative stress stimulations (Avramova 2015; Berry and Dean 2015). Previous research showed that changes of gene expression patterns were usually correlated with changes of the chromatin status (Campos and Reinberg 2009). The molecular mechanisms of the plant memory have two branches: *cis* mechanism and *trans* mechanism, which means a memory generated on chromatin marks (including DNA methylation and histone modifications) and a memory maintained by feedback loops and cytosol partitioning, respectively (Bonasio et al. 2010; Berry and Dean 2015; de Freitas Guedes et al. 2019).

Epigenetic mechanisms play an important role in the regulation of gene

expression through plenty of molecular mechanisms which contribute to epigenetic inheritance in plants, including DNA methylation, histone modifications, RNA molecules and chromatin structure alteration (Chinnusamy and Zhu 2009; Friedrich et al. 2019). It is reported that the changes on the epigenetic level is possible to inherit or transmit to the next generation through mitotic cell divisions (Kinoshita and Seki 2014). The profiles of histone H3 tri-methylations of lysine 4 and lysine 27 (H3K4me3 and H3K27me3) have been studied for five dehydration stress memory genes in *A. thaliana* plants (Liu et al. 2014). The results revealed the existence of distinct memory responses and showed different activities of transcription during the rehydration periods (Liu et al. 2014). H3K27me3 is a well-known chromatin repressive factor for developmentally regulated genes, while it did not block the transcription of dehydration stress-related genes (Liu et al. 2014). It has been reported that the histone modification profiles and the nucleosome occupancy of dehydration responsive genes (including *RD20*, *RD29A* and *galactinol synthase (GOLS2)*) changed during the transition phase from dehydration to rehydration cycle in *A. thaliana* (Kim et al. 2012). The acetylation level of lysine 9 of H3K9ac related to the active state of dehydration-related gene expression (Kim et al. 2012). The presence of RNA polymerase II was increased during dehydration and decreased during the rehydration period, which correlated with transcript profiles (Kim et al. 2012). Correlating active transcription with the alteration of H3K4me3 indicated that this chromatin mark participates in the transcription memory of these genes (Kim et al. 2012). Ding et al. (2012) reported that the relatively high occupancy level of phosphorylation of serine 5 (Ser5P) and H3K4me3 of RNA polymerase II persisted while the transcripts of trainable genes fall to a basal level during rehydration, which suggests the correlation to drought stress memory.

To investigate the possible role of genome-wide DNA methylation differences in drought stress memory, seedlings of *A. thaliana* had been used in a simulated-drought treatment (Colaneri and Jones 2013). However, the results showed no correlation between DNA methylation levels and gene expression patterns in *A. thaliana*

(Colaneri and Jones 2013). Even though evidence increases for epigenetic mechanisms of stress responses and memory in plants, more studies are needed to understand the role of a drought stress memory in adaption of plants to dehydration.

3.3 Cross memory

Due to global warming, plants are more likely to be exposed to different kind of stresses at the same time or at different stages of their life span instead of being exposed to a continuous stress with the same intensity. Thus cross stress tolerance of plants is extremely essential to overcome those stresses which happen during the whole life span. Cross stress tolerance may be obtained by establishing some acclimation mechanisms, such as morphological changes, specific transcription factors accumulation, protective metabolites accumulation, and epigenetic modifications (Munne-Bosch and Alegre 2013; Walter et al. 2013). Heat stress, freezing stress and drought stress will cause cell dehydration and induce acclimation mechanisms, which are partly similar to each other (Beck et al. 2007). Therefore, it is highly possible that the activated acclimation mechanisms in plants caused by one kind of stress can prevent damage from other stresses occurring later, which is termed as cross stress memory (Walter et al. 2013).

All processes involved in cross stress tolerance and cross stress memory are regulated by a multiplex network covering the interaction of multiple external and internal factors, permitting plants to adapt to the changing environment (Munne-Bosch and Alegre 2013). More specifically, previous researches in *A. thaliana* showed that cold responsive genes (eg. C-repeat binding factor) could induce the expression of downstream drought responsive genes (Thomashow 1999; Shinozaki and Yamaguchi-Shinozaki 2000). More recently it was shown that drought stress played a dominant role in inducing cold tolerance in strawberry (*Fragaria × ananassa*) plants (Rajashekar and Panda 2014). The mediterranean *Pinus nigra* exposed to an extreme drought stress displayed frost tolerance to lower

temperatures occurring in the following years (Kreyling et al. 2012). Studies on spring wheat showed that a moderate drought stress during the stem elongation stage could alleviate yield loss caused by heat stress occurring later during the grain filling stage (Wang et al. 2015). Li et al. (2015) found that wheat plants pre-exposed to moderate drought stress at the vegetative stage had improved cold tolerance at the jointing stage by sustaining ROS homeostasis, reducing leaf water loss, decreasing oxidative injuries of the photosynthetic apparatus, and increasing ABA levels. Another type of cross stress memory was reported by Herms and Mattson (1992); they showed that previous experience of abiotic stress (eg. drought stress) could induce herbivore resistance through increasing of carbon-based secondary metabolites.

3.4 Priming of seeds

Seed priming as a low-cost and efficient approach to increase crop yield has been developed to produce tolerant plants against various stresses and solve food security problems of a growing world population (Jisha et al. 2013; Sher et al. 2019). Although seed priming and plant priming, both could contribute to improved stress tolerance, they are different from each other (Li and Liu 2016). Priming is a technique based on water that controls hydration of seeds in water or a solution with low osmotic potential to trigger the metabolic processes during the early phase of seed germination without radical protrusion (Paparella et al. 2015). Research related to seed priming has been widely reported, water, sugars, polyethylene glycol (PEG), hormones, beneficial microbes, solid medium, and micronutrients are used as priming agents (Sher et al. 2019). Therefore the methods of seed priming can be classified into several types, including hydropriming, biopriming, osmopriming, solid matrix priming, nutripriming, hormonal priming, and thermopriming (Paparella et al. 2015; Sher et al. 2019).

It has been widely reported that seed priming is not only promoting seed germination and improving plant growth and crop yield, but it also increases tolerance

to abiotic stress under changing conditions (Sher et al. 2019). Here, we focus on seed priming involved in promoting drought tolerance of plants. In comparison to seedlings obtained from non-primed chickpea seeds, seedlings obtained from seeds primed using mannitol and water showed longer roots and shoots (Kaur et al. 2002). Hydropriming of maize (*Zea mays* L.) significantly improved germination as well as seedling growth under drought stress conditions (Janmohammadi et al. 2008). Primed (treated with H₂O or different concentrations of PEG) and non-primed seeds of four rice cultivars were germinated under drought stress (imitated with PEG) to examine the effects of seed priming of physiological characteristics of rice plants (Sun et al. 2010). The results showed that a suitable concentration of PEG could improve indices of germination, quality and drought tolerance of seedlings under drought stress conditions. The physiological changes were correlated with increased proline, soluble proteins, phenylalanine ammonia lyase (PAL), peroxidase (POD), superoxide dismutase (SOD) and catalase (CAT), and decreased total soluble sugars and malondialdehyde (MDA) (Sun et al. 2010). Hormonal priming was evaluated in seeds of tall wheatgrass (Eisvand et al. 2010). Seed priming using 50 ppm of auxin increased seed germination and the number of seminal roots whereas 100 ppm of gibberellin, 50 ppm of cytokinin, and 50 ppm of ABA improved seed performance under drought stress conditions, respectively (Eisvand et al. 2010). Recently, the effect of seed osmopriming (with CaCl₂ solution) on wheat yield was evaluated in a field experiment (Hussain et al. 2018). The osmoprimed seeds led to increased yield and crop allometry and improved productivity under drought stress, due to establishment of early and uniform tolerance mechanisms (Hussain et al. 2018). Durum wheat (*Triticum durum* cv. Yelken) seeds primed with zinc (Zn) showed better seed vigor and seedling growth in water limited growth medium; possibly the addition of Zinc led to a higher antioxidative potential (Candan et al. 2018). Interestingly, Khan et al. (2019) reported that seed priming with melatonin in a cultivated rapeseed cultivar could detoxify ROS activities through enhancement of antioxidants, potentially regulate stomatal traits, and prevent chloroplast and cell wall degradation under drought stress. These observations could result in to develop drought tolerance

of crop plants. In general, the overall growth of plants is enhanced due to seed priming treatments under drought stress conditions, which could be a hint for future studies of plant priming or plant stress memory.

4 Polysome profiling and translational regulation

4.1 Isolation of polysome RNAs

To gain further insight into regulation of translation, the relative amount of transcripts associated with polysome complexes need to be assessed. It has been demonstrated that polysomes can be isolated from different plant tissues, including organs, whole plants under different conditions, dissected tissue sections, and even mature pollen grains (Mustroph et al. 2009). Polysome mRNA isolation has routinely been accomplished by using an extraction buffer containing magnesium chloride (stabilizing the two subunit ribosome complex), cycloheximide and chloramphenicol (blocking further translocation of the ribosomes to the cytosol and organelles) (Mustroph et al. 2009). After precipitating the cell debris, the supernatant is loaded and separated on continuous sucrose gradients (15-56% (w/v)). The separated fractions are then used for RNA extractions (Mustroph et al. 2009; Juszczak and Bartels 2017).

A critical point during the polysome RNA isolation process is to identify the sucrose gradient fractions which contain the polysome mRNAs. To solve this problem, the antibiotic puromycin is used in the reference fractions during the polysome RNA isolation experiment. Puromycin can cause dissociation of ribosomes during the elongation phase of the translation process (Azzam and Algranati 1973). Simultaneously, the ethylenediaminetetraacetic acid (EDTA) is also used as a disrupter during the polysome purification. EDTA dissociates the subunits of the ribosomes (Chassé et al. 2016). However, EDTA has additional effects on disrupting the gradient profile and leads to high losses of RNA integrity (Chassé et al. 2016). Using puromycin after the lysate preparation does not affect RNA quality (Chassé et

al. 2016). Therefore puromycin has become a common chemical reagent used in controls to isolate polysome mRNAs, and avail the mRNAs translational status analysis (Chass éet al. 2016).

4.2 Polysome profiling

A polysome or polyribosome is a complex of an mRNA molecule and ribosomes which functions to translate mRNAs into polypeptides. Based on the number of associated ribosomes, translated mRNAs can be separated and collected by using sucrose gradients (Smit et al. 2018). The separated polysome RNA is subjected to RNA sequencing to investigate translational alterations, while the unseparated total RNA is used to detect the transcriptional changes (Smit et al. 2018).

Polysome profiling analyzed by polysome fractionation is a powerful method in molecular biology used to assess the association between ribosomes and a given mRNA (Panda et al. 2017). Polysome profiling and ribosome profiling are used in the transcriptome analysis, but these two techniques are different from each other, generating data at different levels of specificity (Piccirillo et al. 2014). Polysome profiling has been developed and used to infer the translational status of a specific mRNA in a specific tissue during the past decade (Chass éet al. 2016). It was reported that large polysomes formed by mRNAs associated with more ribosomes are more likely to be actively translated compared to mRNAs associated with a few ribosomes (Panda et al. 2016). Polysome profiling provides a direct way to detect the translation efficiency of the whole transcriptome or an individual mRNA (Panda et al. 2017). Furthermore, it is very suitable for analyzing genomic data of organisms with limited genetic resources (Chass éet al. 2016).

4.3 Polysome occupancy

Measuring the relative transcript amount of an individual mRNA or a population of mRNAs in polysome complexes and comparing it with the total amount of

transcripts allow to evaluate the translational regulation of a specific gene or all genes in a specific tissue (Mustroph et al. 2009). The ratio between polysomal mRNA abundance and total mRNA abundance of a specific mRNA is described as polysome occupancy, which partly represents the meaning of translational efficiency (Bai et al. 2017). The changes of polysome occupancy of a specific mRNA has been used to estimate the translational status of an mRNA in different growth conditions and different species (Arava et al. 2003; Ingolia et al. 2009; Liu et al. 2012, 2013; Krishnan et al. 2014; Juntawong et al. 2014; Basbouss-Serhal et al. 2015; Bai et al. 2017, 2018).

4.4 Translational regulation

Gene expression is regulated on several levels, such as transcriptional level, translational level, post-translational level and epigenetic level (Hershey et al. 2012). Among these, translational regulation is a cellular response mechanism which controls protein production in response to various physiological and pathological situations (Pradet-Balade et al. 2001; Chassé et al. 2016). Since total mRNAs can be poorly correlated to proteins in their abundance in various species, the amount of polysomal mRNAs may better reflect protein abundances (Wang et al. 2013). The study of translational regulation contributes to explain the differences between transcriptome analysis and proteome analysis and gives rise to a better understanding of regulation of gene expression (Vogel and Marcotte 2012; Chassé et al. 2016).

Various techniques have emerged for studying translated mRNAs, including polysome profiling, ribosome profiling and affinity purification of ribosomes engaged in translation. Polysome profiling is the most commonly used approach (Chassé et al. 2016). Recently, the genome-wide profiling of polysome-associated mRNA and total mRNA was determined during *A. thaliana* seed germination (Bai et al. 2017). The changes of polysome occupancy of thousands of individual mRNAs were limited to two temporal phases (seed hydration and germination), which revealed extensive

translational regulation during seed germination (Bai et al. 2017). Polysome profiling was also performed in dormant and after-ripened *A. thaliana* seeds after imbibition for 6 h and 24 h in the transcription inhibitor cordycepin and in water (Bai et al. 2018). The translational status of the *A. thaliana* samples during photomorphogenesis was examined by polysome profiling, which showed that genes encoding ribosomal proteins are more likely under translational regulation and revealed that mRNAs under translational control have longer half-lives and shorter length (Liu et al. 2012). The dynamics of mRNA association with polysomes were analyzed using polysome profiling in dormant and non-dormant seeds of *A. thaliana* during the imbibition at 25 °C in darkness (Basbouss-Serhal et al. 2015). The results showed that the recruitment of mRNAs to polysomes was a selective and dynamic process in both dormant and non-dormant seeds, and revealed that the GC content of 5' untranslated region had a role in the selective translation occurring during seed germination (Basbouss-Serhal et al. 2015). Kawaguchi et al. (2003) reported that the effect of water deficit on mRNA translation occurred in basal and apical leaves of the tobacco (*Nicotiana tabacum*) plants. A progressive reduction of the amount of polysomes per mRNA caused by water deficit in both old and young leaves, while under well watered conditions the level of polysomes was significantly higher in apical leaves compared to basal leaves (Kawaguchi et al. 2003). The data by Kawaguchi et al. (2003) revealed that translational regulation is an important component of the drought stress response and the translation level of an individual mRNA is distinctly different in leaves of different growth stages.

To sum up, previous research using polysome profiling analysis suggests that polysome profiling plays an essential role in the analysis of genes under translational regulation during different biological processes.

5 The changes of cellular membrane under dehydration stress

5.1 Cell membranes affected by dehydration stress

Research showed that dehydration tolerance of plants depends on the ability to maintain the integrity of cell membranes during dehydration (Bewley 1979). Recent reports showed that desiccation tolerance in plants needs the presence of specific carbohydrates and protective proteins, the activation of mechanisms regulating the expression of relevant genes, the restructuring of membrane lipids and membrane integrity (Giarola et al. 2017). During desiccation, most of the water in plants is lost and the plant size is diminished, which leads to membrane folding and formation of small vesicle (Cruz de Carvalho et al. 2017). Regulating membrane integrity during desiccation is important to avoid leakage during the rehydration stage when the cell volume increases again (Crowe et al. 1992; Cruz de Carvalho et al. 2017). It has been reported that plant membranes could change from a liquid crystalline to a gel phase during dehydration. This might result in membrane fusion and loss of cell compartmentation which causes leakage of cytoplasmic solutes (Crowe et al. 1992; Koster et al. 2010; Cruz de Carvalho et al. 2011).

The integrity of cell membranes as one of the factors most strongly affected by various stresses has often been used as a guidance to monitor the tolerance of plants to various stresses, such as drought, heat or cold (Levitt 1980; Blum and Ebercon 1981; Willing and Leopold 1983). Therefore, the measurements of cell membrane damage have become very useful physiological indices to measure the damage caused by dehydration stress and to evaluate the dehydration tolerance (Sullivan 1972; Blum and Ebercon 1981; Sun et al. 2020). Bajji et al. (2002) reported that the measurement of electrolyte leakage could be used to estimate the extent of cell membrane damage caused by dehydration stress.

5.2 Phosphatidylcholine involved in membrane integrity

Phosphatidylcholine (PC) is a main structural component of cell membranes as well as one of the most abundant phospholipids in plant cells, which is important in keeping the integrity and functionality of cell membranes (Sun et al. 2020). PC also plays a role in multiple physiological functions, such as cell recognition, cell signaling, cellular metabolism and maintaining normal physiological activity, growth and development, and stress defense (Chen et al. 2018). In addition, PC as a precursor is involved in the biosynthesis of various signaling molecules, including phosphatidic acid (PA), lysoPC, arachidonic acid, and diacylglycerol (DAG) (Cui and Houweling 2002). Exton (1994) reported that PC is a main source of secondary lipid messengers and thus plays a vital role in signal transduction. Due to these structural and functional roles of PC, the biosynthesis and catabolism pathways of PC are extremely important for maintaining the homeostasis of PC as well as other lipids (Robinson et al. 1989; Exton 1994; Sun et al. 2020).

Recently, the function of exogenous PC application has been studied. Research on peach seedlings subjected to drought stress showed that exogenous application of PC enhanced the integrity of cell membranes, thereby increasing cell viability, protect leaf cell tissues, and reduce electrolyte leakage (Sun et al. 2020).

5.3 Enzymes involved in phosphatidylcholine synthesis

PC is a ubiquitous phospholipid in most eukaryotic algae and plants (Sato et al. 2016). Due to the important role of PC, it is necessary to study PC synthesis-related enzymes.

In eukaryotes, PC is synthesized through three known pathways, including the Kennedy pathway, the methylation pathway, and base-exchange pathway (Liu et al. 2015). In the Kennedy pathway, there are two branches referred to as CDP-ethanolamine (for the synthesis of phosphatidylethanolamine: PE) and

CDP-choline pathway (for the synthesis of PC) (Gibellini and Smith 2010). For the methylation pathway, PC is produced from PE through three methylation steps: the initial methylation step is catalyzed by PE methyltransferase (PEMT) while the second and third methylation steps are catalyzed by phospholipid methyltransferase (PLMT) (Sato et al. 2016). In the base-exchange pathway, PC is synthesized from other phospholipids (eg. phosphatidylserine: PS) by exchanging the head group with free choline (Liu et al. 2015).

The CDP-choline pathway consists of three enzymatic steps in eukaryotes (Fig. 1). Initially, choline is catalyzed by choline kinase (CK), which is an ATP-dependent phosphorylation step, forming phosphocholine. Secondly, the CTP:phosphocholine cytidyltransferase (CCT) catalyzes CTP and phosphocholine to form CDP-choline and pyrophosphate (PP), which is considered to be a rate-limiting step in CDP-choline pathway of PC synthesis (Gibellini and Smith 2010; Cornell and Ridgway 2015). In this step, the activity of CCT is regulated by signals from the membrane which can sense the relative PC abundance (Cornell and Ridgway 2015). The final reaction of the pathway is catalyzed by CDP-choline 1,2-diacylglycerol cholinephosphotransferase (CPT), using CDP-choline and alkyl-acylglycerol (AAG) or diacylglycerol (DAG) to synthesis PC and the byproducts CMP (Sundler and Akesson 1975; Gibellini and Smith 2010; Cornell and Ridgway 2015).

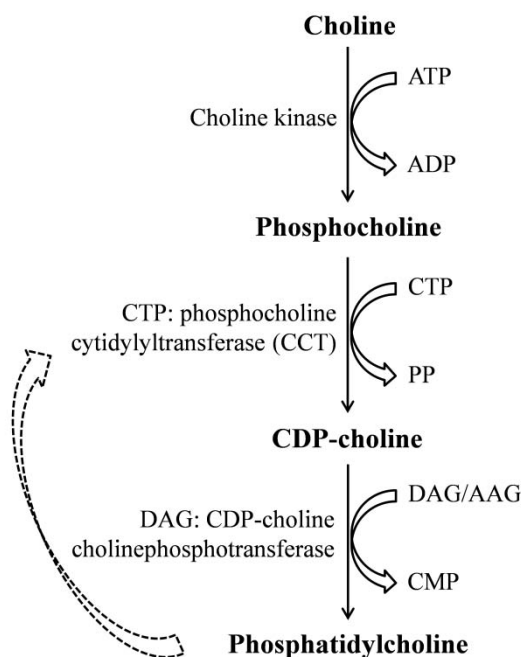


Fig. 1 The CDP-choline pathway for PC synthesis in eukaryotes (Gibellini and Smith 2010; Cornell and Ridgway 2015). The activity of CCT is regulated by signals from the membrane (dotted arrow) related to the relative PC abundance.

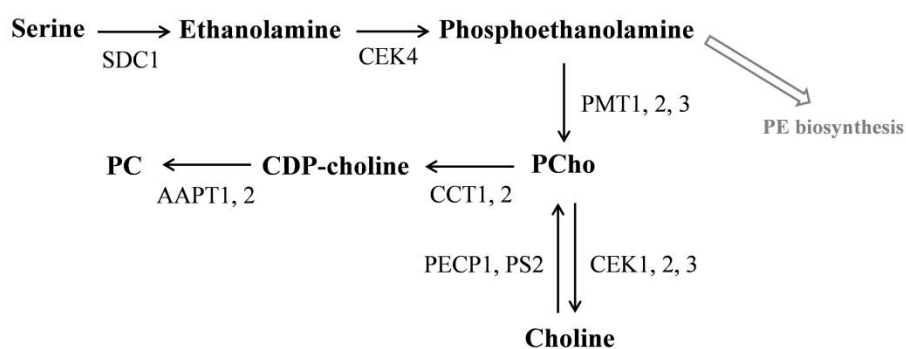


Fig. 2 An updated metabolic pathway for the PC biosynthesis in *A. thaliana* (Liu et al. 2019). SDC1: Serine decarboxylase 1; PMT: S-adenosylmethionine: phospho-base *N*-methyltransferase; CEK: choline/ethanolamine kinase; CCT: phosphorylcholine cytidyltransferase; AAPT: aminoalcohol aminophosphotransferase; PECP1: phosphoethanolamine/phosphocholine phosphatase 1; PS2: phosphate starvation induced gene 2.

Recently, an updated metabolic map of PC biosynthesis in *A. thaliana* was drawn by Liu et al. (2019b) (Fig. 2). In detail, the reaction step is started from the alteration

of serine to ethanolamine using serine decarboxylase 1 (SDC1) (Yunus et al. 2016; Liu et al. 2018). The choline/ethanolamine kinase 4 (CEK4) then phosphorylates ethanolamine to phosphoethanolamine (Lin et al. 2015). The phosphoethanolamine has two different metabolic fates: to synthesize PE or to synthesize PC (Liu et al. 2019b). For the PC synthesis, phospho-base N-methyltransferase (PMT) catalyzes phosphoethanolamine to form phosphocholine (PCho), in which PMT1, PMT2, and PMT3 are redundant in *A. thaliana* (Liu et al. 2019b). Then PCho is converted to CDP-choline in the reaction triggered by CCT1 and CCT2 (Inatsugi et al. 2002, 2009), then CDP-choline is used to form PC through the catalysis of aminoalcoholaminophosphotransferase 1 (AAPT1) and AAPT2 in *A. thaliana* (Liu et al. 2015). Rhodes and Hanson (1993) reported that ethanolamine can be used to produce PCho through PMT activity in angiosperm plants. More recently research showed that knocking out the putative choline /ethanolamine kinases CEK 1, CEK 2, and CEK 3 did not affect PC contents in *A. thaliana* (Lin et al. 2015). In addition, the PC content was not affected by the null mutants of two PCho phosphatases: phosphoethanolamine/phosphocholine phosphatase 1 (PECP1) and phosphate starvationinduced gene 2 (PS2) in *A. thaliana* (Hanchi et al. 2018). Therefore, it can be speculated that the choline phosphorylation pathway might not be the major pathway for PC biosynthesis in *A. thaliana* plants (Liu et al. 2019b).

6 Objectives of this study

This study is comprised of three main projects and focused on the mechanisms related to desiccation tolerance in the desiccation tolerant resurrection plant *C. plantagineum*.

In plants, repeated exposure to dehydration stress or other biotic or abiotic stresses may generate stronger reactions during a subsequent stress event. This phenomenon is referred to as plant stress memory, which has been studied mainly in desiccation sensitive plants. For resurrection plants, *C. plantagineum* as a desiccation

tolerant plant has become an experimental model system to study desiccation tolerance. These conditions stimulated us to address the question whether the desiccation tolerant resurrection plant *C. plantagineum* has a stress memory after exposed to repeated dehydration/rehydration treatment cycles. Therefore, we designed the following experiments: 12 week-old *C. plantagineum* plants were air-dried for 6 h, and then recovered for 18 h. After the same treatments (dehydration and rehydration) were repeated 4 times, the plants were re-watered for 2, 4 or 6 days. Whether the putative memory responses exist in *C. plantagineum* under repeated dehydration treatments was analyzed on the physiological level (including leaf water content, electrolyte leakage, chlorophyll content, proline content, H₂O₂ content, superoxide dismutase activity, sucrose and octulose content analysis, and lipid peroxidation assay) and on the molecular level (including transcript abundance analysis of stress-induced genes, chlorophyll synthesis and degradation-related genes, ROS pathway-related genes; and protein expression of four stress-induced genes). Representative genes were selected from different pathways and it was investigated whether they are trainable genes and may be involved in dehydration stress memory. It was also studied how long the memory can persist after the dehydration had stopped. Understanding the response of desiccation tolerant plants to dehydration stress which occurred repeatedly within short intervals may guide us to find beneficial ways for increasing the yield of crop plants (**CHAPTER 2**).

Strategies for desiccation tolerance and recovery in *C. plantagineum* have been extensively studied, such as changes in morphology and photosynthetic activity, synthesis of protective protein, mRNA binding to polysomes, and sucrose accumulation. However, the basis of such mechanisms is mainly unknown. Currently, RNA-sequencing represents the best method to identify changes in expression of dehydration-induced genes in resurrection plants on a genome-wide level. To obtain genes affected by dehydration and rehydration in *C. plantagineum*, polysomal mRNA was isolated from leaves using sucrose gradient-based fractionation and quantification by RNA sequencing. Combined with total mRNA profiling, we planned to undertake a

comprehensive study of gene expression profiles and of genes under translational control in *C. plantagineum* at four crucial stages (untreated, partially dehydrated, desiccated, and rehydrated). Therefore we analyzed the dynamic profiling and sequence features of genes under translational control. The genes and their interaction networks, and related metabolic pathways may provide a more complete picture of genes and pathways involved in the acquisition of desiccation tolerance and the ability of rapid recovery (**CHAPTER 3**).

The work in **CHAPTER 3** has identified a dehydration induced gene CTP:phosphocholine cytidyltransferase (CCT), which is under translational control during dehydration stress. CCT is a rate limiting enzyme in the CDP-choline pathway for *de novo* phosphatidylcholine (PC) synthesis in plants. In order to analyze the function and characteristics of CCT in *C. plantagineum*, we cloned *CpCCT1* cDNA from *C. plantagineum* and compared the putative amino acid sequence with the desiccation sensitive plant (*A. thaliana*), the animal homolog (*Rattus norvegicus*) and the yeast homolog (*Saccharomyces cerevisiae*). The subcellular localization assay and the tissue specific expression analysis were designed to monitor the localization and tissue specific expression characteristics of CpCCT1. The responses of *CpCCT1* to dehydration, salt stress, cold stress, mannitol and sorbitol treatments, as well as abscisic acid (ABA) and indole-3-acetic acid (IAA) treatments was studied on the transcript and protein level in the leaf and root samples. A yeast complementation assay with CpCCT1 was performed to verify the enzyme activity of CpCCT1. The *CpCCT1* gene promoter region contains several putative DRE and ABRE *cis*-elements, therefore, the promoter activity of *CpCCT1* was analyzed in response to dehydration both in *C. plantagineum* and *A. thaliana* (**CHAPTER 4**).

CHAPTER 2

Transcriptional and metabolic changes in the desiccation tolerant plant *Craterostigma plantagineum* during recurrent exposures to dehydration

Xun Liu¹, Dinakar Challabathula², Wenli Quan³, Dorothea Bartels^{1*}

¹Institute of Molecular Physiology and Biotechnology of Plants (IMBIO), University of Bonn, Kirschallee 1, 53115 Bonn, Germany

²Department of Life Sciences, School of Basic and Applied Sciences, Central University of Tamil Nadu, Thiruvarur, India

³Key Laboratory for Quality Control of Characteristic Fruits and Vegetables of Hubei Province, College of Life Science and Technology, Hubei Engineering University, Xiaogan, Hubei, 432000, China

Abstract

***Main conclusion* Multiple dehydration/rehydration treatments improve the adaptation of *Craterostigma plantagineum* to desiccation by accumulating stress inducible transcripts, proteins and metabolites. These molecules serve as stress imprints or memory and can lead to increased stress tolerance.**

It has been reported that repeated exposure to dehydration may generate stronger reactions during a subsequent dehydration treatment in plants. This stimulated us to address the question whether the desiccation tolerant resurrection plant *Craterostigma plantagineum* has a stress memory. The expression of four representative stress-related genes gradually increased during four repeated dehydration/rehydration treatments in *C. plantagineum*. These genes reflect a transcriptional memory and are trainable genes. In contrast, abundance of chlorophyll synthesis/degradation-related transcripts did not change during dehydration and remained at a similar level as in the untreated tissues during the recovery phase. During the four dehydration/rehydration treatments the level of reactive oxygen species (ROS) pathway-related transcripts, the superoxide dismutase (SOD) activity, proline, and sucrose increased whereas H₂O₂ content and electrolyte leakage decreased. Malondialdehyde (MDA) content did not change during the treatments, which indicates a gain of stress tolerance. At the protein level increased expression of four representative stress-related proteins showed that the activated stress memory can persist over several days. The phenomenon described here could be a general feature of dehydration stress memory responses in resurrection plants.

1 Introduction

Due to global warming air temperature, precipitation capacity and rainfall distribution change more frequently, which possibly lead to more irregular and multiple abiotic stresses, such as drought, heat and cold stress (Wang et al. 2014; Niinemets et al. 2017). Drought is one of the major factors, which can affect growth, survival and productivity of plants throughout their life cycle repeatedly (Avramova 2015; Todaka et al. 2017). It has been observed that tolerance to biotic and/or abiotic stress can be increased when plants are initially exposed to a mild stress (Ramírez et al. 2015). This phenomenon is termed “priming” and it is used in the context of application of chemical agents and biotic stress, and “acclimation” or “hardening” in the context of abiotic stress (Sinclair and Roberts 2005; Hilker et al. 2016; Savvides et al. 2016). Information may be stored from the initial first stress until the subsequent stress; this stored information influences the response to the subsequent stress so that plants can respond more quickly and efficiently and thus tolerance can be enhanced (Bruce et al. 2007; Ding et al. 2012; Li et al. 2014; Ramírez et al. 2015; Liu et al. 2016). A modulated response to a subsequent second stress represents the concept of a stress memory or imprint, which is responsible for providing mechanisms for acclimation and adaptation (Avramova 2015). Since ‘plant memory’ has been described as ‘an ability to access past experience so that new responses incorporate relevant information from the past’ (Pintó-Marijuan et al. 2017), we therefore use ‘memory’ in this work. A plant stress memory is associated with changes in physiology and biochemical parameters. Walter et al. (2011) reported that the relative leaf water content does not change significantly between two recurrent drought stresses, but the maximum quantum efficiency (F_v/F_m) and maximum fluorescence (F_m) are reduced. Studies demonstrated that a pre-exposition to cold stress can activate the sub-cellular antioxidant systems by increasing activities of SOD, APX and CAT which depress the oxidative burst in the photosynthetic apparatus, and thus the tolerance to a subsequent cold stress is enhanced (Li et al. 2014). It was observed that the photosynthetic rate and the sugar content increase, the stomata aperture

decreases, the ROS homeostasis sustains and the grain yield increases when plants were exposed to a second abiotic stress (Wang et al. 2014, 2015; Li et al. 2015; Virilouvet and Fromm 2015; Hu et al. 2016). Plant stress memory is mediated by proteins, transcription factors and modifications on the epigenetic level such as DNA methylation and demethylation, histone modifications and small RNAs (Chinnusamy and Zhu 2009). Besides increasing stress tolerance priming for a stress memory has also sometimes negative impacts as it may compromise growth of plants and biomass production (Chen and Arora 2012). The transcriptional changes induced by the pre-treatment may contribute to cope with the subsequent stress treatments by involving stress memory effects (Hu et al. 2016). Previous experiments demonstrated that different genes (*RD29A*, *RD29B*, *COR15A*, *RAB18*, *WRKY70*, jasmonic acid-associated genes and ‘revised-response’ memory genes) behave differently during repeated exposures to dehydration and memory and non-memory genes can be distinguished (Liu et al. 2016). Memory genes (or trainable genes) alter transcriptional responses to a subsequent stress, while ‘non-memory’ genes (or non-trainable genes) respond in the same way to each stress (Alvarez-Venegas et al. 2007; Ding et al. 2012; Liu et al. 2014, 2016; Avramova 2015). However, the process is so far not well studied and a more detailed analysis is required of the physiology and the molecular basis in plants.

Understanding the response of plants to stresses which occur repeatedly within short intervals may lead to beneficial treatments also in crop plants. Memory responses have been identified in several angiosperm plants (such as potato, *Arabidopsis* or perennial ryegrass) (Ramírez et al. 2015; Hu et al. 2016; Liu et al. 2016).

C. plantagineum is a desiccation tolerant plant which loses nearly all cellular water and goes to a quiescent state during desiccation. Upon water availability the plant rehydrates and restores full metabolic activity (Bartels et al. 1990). This is a good experimental system to study the dehydration stress-induced memory responses

in resurrection plants. We were interested to know how the desiccation tolerant resurrection plant *C. plantagineum* responds to repeated dehydration treatments with short time intervals and whether this plant has the capacity to recover from repeated stress treatments. Therefore, we analyzed whether memory responses exist in *C. plantagineum* under repeated dehydration treatments on the physiological and molecular levels and how long the memory persists after the stress relief. Representative genes from different pathways were selected and it was investigated whether they are trainable genes and could be involved in dehydration stress memory.

2 Materials and methods

2.1 Plant growth and stress treatments

C. plantagineum was propagated vegetatively and grown in artificial clay pebbles (Lanstedt Ton, Gebr. Lenz GmbH, Bergneustadt, Germany) in individual pots with nutrient solutions according to Bartels et al. (1990). The artificial clay pebbles are porous small granules (8-12mm). Dehydration stress was applied to 12 week-old plants by removing the plants from the artificial clay pebbles. The roots were gently washed to remove any remaining pebbles. Then plants were air-dried for 6 h in light conditions. This exposure was recorded as stress 1 (S1) and resulted in the decrease of the fresh tissue weight to 65% of the untreated state (F). It was established in preliminary experiments that if the fresh tissue weight decreased to 65% of the F state, plants could recover fully after rehydration, indicating that this level of water loss is reversible and non-lethal. After dehydration plants were placed in a controlled growth chamber (120-150 $\mu\text{mol m}^{-2} \text{s}^{-1}$ light, 22 °C and 30% humidity) with their roots in water for 18 h (including a dark period of 6 h) to recover (R1). The same treatments (dehydration and rehydration) were repeated 4 times until stress 4 (S4). After S4 plants were re-watered for 2, 4 or 6 days and these samples are termed R2d, R4d and R6d. Samples were harvested at each time point for further analysis. The treatments are depicted in the scheme in Fig 1a. In each experiment at least 30 plants were used, of which 6 plants were used as control. The control plants were kept under the same light and temperature conditions as the treated plants. At least three independent biological replications were done for each experiment and three to five technical repetitions in each biological experiment.

2.2 Relative water content measurement

To check the water status of the plants at the dehydration and rehydration stages, the relative water content was measured, according to the formula: $\text{RWC}(\%) =$

$[(FW - DW)/(TW - DW)] \times 100\%$ where FW is the fresh weight of leaves, TW is turgid weight of the same leaves after submerged in water for 24 h and DW is the dry weight of the same leaves after 24 h incubation at 80 °C (Ding et al. 2012; Quan et al. 2016a).

2.3 Assay of electrolyte leakage

For electrolyte leakage assays at least 4 leaves were used in one repetition, and 5 technical repetitions and 3 biological repetitions were done. Leaves were cut into squares of about 1 cm side length and shaken at 160 rpm (Innova 4000 incubator shaker, New Brunswick Scientific, USA) in Milli-Q water for 4 h at room temperature before measuring the initial conductivity using a conductivity meter (Qcond 2400, VWR International, USA). Then samples were boiled for 30 min. The conductivity of the samples was measured after they had been cooled down to room temperature. Electrolyte leakage was calculated as the ratio of initial conductivity and the conductivity of the boiled samples (Quan et al. 2016b).

2.4 Determination of chlorophyll content

Plant leaves (dry weight: 20-60 mg) were ground under liquid nitrogen and homogenized in 2 ml of 80% (v/v) acetone. The mixtures were incubated for 30 min in the dark with shaking and centrifuged for 5 min at 12000 g at room temperature. The chlorophyll content was measured at 663 nm (OD 663) and 645 nm (OD 645) and calculated using the formula:

$$C \text{ (mg/g DW)} = 0.002 \times (20.2 \times \text{OD } 645 + 8.02 \times \text{OD } 663) / \text{g DW}$$

, where C corresponds to the total chlorophyll content (Missihoun 2011).

2.5 Quantification of proline content

Proline levels were determined from leaves of treated plants according to Liu and

Chan (2015). Proline was extracted from 0.5 g leaf tissue by adding 5 ml of 3% (w/v) sulfosalicylic acid and subsequently boiled for 10 min. Two ml supernatant was transferred to a mixture of 2 ml of 100% (v/v) glacial acetic acid and 2 ml of ninhydrin acid (1.25 g ninhydrin dissolved in 30 ml of 100% (v/v) glacial acetic acid and 20 ml of 6 mol/L phosphoric acid). Then the compounds were boiled for 30 min. After cooling to room temperature, 4 ml of toluene was added. The upper phase was transferred to a new tube after vortexing for 30 s. After centrifugation for 5 min at 3000 g, the upper organic phase was collected and the OD was measured at 520 nm. In parallel, L-proline was used for preparing a standard curve (Liu and Chan 2015). The proline content was calculated based on the standard curve as follows:

$$\begin{aligned} \text{proline } (\mu\text{g/g DW}) & \\ &= (\text{concentration derived from a standard curve} \\ &\times \text{volume of the extract}) / \text{g DW} \end{aligned}$$

2.6 Assay of H₂O₂ content

The H₂O₂ content was measured according to Velikova et al. (2000). Leaf material (20-60 mg) was ground with liquid nitrogen and homogenized in 2 ml of 0.1% (w/v) trichloroacetic acid. The mixture was incubated on ice for 5 min and centrifuged for 10 min at 13000 g at 4 °C. After centrifugation 0.5 ml of the supernatant was transferred into a mixture of 0.5 ml of 10 mM potassium phosphate buffer (pH 7.0) and 1 ml of 1 M potassium iodide to start the reaction. After keeping the compounds in the dark for 20 min at room temperature, the absorbance was read at 390 nm. In parallel, H₂O₂ standards (5, 10, 25, 50 μM) were prepared for a standard curve. The H₂O₂ content was calculated based on the standard curve as follows:

$$C (\mu\text{mol/g DW}) = (\text{concentration derived from a standard curve} \times \text{volume of the extract}) / \text{g DW} ,$$

where C corresponds to the H₂O₂ content.

2.7 Lipid peroxidation assay

The MDA was measured as the end product of the lipid peroxidation process according to Hodges et al. (1999) and Kotchoni et al. (2006). Briefly, 1 ml pre-chilled 0.1% (w/v) TCA solution was used to homogenize the leaf tissue (20-60 mg) which was ground with liquid nitrogen. The homogenate was centrifuged at 13000 rpm at 4 °C for 5 min. One volume of 20% (w/v) TCA, 0.01% (w/v) butylated hydroxytoluene (BHT) and 0.65% (w/v) thiobarbituric acid (TBA) mixture was added to 500-600 µl supernatant for the last step. The compound was incubated at 95 °C in a water bath for 25 min. Absorbances were read at 440 nm (OD 440), 532 nm (OD 532) and 600 nm (OD 600), respectively. The MDA content was determined by the following formula:

$$\begin{aligned} & \text{MDA equivalents (nmol/g DW)} \\ &= [(A - B) / 157\,000] \times 1\,000\,000 \\ & \times \text{total volume of the extracts ((ml)) / g DW, where A} \\ &= [(OD\,532 - OD\,600)] \text{ and } B = [(OD\,440 - OD\,600) \times 0.0571] \end{aligned}$$

2.8 Determination of superoxide dismutase activity

Superoxide dismutase activity was measured by the 4-nitro-blue tetrazolium chloride (NBT) illumination method as described by Liu and Chan (2015).

2.9 Sugar extraction and analysis

Sugars were extracted from leaf tissues of *C. plantagineum* as described by Zhang et al. (2016). Leaf material (1 g) was ground to a fine powder in liquid nitrogen and extracted twice with 80% (v/v) methanol at 4 °C. After centrifugation for 5 min at 5000 g at 4 °C, the supernatant was transferred to a new tube. A dry sediment was obtained after evaporation at 25 °C under reduced pressure for about 3 h. The sediment was dissolved in water and extracted three times with chloroform. The

aqueous phase was centrifuged at 10 000 g, 4 °C for 30 min. The exchange resin (Dowex 50 WX8 and Dowex IX8) was added to the aqueous phase (5 g/100 ml) to remove charged molecules. Then the aqueous phase containing the sugar fraction was stirred for 1 h before the gas chromatography/mass spectrometry (GC/MS) analysis.

The extracted sugars were first analysed by thin layer chromatography according to Zhang et al. (2016)

For the sucrose and octulose content measurement, 10 µg xylitol was used as internal standard. The following steps were done according to Zhang et al. (2016). Data analysis was performed with GC ChemStation [Rev.B.03.02 (341), Agilent Technologies, Böblingen, Germany].

2.10 RNA isolation and reverse transcription-PCR

Total RNA was extracted according to Valenzuela-Avenidaño et al. (2005). Reverse transcription (RT)-PCR was performed as described by Zhao et al. (2017). Gene-specific primers are listed in Table S1. The transcript of the *EF1α* gene was used as the internal reference for *C. plantagineum* (Giarola et al. 2015). The relative gene expression level was determined by Image-J (<https://imagej.nih.gov/ij/>). Fold changes of each gene at different time points were analyzed by setting F phase as 1.

2.11 Protein analysis

Crude protein extracts were prepared according to Laemmli (1970) by using Laemmli-sample buffer (62.5 mM Tris-HCl, pH 6.8, 10% (v/v) glycerol, 2% (w/v) SDS, 0.1 M DTT, 0.005% (w/v) bromophenol blue). Pre-chilled transfer buffer was used to transfer proteins separated on a 10% polyacrylamide SDS gel onto a nitrocellulose Protran BA-85 membrane (Towbin et al. 1979). The transferred proteins were visualized by staining the membrane with 0.2 % (w/v) Ponceau S-red solution for 30 min. After destaining, the membrane was incubated in blocking solution (1×

TBS, 4% (w/v) skimmed milk powder and 0.1% (v/v) Tween-20) at room temperature for 60 min. Polyclonal antibodies were used for protein detection. The presence of the target protein was detected on the membrane by chemiluminescence under a CCD camera (Intelligent Dark Box II, Fujifilm Corp.). The relative protein expression level was determined by Image-J (<https://imagej.nih.gov/ij/>). Fold changes of each protein at different time points were analyzed by setting F phase as 1.

2.12 Cluster and correlation analysis

Hierarchical cluster analyses were performed using the Cluster 3.0 (<http://bonsai.hgc.jp/~mdehoon/software/cluster/software.htm>) by the uncentered correlation and average linkage method and the resulting tree figures were displayed using Java Treeview (<http://jtreeview.sourceforge.net/>) (Shi et al. 2014).

Correlation analysis was done in Excel (Microsoft 2010). Electrolyte leakage is given on the x-axis and the measurements for the other parameters are given on the y-axis (Shi et al. 2012).

2.13 Statistical analysis

SPSS 20.0 software (IBM, USA) was used in this study for statistical analyses. The differences were performed by one way ANOVA, and at least 3 independent biological replicates and 3-5 technical replicates within each biological experiment were done for each parameter. The results shown are means \pm SE. The vertical bars with different lower-case letters are significantly different from each other at $P < 0.05$.

3 Results

3.1 Dehydration stress-trained *C. plantagineum* plants

The phenotype of *C. plantagineum* plants subjected to four cycles of 6 h air-drying and 18 h rehydration is shown in figure 1b. During the four consecutive cycles of stress (S1-S4) and recovery (R1-R3) the plants lost water faster and wilted faster in the S1 phase than plants in the S2, S3, and S4 phases (Fig. 1c). The RWC in the R1, R2 and R3 phases were always similar to the RWC of untreated leaves (F) (Fig. 1d). This shows that the plants had fully recovered after each rehydration (R1, R2 and R3), although they had lost water during each air-drying treatment.

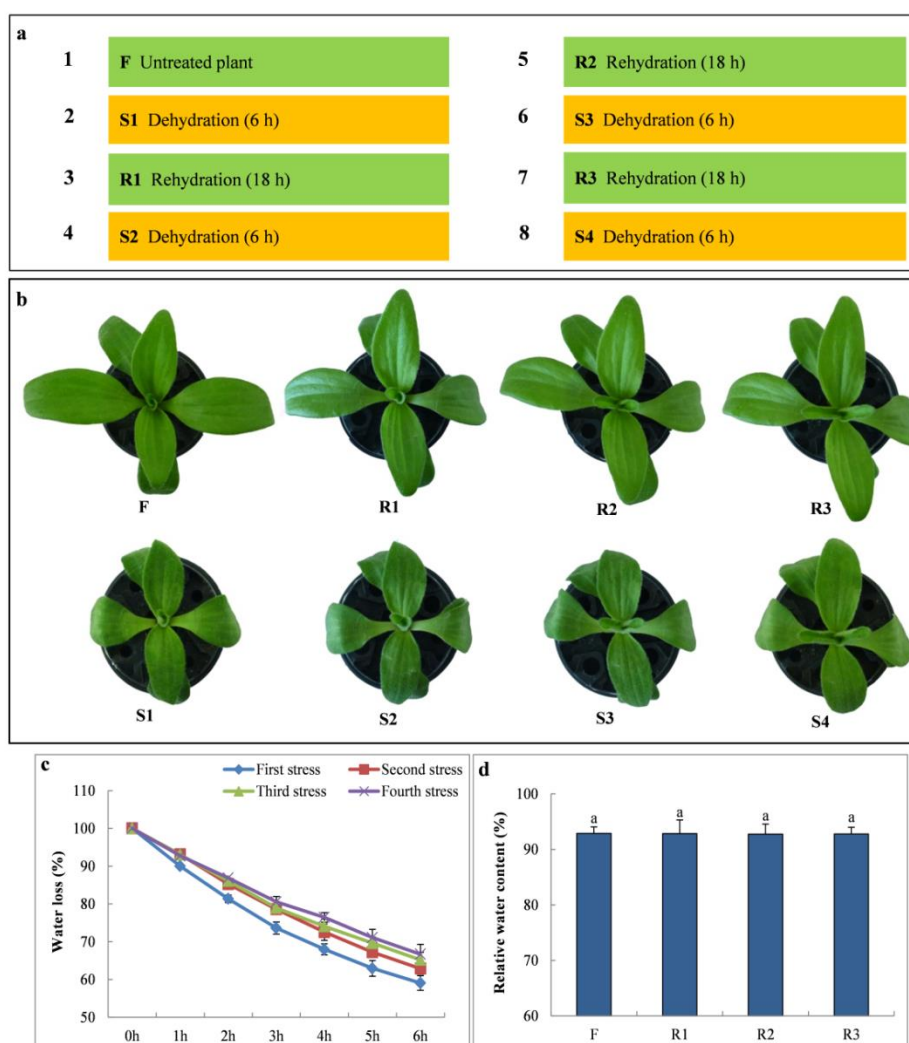


Fig. 1 The assessment of dehydration tolerance and water status during 4 cycles of dehydration. (a)

The experimental design of dehydration/rehydration applications (see details in Materials and methods). **(b)** Appearance of *C. plantagineum* plants during four consecutive cycles of stress (S1-S4) and subsequent recovery (R1-R3) treatments. **(c)** Fresh weight of plants after experiencing the first dehydration (blue line), second (red line), third (light green line) and fourth (purple line) stress cycle. **(d)** Relative water content of plant leaves in untreated plants before the start of the dehydration (F) state and after recovery (R1-R3) phases. Values in **(c)** and **(d)** were calculated from 3 independent biological repetitions and 5 technical repetitions within each biological experiment (means \pm SE). The vertical bars with different lower-case letters are significantly different from each other at $P < 0.05$ (one-way ANOVA). Other details are given in Materials and methods.

3.2 Changes in physiological parameters during repeated dehydration and rehydration in leaves of *C. plantagineum*

After repetitive dehydration-stress/recovery electrolyte leakage and H₂O₂ content decreased from the S1 phase to the S4 phase. The H₂O₂ content at the S4 phase did not differ from the untreated state. Electrolyte leakage and H₂O₂ content stayed at the same level as in the untreated state during all phases of recovery (Fig. 2a, b). MDA levels, SOD activity and proline content gradually increased during the four dehydration treatments and remained at a relatively low level in F and R1-R3 phases (Fig. 2c, d, e). The increase of the MDA and SOD activity were similar during the four dehydration phases, respectively (Fig. 2c, d). The total chlorophyll content did not change significantly throughout the treatments (Fig. 2f).

Changes in sucrose and octulose are major metabolic alterations in *C. plantagineum* during dehydration/rehydration (Bianchi et al.1991). Therefore sugars were analysed during the recurrent stress experiment according to Zhang et al. (2016). The sucrose content gradually increased during the dehydration stages, even though the content declined at each recovery stage, while the octulose content stayed at a high level during the whole process (Fig. 2g, h, Fig. S1, Fig. S2).

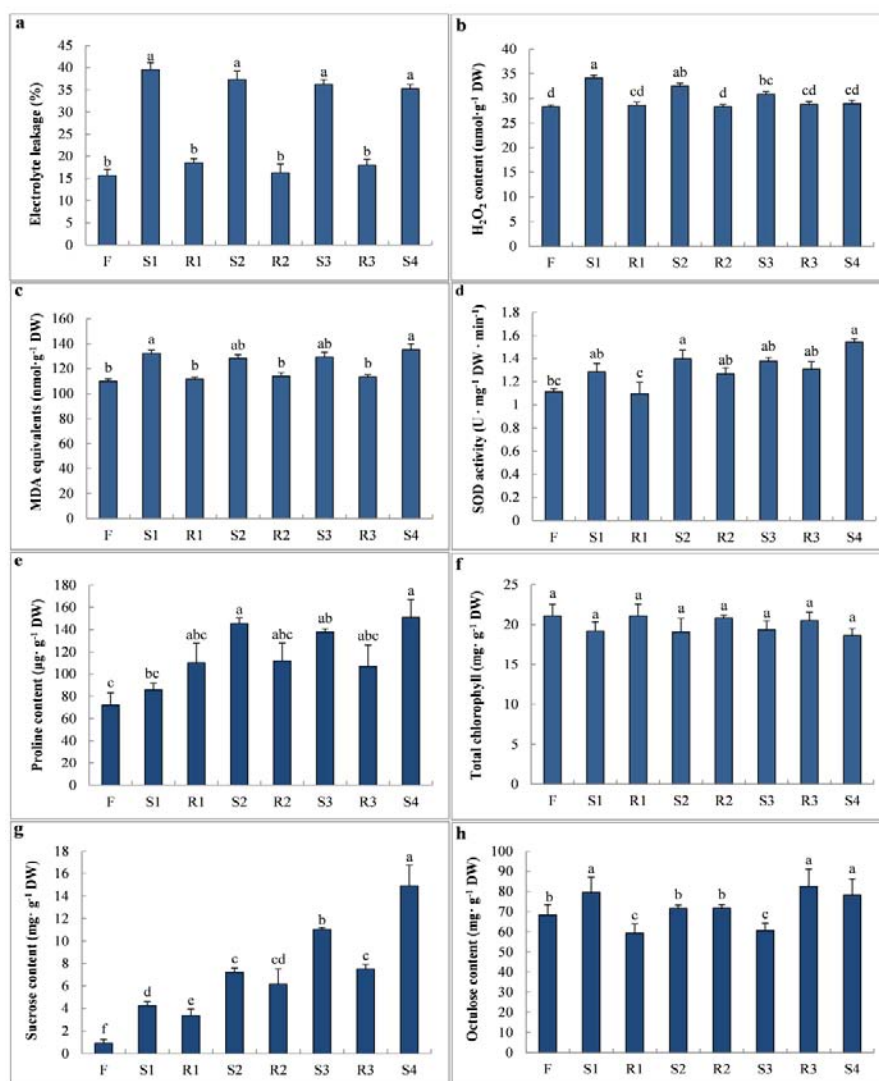


Fig. 2 Quantitative comparison of physiological parameters in *C. plantagineum* during multiple exposures to dehydration. Changes in electrolyte leakage and H₂O₂ content during 4 consecutive cycles of stress (S1-S4) and recovery (R1-R3) treatments (**a**, **b**). Changes in MDA content and SOD activity during 4 dehydration and recovery treatments (**c**, **d**). Changes in proline and total chlorophyll content during 4 stress/recovery treatments (**e**, **f**). Changes of sucrose and octulose content were analyzed during 4 dehydration and recovery treatments (**g**, **h**). Values in (**a-f**) were calculated from 3 independent biological repetitions and 5 technical repetitions within each biological experiment (means ± SE) and Values in (**g**, **h**) were calculated from 3 independent biological repetitions and 3 technical repetitions within each biological experiment (means ± SE). The vertical bars with different lower-case letters are significantly different from each other at $P < 0.05$ (one-way ANOVA). Other details are given in Materials and methods.

3.3 Correlation of electrolyte leakage with other physiological parameters under the repetitive dehydration and rehydration conditions

The correlation was analyzed between electrolyte leakage and other physiological parameters during four cycles of dehydration. The leaf RWC and chlorophyll content showed a negative linear correlation with the electrolyte leakage during the dehydration process ($R^2 = 0.99, 0.89$, respectively) (Fig. 3a, b) which means an association with dehydration-induced cell injury in *C. plantagineum* during the S1-S4 phases. However, there was no linear correlation between electrolyte leakage and the accumulation of SOD activity and osmolytes (proline, sucrose and octulose) ($R^2 = 0.47, 0.26, 0.27$, and 0.02 , respectively) (Fig. 3c-f). A positive correlation was observed for the MDA and H_2O_2 content with electrolyte leakage ($R^2 = 0.92, 0.66$, respectively) (Fig. 3g, h).

3.4 Transcript accumulation during recurrent stress treatments

Transcript levels of four selected stress-induced genes were determined during the repeated dehydration/rehydration treatments (Fig. 4). Figure 4a shows the transcript abundance of late embryogenesis abundant (LEA) genes (*LEA-like 11-24*, *LEA2 6-19* and *LEA 13-62*), and early dehydration responsive 1 (*EDR1*). The results show that after S1 the later dehydration treatments induced higher expression levels of the four selected genes than during the first dehydration. The *LEA-like 11-24*, *LEA2 6-19* and *EDR1* gene reached the highest expression level at the S2 stage, whereas the *LEA 13-62* gene had a transcription peak at the S3 stage during the four cycles of dehydration. The four stress-induced transcripts accumulated during the repeated dehydration treatments in the S1, S2, S3 and S4 phases (Fig. 4b-e).

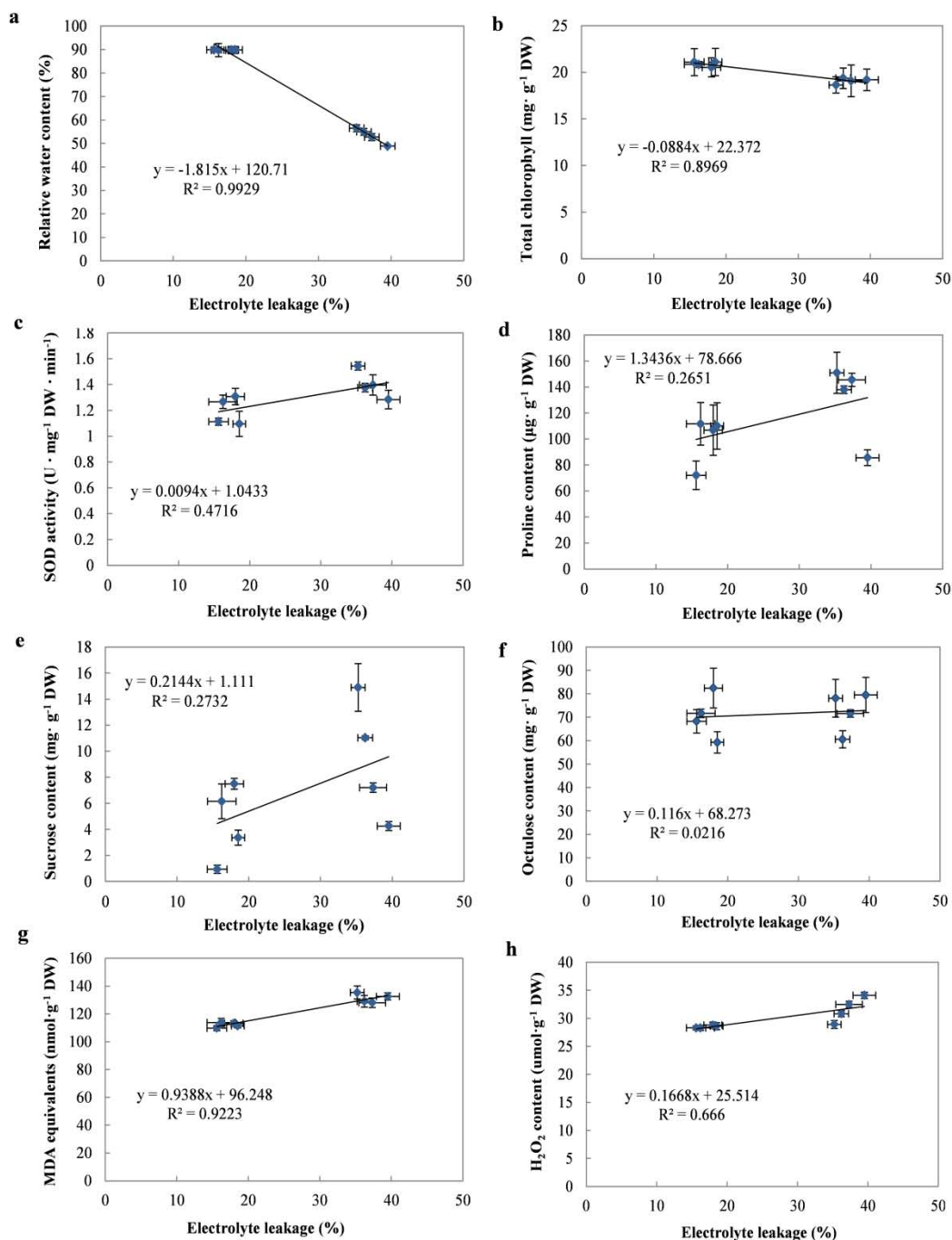


Fig. 3 Correlation between electrolyte leakage and other physiological parameters during multiple exposures to dehydration stress. Correlation of electrolyte leakage with RWC (**a**), total chlorophyll (**b**), SOD activity (**c**), proline content (**d**), sucrose content (**e**), octulose (**f**), MDA content (**g**), and H_2O_2 content (**h**) during 4 consecutive cycles of dehydration and rehydration treatments. Values in (**a-h**) were calculated from 3 independent biological repetitions and 3-5 technical repetitions within each biological experiment (means \pm SE).

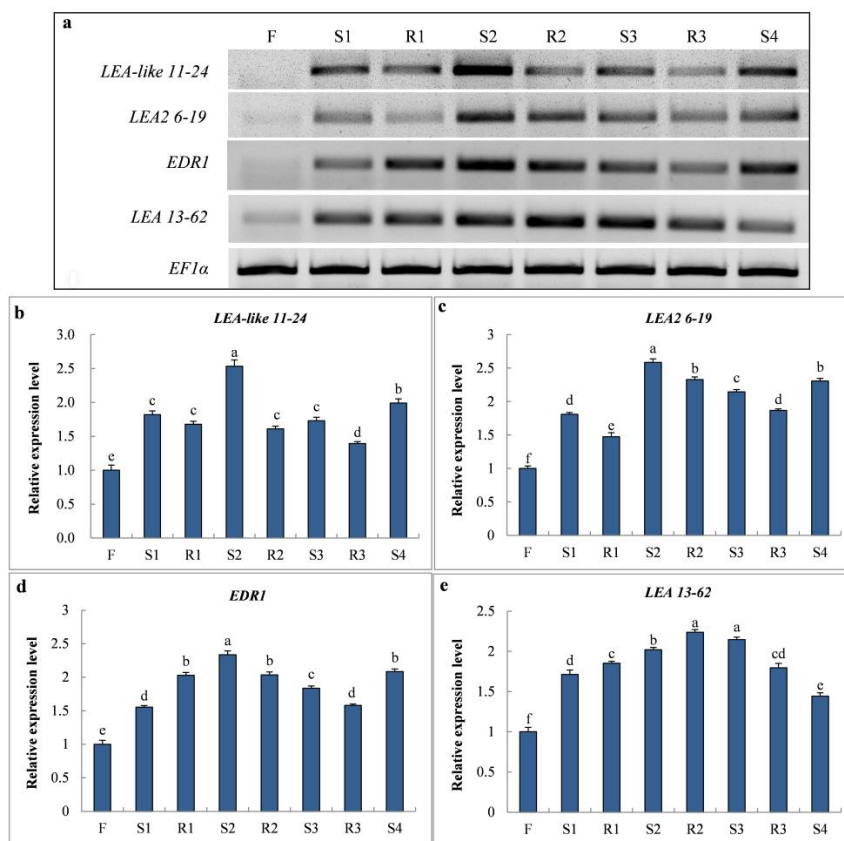


Fig. 4 (a) Transcript levels of stress-induced genes in *C. plantagineum* during multiple exposures to dehydration stress. Transcript abundance of *LEA-like 11-24* (b), *LEA2 6-19* (c), *EDR1* (d) and *LEA 13-62* (e) genes measured by semi-quantitative PCR. Fold changes of each gene at different time points were analyzed by setting the level at F phase as 1 using the Image-J software (b-e). *EF1α* was used as an internal control. Values in (b-e) were calculated from 3 independent biological repetitions (means \pm SE). The vertical bars with different lower-case letters are significantly different from each other at $P < 0.05$ (one-way ANOVA).

A decline of photosynthesis during dehydration and its recovery during rehydration is characteristic for the homiochlorophyllous resurrection plant *C. plantagineum*. Therefore chlorophyll synthesis and degradation-related genes were analyzed during the dehydration/rehydration cycles. Transcript abundance of chlorophyll synthesis-related genes is shown in Fig. 5a. During dehydration the transcript levels of Mg-protoporphyrin IX methyltransferase (*CHLM*), porphobilinogen deaminase (*PBGD*), glutamate-1-semialdehyde (*GSA*), 5-aminolaevulinic acid dehydratase (*ALAD*), coprogen oxidase (*CPO*) and

chlorophyll synthase (*CHLG*) decreased and during rehydration the transcripts of all six genes remained at a similar level as in the untreated state, except for *PBGD*, *GSA* and *CPO* which were reduced in R1, R3, R1 and R2, respectively (Fig. 5b-g).

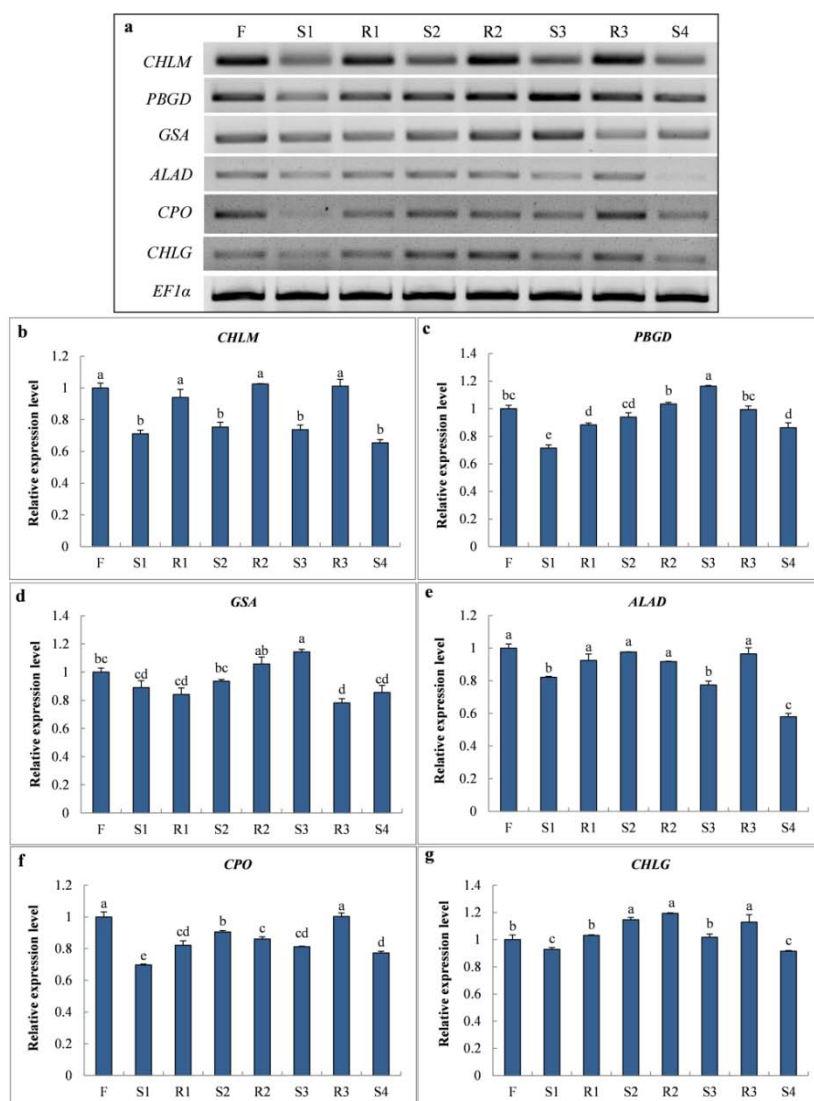


Fig. 5 (a) Transcript levels of chlorophyll synthesis-related genes in *C. plantagineum* during multiple exposures to dehydration stress. Transcript abundance of *CHLM* (b), *PBGD* (c), *GSA* (d), *ALAD* (e), *CPO* (f) and *CHLG* (g) genes were measured by semi-quantitative PCR. Fold changes of each gene at different time points were analyzed by setting the level at F phase as 1 using Image-J software (b-g). *EF1α* was used as an internal control. Values in (b-g) were calculated from 3 independent biological repetitions (means \pm SE). The vertical bars with different lower-case letters are significantly different from each other at $P < 0.05$ (one-way ANOVA).

The changes in transcript abundance of the chlorophyll degradation-related genes red chlorophyll catabolite reductase (*RCCR*), pheophorbide a oxygenase (*PaO*), pheophytinase (*PPH*) and non-yellowing 1 (*NYEI*) showed an opposite trend to the chlorophyll synthesis-related genes during four cycles of dehydration. During the dehydration treatments the transcript levels of the four genes (*RCCR*, *PaO*, *PPH* and *NYEI*) increased at each time point, except for *PaO* in the S4 phase which was not significantly different from the untreated state (Fig. 6).

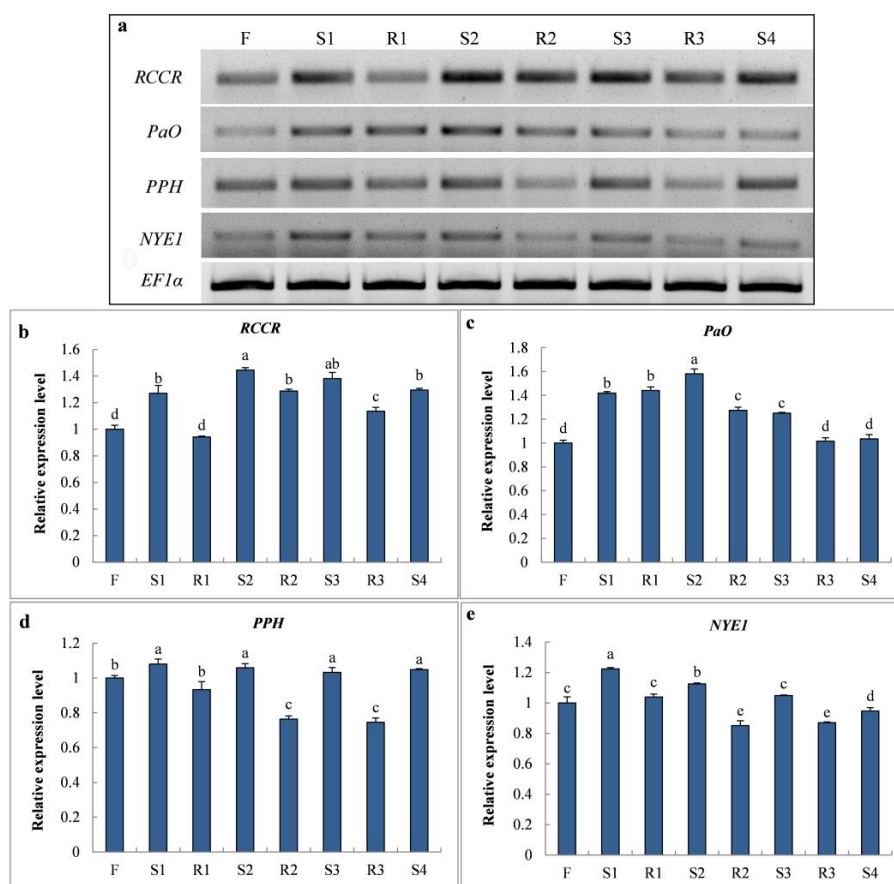


Fig. 6 (a) Transcript levels of chlorophyll degradation-related genes in *C. plantagineum* during multiple exposures to dehydration stress. Transcript abundance of *RCCR* (b), *PaO* (c), *PPH* (d) and *NYEI* (e) genes were measured by semi-quantitative PCR. Fold changes of each gene at different time points were analyzed by setting the level at F phase as 1 (b-e). *EF1α* was used as an internal control. Values in (b-e) were calculated from 3 independent biological repetitions (means \pm SE). The vertical bars with different lower-case letters are significantly different from each other at $P < 0.05$ (one-way ANOVA).

As markers for stress defense four ROS pathway-related genes manganese superoxide dismutase (*Mn-SOD*), copper/zinc superoxide dismutase (*Cu/Zn-SOD*), catalase (*CAT*) and ascorbate peroxidase (*APX*) were analyzed. The transcript patterns of the four genes changed at each time point (Fig. 7a). At the S4 stage, the transcript levels of *Mn-SOD*, *Cu/Zn SOD* and *CAT* were reduced compared to the untreated state whereas the *APX* transcript did not change between the S4 and F phases (Fig. 7b-e).

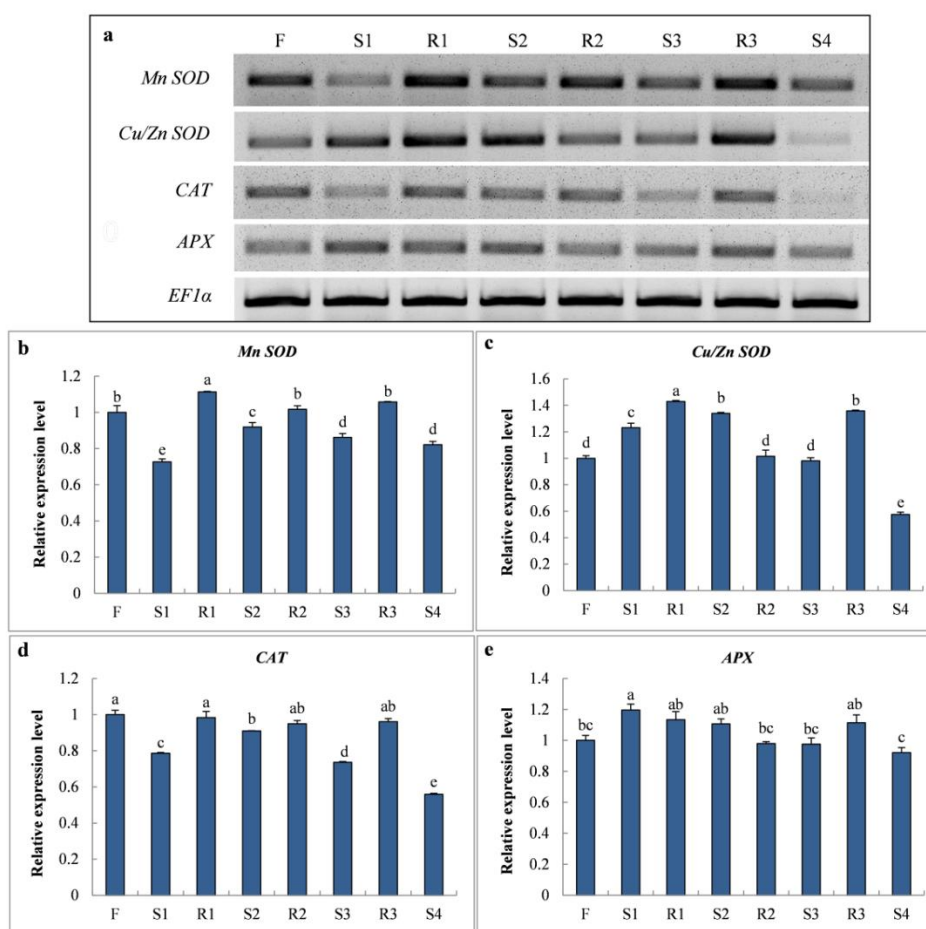


Fig. 7 (a) Transcript levels of ROS pathway-related genes in *C. plantagineum* during multiple exposures to dehydration stress. Transcript abundance of *Mn-SOD* (b), *Cu/Zn-SOD* (c), *CAT* (d) and *APX* (e) genes were measured by semi-quantitative PCR. Fold changes of each gene at different time points were analyzed by setting the level at F phase as 1 (b-e). *EF1α* was used as an internal control. Values in (b-e) were calculated from 3 independent biological repetitions (means \pm SE). The vertical bars with different lower-case letters are significantly different from each other at $P < 0.05$ (one-way ANOVA).

To compare the transcripts of the different pathways a hierarchical cluster analysis was done. The graph shows that the transcript levels of the four stress-related genes (*LEA-like 11-24*, *LEA2 6-19*, *EDR1* and *LEA 13-62*) accumulated throughout dehydration treatments. However, the genes (*CHLM*, *PBGD*, *GSA*, *ALAD*, *CPO*, *CHLG*, *RCCR*, *PaO*, *PPH*, *NYE1*, *Mn SOD*, *Cu/Zn SOD*, *CAT* and *APX*) stayed at similar levels or were even reduced by the end of the treatment compared with the untreated state (Fig. 8a).

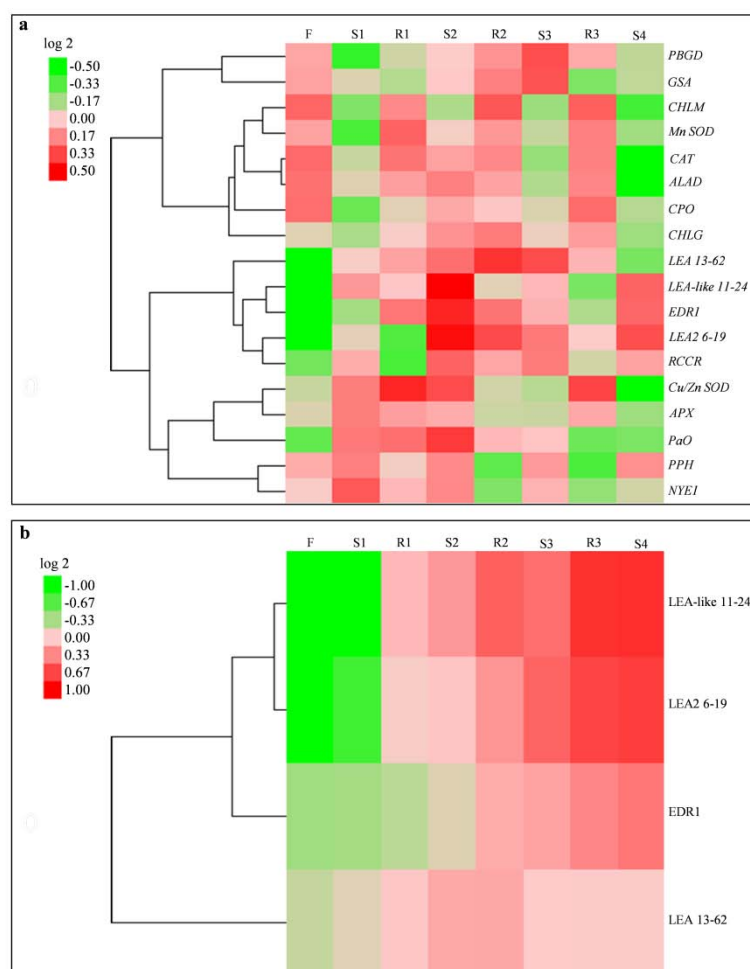


Fig. 8 (a) Hierarchical cluster analyses of different kinds of genes/proteins responding to 4 cycles of dehydration stress. **(b)** The relative data of transcript levels of all tested genes were chosen for cluster analysis. The relative expression abundance of 4 stress-induced proteins was chosen for cluster analysis. All these data were quantified as fold change relative to the untreated state (F) which was set as 1. The tree figure was obtained by using Cluster 3.0 software and Java Treeview. The cluster colour bar was shown as log₂ fold change.

3.5 Expression patterns of stress-induced proteins

The abundance of four stress-induced proteins (LEA-like 11-24, LEA2 6-19, EDR1 and LEA 13-62) was analyzed by immunoblots (Fig. 9). Equal loading of proteins was monitored by staining the membrane with Ponceau S (red bands) (Fig. 9a). The relative fold change of each protein was measured by setting the untreated state as 1. The results showed that the abundance of the four stress-induced proteins gradually increased during four cycles of dehydration. The abundance of LEA-like 11-24, LEA2 6-19 and EDR1 proteins increased and reached the highest level at S4. The expression level of LEA 13-62 had a peak at the S2 phase, then gradually decreased in the following treatments, but the expression level in S4 was still higher than that at the untreated state (Fig. 9b-e). A hierarchical cluster analysis of the four stress-induced proteins showed that the abundance of LEA-like 11-24, LEA2 6-19 and EDR1 proteins increased during the repeated dehydration treatments except for LEA13-62, which slightly decreased after the R2 phase, but was still higher than that at the untreated state (Fig. 8b). These results demonstrate that the stress-related proteins increased during the treatment and the protein changes correlate directly with the transcript levels.

3.6 Dehydration-stress memory

The question was raised as how long the stress memory can persist in the absence of stress stimulation. The protein abundance of four stress-induced genes is shown in Fig. 10a. The LEA-like 11-24 and LEA 13-62 proteins were retained for 2 and 4 days, and the relative protein levels at R2d and R4d were both significantly higher than at the untreated state but at R6d the expression level of the two proteins did not differ from the untreated state (Fig. 10b, e). The EDR1 protein persisted for 3 days, and the protein disappeared after 4 days of re-watering (Fig. 10d). The LEA2 6-19 protein gradually decreased from R2d to R6d, but was significantly higher during re-watering conditions than in the untreated state (Fig. 10c).

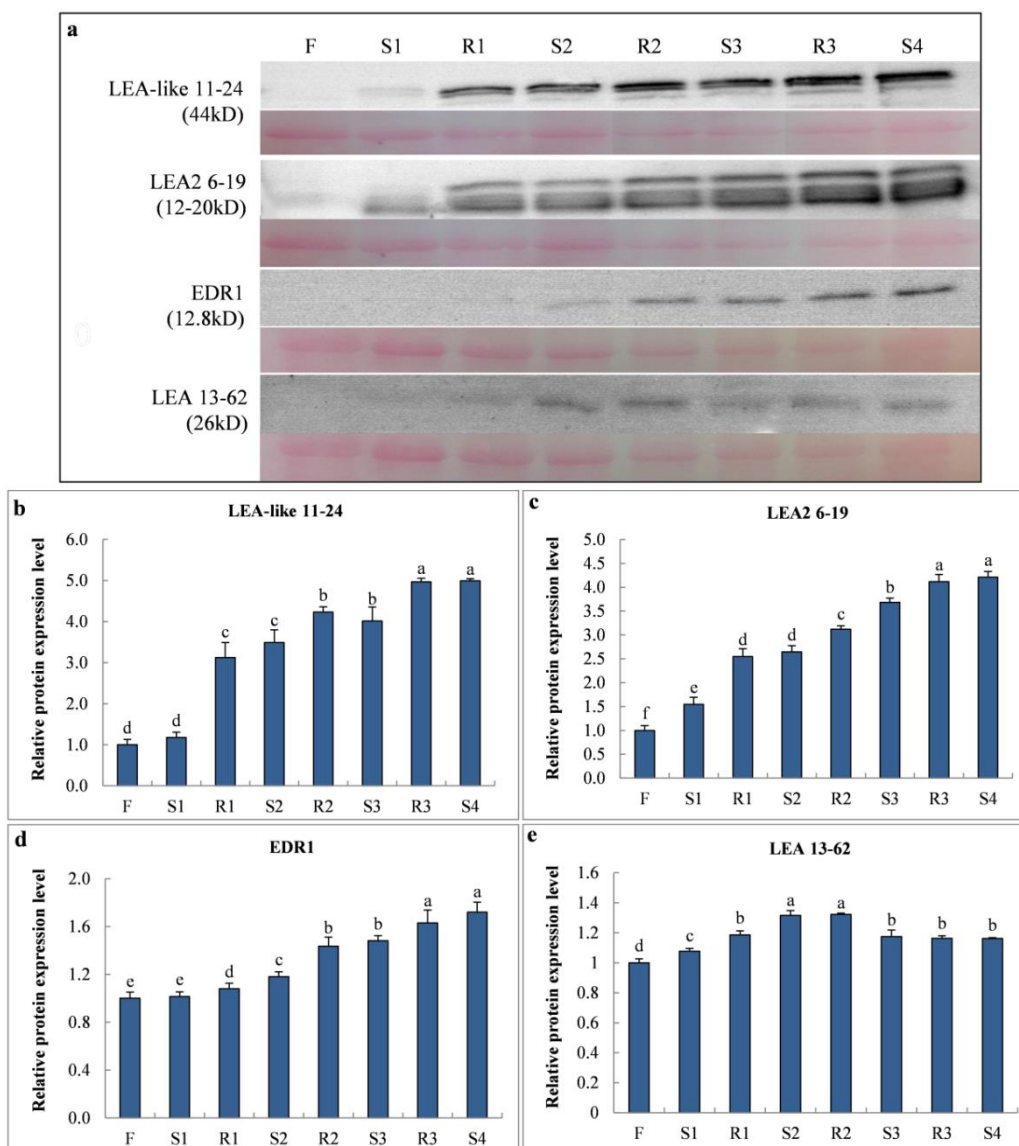


Fig. 9 (a) Expression abundance of stress-induced proteins in *C. plantagineum* during multiple exposures to dehydration stress. (b) Expression levels of LEA-like 11-24, (c) LEA2 6-19, (d) EDR1 and (e) LEA 13-62 proteins were measured by Western blot. Equal loading of proteins was monitored by staining the membrane with Ponceau S (red bands). Fold changes of each protein at different time points were analyzed by setting the level at the F phase as 1 (b-e). Values in (b-e) were calculated from 3 independent biological repetitions (means \pm SE). The vertical bars with different lower-case letters are significantly different from each other at $P < 0.05$ (one-way ANOVA).

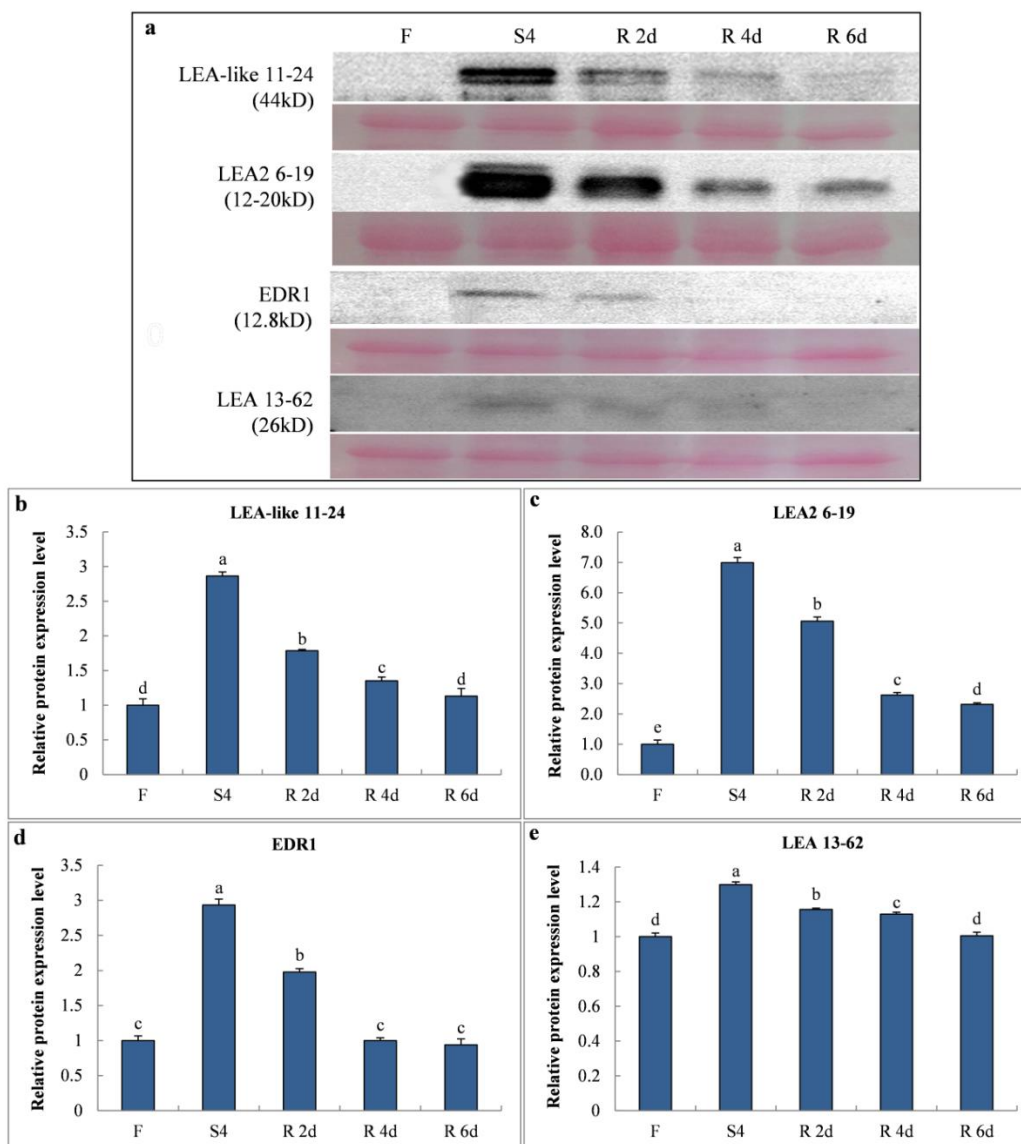


Fig. 10 Dehydration stress memory. (a) Expression levels of LEA-like 11-24 (b), LEA2 6-19 (c), EDR1 (d) and LEA 13-62 (e) proteins were analyzed by Western blot after 2d, 4d or 6d recovery. Equal loading of proteins was monitored by staining the membrane with Ponceau S (red bands). Fold changes of each protein at different time points were analyzed by setting the level at the F phase as 1 (b-e). Values in (b-e) were calculated from 3 independent biological repetitions (means \pm SE). The vertical bars with different lower-case letters are significantly different from each other at $P < 0.05$ (one-way ANOVA).

4 Discussion

In nature plants are usually exposed to repeated cycles of dehydration that differ in duration and intensity. Responses of plants to reiterated dehydration are different from those to a single exposure to dehydration (Fleta-Soriano and Munné-Bosch 2016). Previous stress encounters are remembered through the accumulation of transcripts and some metabolites (involved in carbon and energy metabolism as well as amino acid or fatty acid biosynthesis and others) after pre-exposure to stress conditions (Bruce et al. 2007; Hu et al. 2016; Sun et al. 2018).

4.1 Metabolites during dehydration/rehydration

Minimizing water loss is a key factor for survival of plants experiencing dehydrations, and plants can acclimate to dehydration by reducing the water loss rate (Yoo et al. 2010; Hu et al. 2012; Shi et al. 2012). During the four repetitive dehydration/rehydration treatments in this study the water loss rate in *C. plantagineum* leaves decreased from S1 to S4, and the RWC reached the same level as in the untreated state after each recovery (R1, R2 and R3) (Fig. 1c, d). A similar trend was also observed in desiccation sensitive *A. thaliana* plants during mild dehydration and rehydration conditions (Ding et al. 2012).

During dehydration the electrolyte leakage is increased due to disturbance of cell membranes (Zhao et al. 2011). Oxidative stress is caused by excessive production of ROS which can lead to damage of nucleic acids and proteins as well as lipid peroxidation. The SOD activity increases to scavenge the over-production of ROS and protects plants from oxidative damage, functioning as the first stage of antioxidant defense (Mittler 2002; Apel and Hirt 2004; Mittler et al. 2004; Liu and Chan 2015). In the study presented here the SOD activity gradually increased during S1-S4, the levels of electrolyte leakage and H₂O₂ content decreased and no significant changes of MDA content was observed during the four cycles of dehydration treatments (Fig. 2a, b, c,

d). Repeated dehydration did not lead to increased accumulation of stress metabolites, but the opposite behavior was observed which implies that repeated stress treatments make the *C. plantagineum* plants more robust to dehydration.

Osmotic adjustment and cellular compatible solute accumulation are widely recognized as plant adaptation to dehydration (Blum 2017). According to previous studies, high proline content provides an advantage for plants under dehydration stress (Lu et al. 2009; Zhao et al. 2011). An increase of proline and sucrose was observed in *C. plantagineum* leaves during the four cycles of dehydration and rehydration (Fig. 2e, g). Electrolyte leakage as an indicator of cell membrane stability has been used to evaluate the extent of cell injury (Hu et al. 2010; Shi et al. 2012). The analysis of the H₂O₂ and MDA values as well as RWC and total chlorophyll content showed the highest positive and negative correlation with electrolyte leakage, respectively (Fig. 3).

4.2 Gene expression patterns

Multiple consecutive stress/recovery treatments can alter transcriptional responses to a subsequent stress (Goh et al. 2003; Ding et al. 2012; Liu et al. 2014, 2016; Hu et al. 2016). Genes involved in ABA/abiotic stress responses are signatures for memory genes in which trainable LEA genes represent a major component (Ding et al. 2013). The *LEA 2 6-19* and *LEA-like 11-24* genes are involved in ABA signalling pathways (Michel et al. 1994; Van den Dries et al. 2011). The increasing accumulation of transcripts and proteins of stress-related genes and an altered accumulation of dehydration-responsive metabolites during repetitive exposures to dehydration suggest that an earlier stress exposure is memorized by *C. plantagineum* (Fig. 2, 4, 9). The hierarchical cluster analysis of the accumulation of stress-related genes/proteins during repetitive dehydration and rehydration indicates the formation of a stress memory during the accumulation process (Fig. 8). It has been suggested that the stress memory improves tolerance to subsequent stress exposures. This

includes tolerance to dehydration-related stresses but it may also be beneficial for the desiccation tolerant plants to cope with other stresses than dehydration.

4.3 Photosynthesis-related processes

Photosynthesis is very sensitive to dehydration stress in both desiccation tolerant and sensitive species (Challabathula et al. 2018). The photosynthetic apparatus is susceptible to injury during dehydration but can quickly be repaired upon rehydration and photosynthetic activity is restored in *C. plantagineum* in contrast to most angiosperm plants (Challabathula et al. 2012). Changes in chlorophyll content can be considered as an indicator for plant dehydration tolerance (Li et al. 2006). In our consecutive dehydration/rehydration treatment system the total chlorophyll content in *C. plantagineum* leaves was at a similar level as the untreated state during the recovery (R1, R2 and R3), indicating that the plants had fully recovered after each treatment which is consistent with phenotypic observations and relative water content measurements (Fig. 1b, d, Fig. 2f). Consistently, the transcript levels of chlorophyll synthesis-related genes decreased during dehydration and increased during recovery whereas degradation-related transcripts and proteins increased at each dehydration stage and declined during recovery (Fig. 5, 6).

4.4 Stress memory

The results presented here are in agreement with a dehydration stress memory as already observed in *Arabidopsis* or as observed for drought hardening in horticultural plants (Kozlowski and Pallardy 2002; Ding et al. 2012). Stress memory will fade off, if the signals of stress stimulation disappear. The duration of the transcriptional memory for stress-related genes *RD29B*, *RAB18*, *ACO1*, *JAZ9* and *TRAF1* in desiccation sensitive *Arabidopsis* plants persisted for five days under dehydration conditions (Ding et al. 2012; Liu et al. 2016). In another study, the transcriptional memory in trained perennial ryegrass plants sustained for up to four days after cycles of salt stress (Hu et al. 2016). In *C. plantagineum* dehydration stress-induced memory

responses could persist up to six days after the stress stimulation disappeared under the conditions applied here (Fig. 10).

The present study supports the notion that pre-exposure to multiple dehydration treatments could improve the stress-response to the subsequent encounter at physiological and molecular levels. Upon the first dehydration signal plants respond by expressing stress-related transcripts/proteins (Fig.11). Upon subsequent exposures to stress dehydration responsive transcripts/proteins accumulate further which suggests that plants memorize the first stress and are able to prepare for the subsequent stress. This shows that memory responses exist in *C. plantagineum* for stress responsive transcripts/proteins and that it takes at least six days for the memory to fade off, if the stress is not re-imposed. This phenomenon is most likely a general feature of the dehydration stress memory response in resurrection plants and may induce cross-protection to other environmental cues besides dehydration.

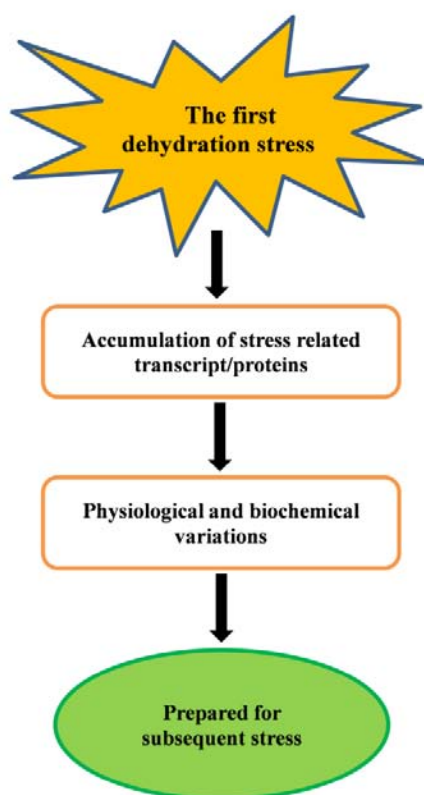


Fig. 11 A model for dehydration stress memory in *C. plantagineum*.

Acknowledgements

Xun Liu is supported by the China Scholarship Council (2016-2020). Dinakar C acknowledges the support from the Indian National Science Academy (INSA-India) and Deutsche Forschungsgemeinschaft-GZ:BA712/19-1 (DFG, Germany). The authors would like to thank Christiane Buchholz for growing the plants and Prof. Dr. Lukas Schreiber and Dr. Viktoria Zeisler-Diehl (IZMB, University of Bonn) for supporting the measurements of sucrose and octulose.

Author contribution statement

DB, DC and XL conceived and designed the experiments. XL performed the experiments and wrote the article. XL and WQ analyzed the data. DB, DC and WQ revised the article. DB supervised and corrected the writing.

Supporting data

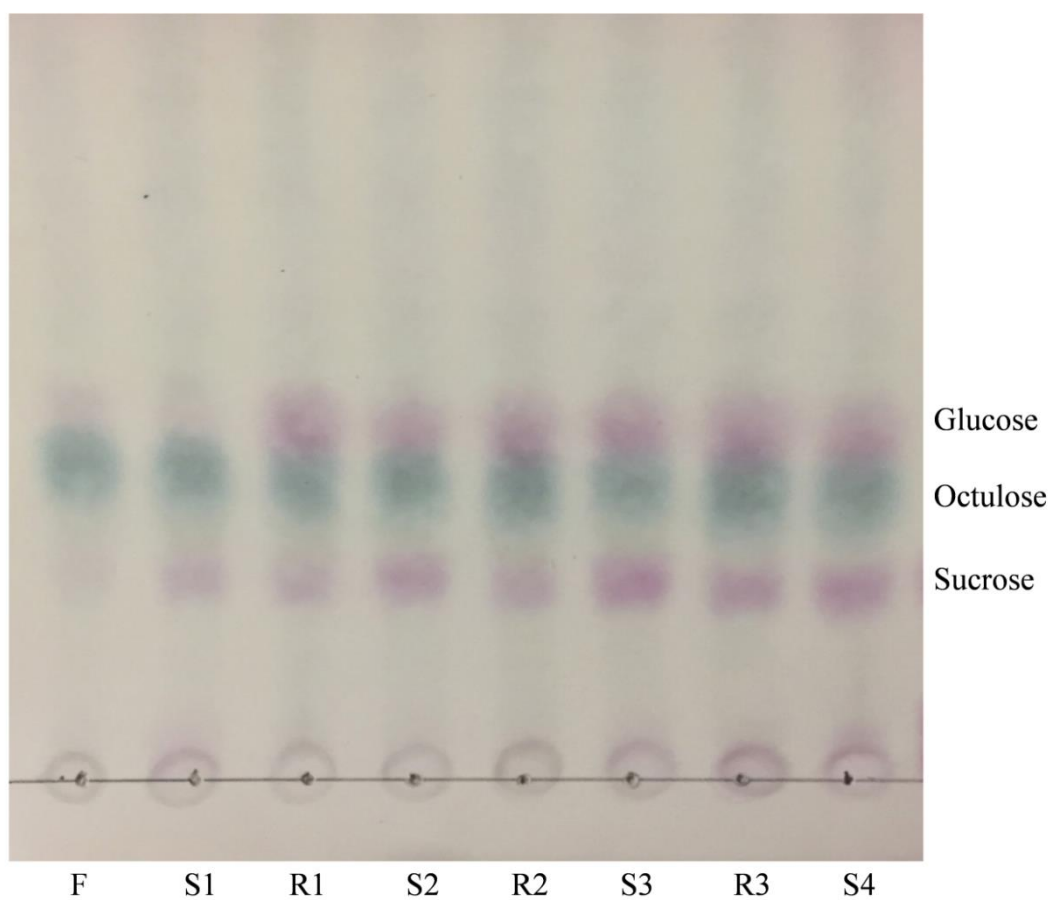


Fig. S1 Thin layer chromatography of sugars extracted from *C. plantagineum* leaves.

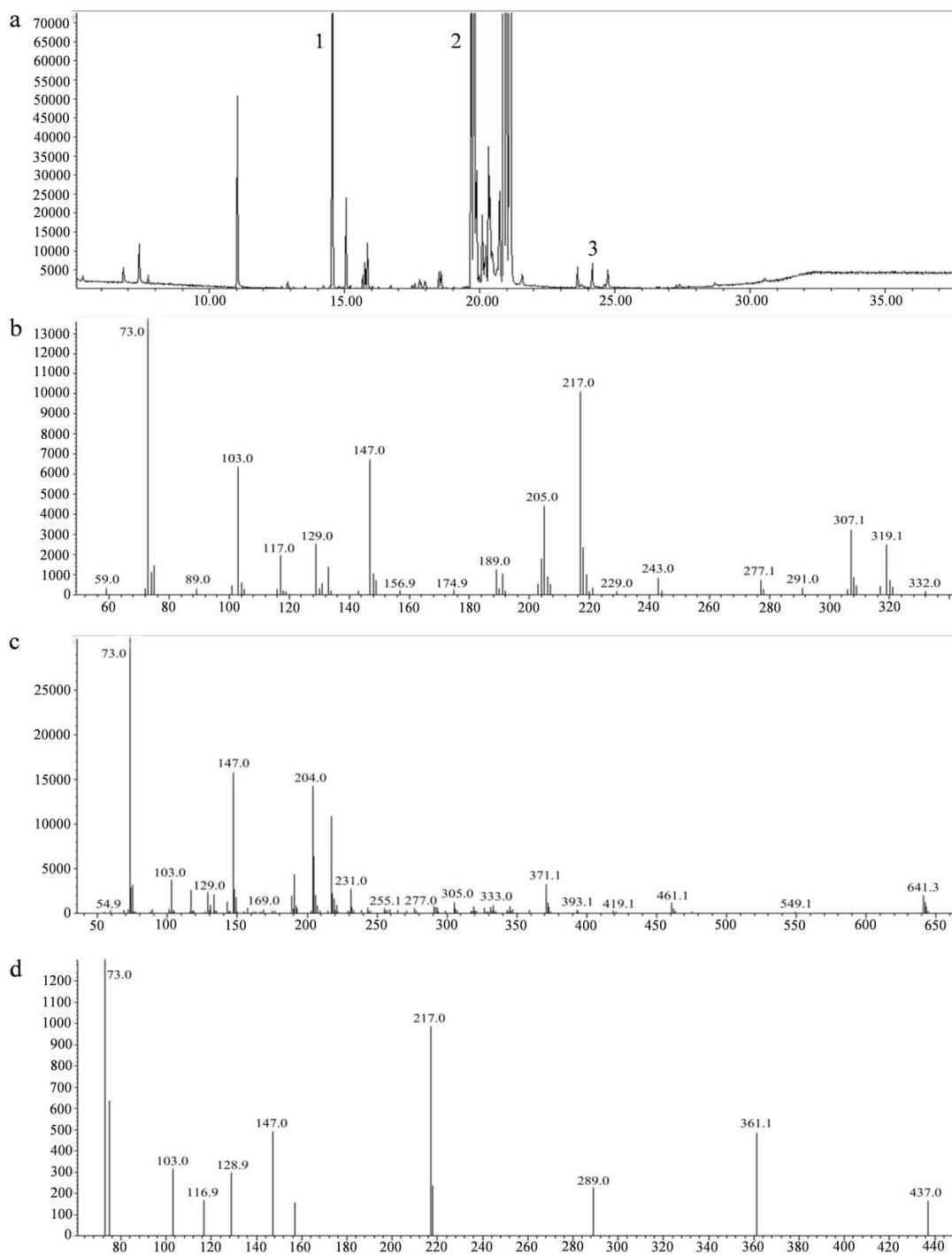


Fig. S2 (a) The chromatogram of sucrose (peak 3) and octulose (peak 2) extracted from *C. plantagineum* leaves, and the internal standard xylitol (peak 1). The fragmentation patterns of xylitol (b), octulose (c) and sucrose (d).

Table S1 List of primer sequences used for gene expression analysis.

Category	Gene	Primer sequence
Reference	EF1 α	Forward: AGTCAAGTCCGTCGAAATGC Reverse: CACTTGGCACCCCTTCTTAGC
Stress responsive genes	LEA-like 11-24	Forward: TCGGAAGACGAGCCTAAGAA Reverse: ACAGCGCCTTGTCTTCATCT
	LEA2 6-19	Forward: ACACCGACGAGTACGGAAACC Reverse: CGCCGGGAAGCTTCTCTTTG
	EDR1	Forward: TTGAACCGAGGGACGATG Reverse: GTTTAACGTTGCAAGGATTGTCTC
	LEA 13-62	Forward: CCTGGCATCATGAGAAGGAT Reverse: GAACTCTGAATCGCCCTGAC
Chlorophyll synthesis related genes	CHLM	Forward: GAGAAACAGGCCAAAGAAGAGC Reverse: CCAGAGAAGCTAAGTGGGCTATC
	PBGD	Forward: GAAGGCGTAGTACAAGCGACA Reverse: GTCTACATCCACGACGATTTCC
	GSA	Forward: CGGAGCACTTCTCATATTCGAC Reverse: CTAGTAAATCCCGCCTCGAACT
	ALAD	Forward: GTAGTCTCTTTGAGGCCCACTTC Reverse: CGTATTGTCCGAGGCACTAATC
	CPO	Forward: GAATCCCTCTCAGGTCAATGG Reverse: ACTCTCGATCCTACCTCCTGTCT
	CHLG	Forward: GAATGCCAGTGCTTTGAACC Reverse: ACAAGTGGAGGCCATGTAAGT
ROS detoxification	Mn SOD	Forward: CCTGCCCTTTTCCACAGATA Reverse: ATGCTCCCAGACATCAATGC
	Cu/Zn SOD	Forward: GCAAGGTTTACATCGGTGCT Reverse: AAATCGACCTCCTCCAATCC
	CAT	Forward: GGTGGAGAACCGGACAATAA Reverse: GTACCGTCCATCGAGTGCTT
	APX	Forward: GCATCCTCATCAGCAGCATA Reverse: GATGCTACCAAGGGTCTGA
Chlorophyll degradation related genes	RCCR	Forward: GTTCAACACTTCGGCGATTT Reverse: GTGCCTGTGCGAGGTTTGAGT
	PaO	Forward: ATCCCGAGGAACGACCAT Reverse: ATCAATCGATGTCTGCGTGT
	PPH	Forward: CTTCTCCAACAAGCCTCTG Reverse: GCAGAAAAGAAAGGGCTGTG
	NYE1	Forward: GTGGCCATTTTCTGCTTGAT Reverse: TCGAGACATGGCTGAGGAAT

CHAPTER 3

Translational regulation during dehydration and rehydration in *Craterostigma plantagineum* revealed by polysome profiling

Xun Liu

Institute of Molecular Physiology and Biotechnology of Plants (IMBIO), University of Bonn,
Kirschallee 1, 53115 Bonn, Germany

Abstract

The genome-wide total mRNA and polysome associated mRNA profiling revealed the polysome occupancy of each gene during four stages of dehydration and rehydration cycle in *C. plantagineum*. By comparing the polysome occupancy between each stage and the next time point, there were two phases with extensive changes under the translational control: from partial dehydration to desiccation (termed D/M group) and from desiccation to rehydration (termed R/D group). mRNAs had a positive trend to associate with ribosomes during desiccation which might contribute to RNA stability in *C. plantagineum*. The different dynamic patterns between up-regulated or down-regulated gene sets in the D/M group and R/D group indicated different regulatory mechanisms at different stages of dehydration and rehydration cycle in *C. plantagineum*. Sequence features, including transcript length, GC content, GC3 content, effective number of codons and enriched motifs correlated with the translational regulation occurring in the D/M group and R/D group. The significant different features in the two groups indicated different regulatory mechanisms of translation during dehydration and rehydration. GO term and MapMan pathway analysis revealed that genes under translational regulation in the D/M group and R/D group involved in several pathways including major carbohydrate (CHO) metabolism, signal transduction, kinase activity, transcription factor activity, cell wall, lipid metabolism and hormone metabolism. Our data showed that several transcription factor families, such as zinc finger, WRKY, NAC and ARF, involved in the translational regulation during dehydration and rehydration. This work here uncovers an important layer of regulation of gene expression related to plants desiccation tolerance and recovery process in resurrection plants.

1 Introduction

Dehydration stress is one of the most important environmental factors, which can affect growth, survival and productivity of plants (Todaka et al. 2017). Most angiosperm plants are desiccation sensitive, especially in the vegetative stage, and cannot survive when the relative cellular water content is lower than 60% (Giarola et al. 2017). One exception are the resurrection plants which have a unique characteristic: they recover from extreme dehydration (water loss up to 90%) and renew active metabolism after re-watering (Gaff 1971). Among them, *C. plantagineum* is such an extreme desiccation tolerant plant, which belongs to the *Linderniaceae* family (Bartels and Salamini 2001; Phillips et al. 2008). According to the previous studies, *C. plantagineum* mainly acquires tolerance through protection mechanisms during dehydration stress, such as changes in morphology, increase of protective proteins, decrease of photosynthetic activity, mRNA binding to polysomes and sucrose accumulation etc. (Bianchi et al. 1991; Challabathula et al. 2012; Giarola et al. 2015; Giarola and Bartels 2015; Juszczak and Bartels 2017). Comparative analysis of *in vitro* translated mRNA samples from *C. plantagineum* suggests that events taking place during rehydration only contribute to a full metabolic recovery and most molecules essential for desiccation tolerance accumulate during dehydration (Bernacchia et al. 1996). However, research in *Craterostigma wilmsii* suggests that additionally repair mechanisms during rehydration have the ability to repair inadequate protection or incurred damage (Cooper and Farrant 2002). Strategies for desiccation tolerance and recovery have been extensively discovered, whereas the basis of these mechanisms is often unknown. To obtain a more complete picture of genes and pathways involved in the acquisition of desiccation tolerance and the ability of rapid recovery, we undertook a comprehensive study of gene expression profiles and genes under translational control in *C. plantagineum* at four crucial stages during dehydration and rehydration.

The association of mRNAs with polysomes implies an active translation status

which is under tight regulatory control (Liu et al. 2013). Based on the different numbers of polysomes associated with mRNA, polysomal profiling can be separated by using sucrose gradient-based fractionation (Jackson and Larkins 1976; Barkan 1993, 1998). Then the polysomal mRNA and total mRNA profiles can be quantified by using RNA sequencing (Layat et al. 2014; Lin et al. 2014; Bai et al. 2017, 2018). The ratio between the polysomal mRNA abundance and the total mRNA abundance of a specific mRNA is termed polysome occupancy (Bai et al. 2017). The polysome occupancy reflects translational efficiency and significant changes of polysome occupancy for a specific gene indicate that this gene is under translational regulation (Arava et al. 2003; Ingolia et al. 2009; Bai et al. 2017, 2018). Previous research on *Arabidopsis thaliana*, *Saccharomyces cerevisiae* and *Aspergillus fumigatus*, demonstrate that the translational status of each mRNA can be estimated by changes of polysome occupancy (Arava et al. 2003; Ingolia et al. 2009; Liu et al. 2012, 2013; Krishnan et al. 2014; Juntawong et al. 2014; Basbouss-Serhal et al. 2015; Bai et al. 2017, 2018).

A goal of this study is to identify genes under translational regulation during four stages of dehydration and rehydration in *C. plantagineum*. Therefore we investigated the changes of total mRNA abundance and polysomal mRNA abundance through RNA sequencing. During the four different hydrated stages in dehydration and rehydration, genes were identified with different polysome occupancy in different groups. In the dehydration process, fewer genes with changed polysome occupancy emerged during early dehydration (water loss less than 30%) compared to desiccation (relative water content lower than 5%). Intriguingly, changes of polysome occupancy were caused by different reasons in a specific group (with increased or decreased polysome occupancy). Thus, this study identified several different sets of genes under translational control. The expression profiles of these genes were analyzed and the genes were related to specific pathways. This contributes to understanding the regulation of gene expression related to desiccation and recovery.

2 Materials and methods

2.1 Plant material and growth conditions

C. plantagineum was propagated vegetatively and grown in individual pots with nutrient solutions in a climate-controlled growth chamber (Model AR-75L, Percival Scientific, CLF, Emersacher, Germany) at a day/night temperature of 22/18 °C with 8 h light and 16 h dark photoperiod according to Bartels et al. (1990). For dehydration/rehydration treatments, 12 week-old fully developed plants were dehydrated in individual pots in a controlled growth room with 16 h light and 8 h dark photoperiod (120-150 $\mu\text{E m}^{-2} \text{s}^{-1}$ light, 22 °C and humidity 30%) for 0 d (untreated, C), 3 d (partial dehydration, M) or 10 d (desiccation, D) and rehydrated for 2 d (rehydration, R) under the same conditions. The treatments are depicted in the scheme in Fig. 1a. The plant leaves were harvested at each time point (with three independent biological replications), frozen and ground in liquid nitrogen. After being freeze-dried samples were stored at -80 °C for further analysis.

2.2 Relative water content measurement

The relative water content (RWC) in leaves was calculated following the formula: $\text{RWC (\%)} = [(\text{FW} - \text{DW}) / (\text{TW} - \text{DW})] \times 100\%$. FW means the fresh weight, TW means the turgid weight (after submerged in water for 24 h) and DW means the dry weight (after 24 h incubation at 80 °C) (Ding et al. 2012; Quan et al. 2016a).

2.3 Total mRNA and polysomal mRNA isolation

Total mRNAs were extracted from untreated, partial dehydrated, desiccated and rehydrated leaves of *C. plantagineum* according to Valenzuela-Avenidaño et al. (2005).

Polysomal mRNAs were isolated from the same leaf materials mentioned above according to Juszczak and Bartels (2017). In detail, 150 mg (DW) of freeze-dried

sample was extracted with 1 mL freshly prepared extraction buffer. After centrifugation for 5 min at 13000 g at 4 °C, the supernatant was transferred to a new 2 mL tube and added 10% (w/v) sodium deoxycholate (1/20 volume). The compound was loaded on the well-prepared continuous sucrose gradients (15-56% (w/v)) and separated by ultracentrifugation for 80 min at 45 000g at 4 °C. Ten fractions (410 µL each) were fractionated from the gradient after centrifugation. RNAs were extracted from each fraction and purified by using 2.5 M LiCl. Optical density at 260 nm (OD₂₆₀) was measured for the RNA extracted from each fraction. The gradients supplemented with 20 mM puromycin (as a control) were used to identify fractions containing polysomes. The fractions corresponding to polysomes were pooled for further analysis followed by purification with RNA binding columns from Gene Matrix Universal RNA Purification Kit (EURx, Gdansk, Poland). All procedures were performed using at least three independent biological replicates.

2.4 RNA sequencing analysis

Total mRNAs and polysomal mRNAs from untreated, partial dehydrated, desiccated and rehydrated leaves of *C. plantagineum* were used for RNA sequencing analysis. The purity and integrity of mRNAs were checked by GATC Biotech (Konstanz, Germany). RNA sequencing analysis was performed by GATC Biotech (Konstanz, Germany). Briefly, 3 µg RNA of each sample were used to generate sequencing libraries. The libraries were sequenced on an Illumina HiSeq platform and 50 bp paired-end reads were generated. After removing low quality reads and adapter sequences, clean reads were generated. The cleaned reads were mapped to the assembled sequences, then the mapped reads were calculated and the gene expression abundance was estimated to obtain RPKM (reads per kilo base per million mapped reads) (Li and Dewey 2011).

2.5 cDNA synthesis and quantitative RT-PCR (RT-qPCR)

2 µg of RNA per each sample were used for cDNA synthesis according to Zhao

et al. (2017). Each cDNA sample was diluted 15 times before preparing the RT-qPCR reaction. 5 μ L of the diluted sample was added for a 20 μ L RT-qPCR reaction (Giarola et al. 2015).

Gene specific primers were designed in the 3' region of the transcript to amplify a 70-118 bp amplicon using Primer 3 software (version 0.4.0) (Untergasser et al. 2012; Koressaar and Remm 2007). The secondary structures of target sequences were monitored by using the M-fold web server (<http://mfold.rutgers.edu/?q=mfold/DNA-Folding-Form>) with settings as 50 mM Na⁺ and 25 mM Mg²⁺ ionic conditions (Zuker 2003). To confirm the specificity of the PCR products, target amplicons were sequenced. The primer specificities were confirmed by RT-qPCR with the analysis of melting-curve (Giarola et al. 2015). The primer pairs and amplicon characters of eight candidate genes and reference genes are listed in Table S1.

The RT-qPCR was performed in a PCR plate with Maxima SYBR Green qPCR Master Mix (Thermo Fisher Scientific, St Leon-Rot, Germany) in the Mastercycler[®] ep realplex² (Eppendorf AG, Hamburg, Germany) PCR machine as described by Giarola et al. (2015). Detailed fold change of each gene was analyzed by using the $2^{-\Delta\Delta CT}$ method (Livak and Schmittgen 2001). The elongation factor 1-alpha (*EF1a*) and glyceraldehyde-3-phosphate dehydrogenase (*GAPDH*) were used as internal controls (Giarola et al. 2015). The RT-qPCR for each candidate gene and reference gene was performed with three independent different biological repetitions and three technical repetitions within each biological repeat.

2.6 Data analysis

The genes did not exceed the noise threshold ($\log_2 \text{Exprs} \leq 4$ in all samples) were removed. The differential expression between two different samples was identified using the DESeq2 package (Love et al. 2014). Genes (for both polysomal mRNA and total mRNA) are regarded as differentially expressed when \log_2 fold change > 1 and P

< 0.05 after controlling FDR (Benjamini and Hochberg 1995). Polysome occupancy of each mRNA was analyzed by comparing the normalized levels of the polysomal mRNA and total mRNA (Basbouss-Serhal et al. 2015).

The annotated TAIR IDs of *C. plantagineum* genes with significant change were used for GO term and pathway enrichment analyses with Classification SuperViewer program (http://bar.utoronto.ca/ntools/cgi-bin/ntools_classification_superviewer.cgi) (Alam et al. 2018). The normalized frequency (NF) was calculated according to Provar and Zhu (2003). Hierarchical cluster analyses were carried out in the Cluster 3.0 software (<http://bonsai.hgc.jp/~mdehoon/software/cluster/software.htm>) using the average linkage and uncentered correlation method, and revealed by Java Treeview software (<http://jtreeview.sourceforge.net/>) (Shi et al. 2014). The overview of genes under translational regulation was generated using MapMAN software (Version 3.6.0RC1) (<http://mapman.gabipd.org/home>). The dynamics of genes under translational control were highlighted in correlation plots using GraphPad Prism 7 software.

2.7 Analysis of interaction networks

The interaction networks of up-regulated transcription factors in the D/M and R/D group were constructed using STRING database (<https://string-db.org/>) with high confidence (combined score>0.7) (Szklarczyk et al. 2017). The interaction data collected from STRING database were then analyzed with Cytoscape software (Version 3.7.1) (<http://www.cytoscape.org/>).

2.8 RNA sequence feature analysis

The full length coding DNA sequence (CDS) of genes under translational control in the D/M group and R/D group were obtained from the whole genome database of *C. plantagineum* (unpublished). Since there is no 5' untranslated region (5'UTR) and 3'UTR sequence of *C. plantagineum* available at present, upstream sequences (50 nt,

100 nt and 200 nt) from the ATG start codon and downstream sequences (50 nt, 100 nt and 200 nt) from the stop codon were taken from the genome database (unpublished) and treated as 5'UTR and 3'UTR sequences, separately.

The GC contents were analyzed separately for CDS, 5'UTR and 3'UTR. The GC levels in the third position of codons (GC3) were also evaluated for the coding sequences. After removing coding sequences shorter than 300 nt (100 codons), the codon bias were analyzed by using the effective codon number (N_c) index (Bai et al. 2017).

2.9 Motif analysis

DNA motif analyses for CDS, 5'UTR and 3'UTR were performed on MEME suite (Bailey et al. 2009). The width of motif was set to 6-10 nucleotides. Obtained motifs with a P -value ≤ 0.001 were considered as significant outcomes.

3 Results

3.1 RNA profiling reveals translational activation during four stages of dehydration and rehydration cycle in *C. plantagineum*

Four samples (untreated, partial dehydrated, desiccated and rehydrated) representing critical physiological conditions during the dehydration/rehydration cycle of *C. plantagineum* were prepared for RNA sequencing. The relative water content of leaves for the four time points (C, M, D and R) were around 93%, 67%, 5% and 80%, respectively (Fig. 1b). The phenotypes of *C. plantagineum* plants subjected to the dehydration and rehydration cycle are shown in Fig. 1c. RNA profiles were determined by measuring the absorbance at 260 nm of RNAs extracted from the sucrose gradient fractions. The RNA absorbance profiles were determined based on both equal DW (Fig. 1d) and equal RNA level (Fig. 1e) in the samples. The RNA profiles changed significantly during the dehydration and rehydration cycle. In Fig. 1d, the RNA abundance in the desiccated stage was higher than in other stages based on the same dry weight of leaves. The desiccated sample had a higher amount of polysomal mRNA (RNA extracted from fractions 6-10) when equal RNA levels were considered. This reveals that mRNAs actively bind to polysomes in desiccated samples (Fig. 1e).

3.2 Polysomal profiling of *C. plantagineum* during the dehydration and rehydration cycle

To investigate the relations of transcription and the translation during the four stages of dehydration and rehydration in *C. plantagineum*, total mRNA (T) and polysomal mRNA (P) expression levels were analyzed by RNA sequencing. In total, 281,825,230 raw reads were generated. After removing low quality reads from raw data, 276,733,392 clean reads were generated for the samples used in this study. The data normalization had been done by using RPKM. The 11403 genes that passed the

noise filter ($\log_2\text{Exprs} > 4$) during the dehydration and rehydration cycle were used for further analysis. To confirm the RNA sequencing data, RT-qPCR had been performed with eight selected genes. The expression ratios measured by RT-qPCR correlated very well with the data from RNA sequencing (Fig. S1). The dissociation curves of eight selected genes showed the specificity of the RT-qPCR by amplifying a single amplicon (Fig. S2).

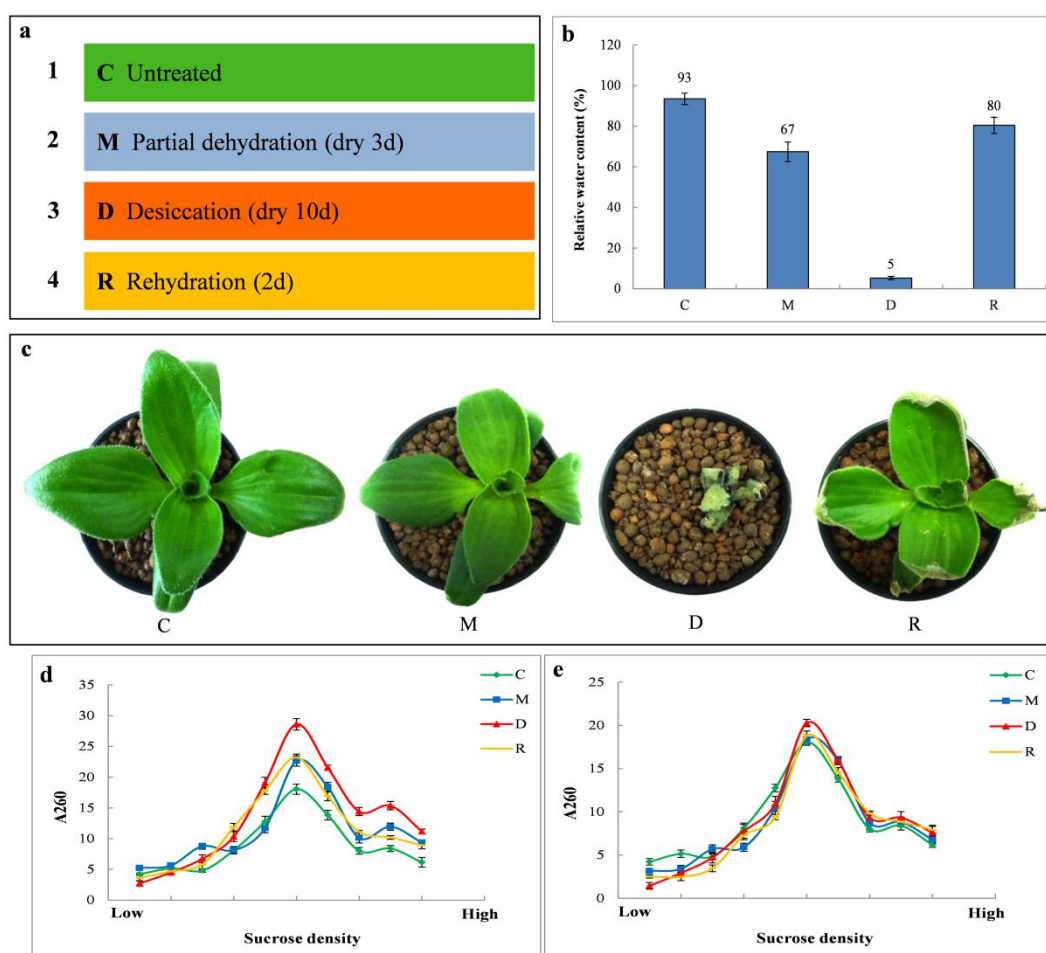


Fig.1 Polysome profiling during four stages of dehydration and rehydration. **(a)** The four samples used and time they have been treated (see details in Materials and methods). **(b)** Relative water content of *C. plantagineum* leaves in untreated (C), partial dehydration (M), desiccation (D) and rehydration (R) stages. Values in **(b)** were calculated from three independent biological replicates and five technical repetitions within each biological experiment (means \pm SE). **(c)** Phenotypes of *C. plantagineum* plants during four stages of dehydration and rehydration cycle. **(d)** Absorbance

profiles of fractionated RNAs (with 15-56% (w/v) continuous sucrose gradients) for the four time points during the dehydration and rehydration cycle according to equal dry weight. (e) Representative absorbance profiles of fractionated RNAs (with 15-56% (w/v) continuous sucrose gradients) for four stages of dehydration and rehydration cycle based on identical RNA loading. Values in (d) and (e) were calculated from five independent repetitions (means \pm SE).

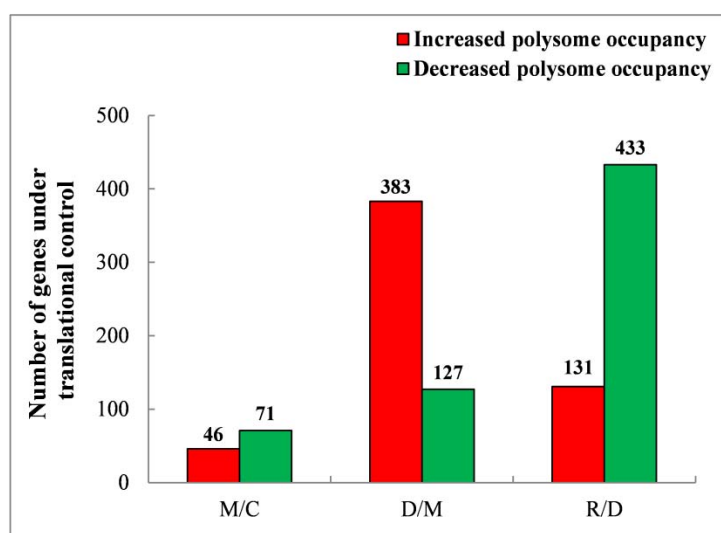


Fig. 2 Number of genes under translational control during four stages of dehydration and rehydration in *C. plantagineum*. The number of genes with changed polysome occupancy (means the ratio of polysomal mRNA level/total mRNA level) in different stages of dehydration and rehydration cycle in *C. plantagineum*. The M/C, D/M and R/D represent partially dehydrated samples (M) compared to untreated samples (C), desiccated samples (D) compared to partially dehydrated samples (M), and rehydrated samples (R) compared to dehydration samples, respectively.

By comparing the polysome occupancy between two consecutive time points, we found that there are two phases with extensive changes of translational control: from partial dehydration to desiccation (D/M group), and from desiccation to rehydration (R/D group) (Fig. 2). The polysome occupancy changes between every two samples with P -value < 0.05 and fold change > 2 were considered to be significant. In total 510 genes in the D/M group and 564 genes in the R/D group are under translational regulation. In the D/M group 383 genes were up-regulated and 127 genes were

down-regulated, while for the R/D group 131 genes were up-regulated and 433 genes were down-regulated (Fig. 2).

3.3 Dynamics of genes under translational regulation

The total mRNA abundance and polysomal mRNA abundance of the four time points are highlighted in correlation plots to show the transcriptional and translational dynamics of genes under translational regulation in the D/M and R/D group in *C. plantagineum* (Fig. 3). The correlation plots showed that the up-regulated genes under translational control in D/M group are weakly associated with polysomal of the untreated stage. From the M to the D phase, the polysomal association increased. The opposite pattern was observed for the down-regulated genes. The translationally up-regulated genes in the R/D group were less associated with polysomes in desiccated stage than other stages, but the level of polysome association was higher in the rehydrated stage compared to the desiccated stage. The down-regulated genes in the R/D group had a completely opposite trend.

In general, differential transcription, translation efficiency or the combination of both can cause the change of polysome occupancy. In Fig. 4, we compared these effects separately, thus different regulatory mechanisms emerged. In total, there are 22 subgroups with nine categories in the D/M group and R/D group which have been identified with their different regulation during dehydration and rehydration. The D/M up-regulated group primarily severely declines on the transcription level, while the D/M down-regulated group is mostly affected by a dramatic decrease on the polysomal level (Fig. 4). The sharp increase on the translation level influenced genes in the R/D up-regulated group. The opposite pattern was observed in the R/D down-regulated group (Fig. 4).

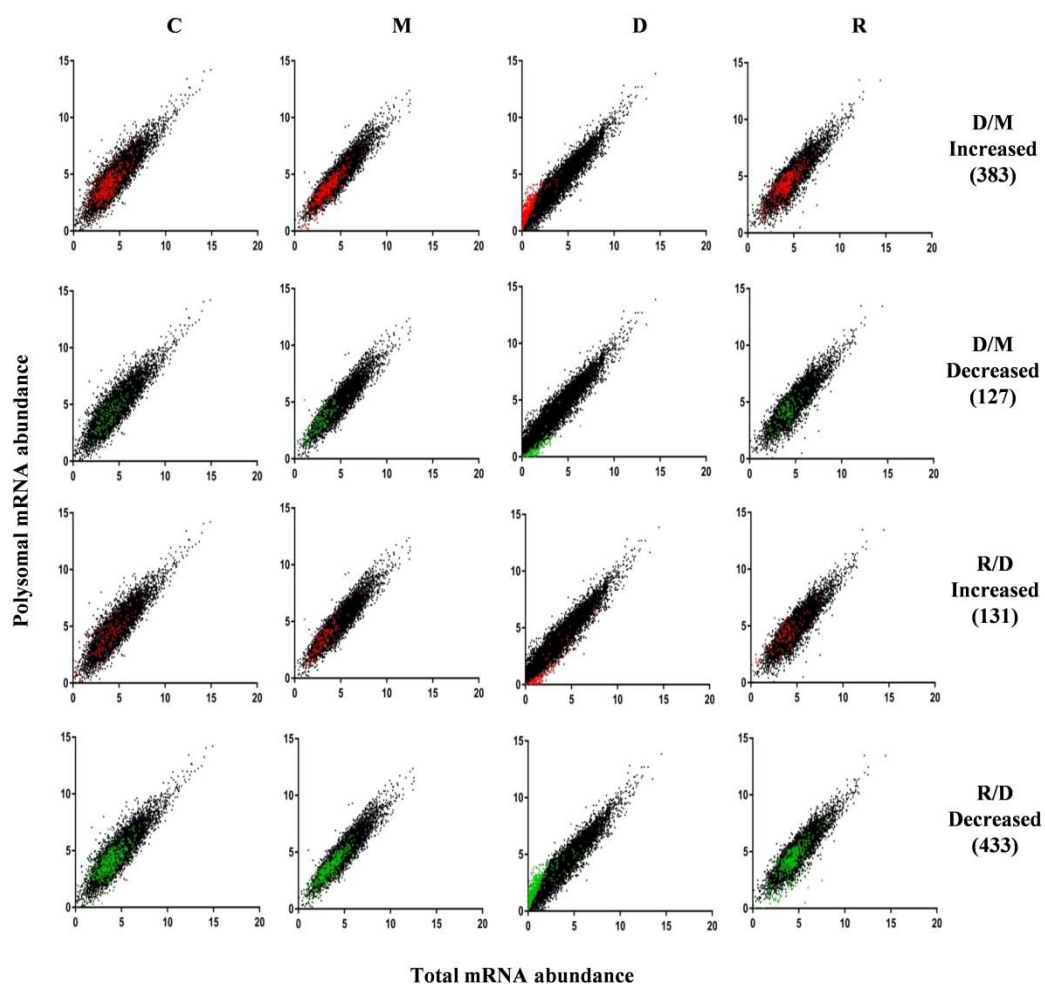


Fig. 3 Dynamics of genes under translational control in the D/M group and R/D group. The abundance of total mRNAs (x-axis) and polysomal mRNAs (y-axis) following the dehydration and rehydration cycle (C, M, D, R) are plotted as black dots. Genes with increased polysome occupancy are plotted as red dots and genes with decreased polysome occupancy are plotted as green dots in both the D/M group and the R/D group.

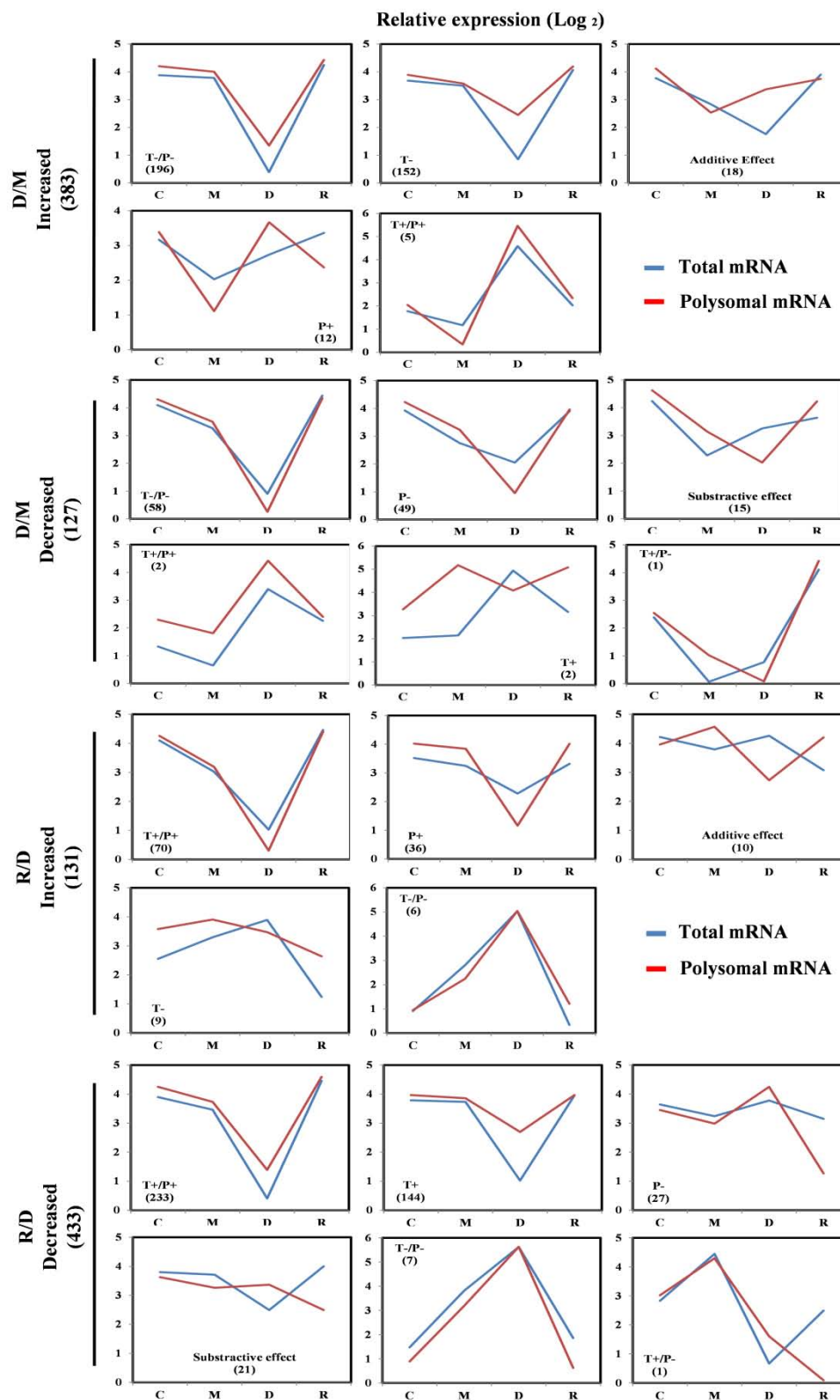


Fig. 4 The profiles of total mRNAs and polysomal mRNAs of genes under translational regulation during four stages of dehydration and rehydration in *C. plantagineum*. Based on the changes of total mRNA and polysomal mRNA abundance, genes in the D/M group and R/D group are divided

into different subgroups. In total, there are 22 subgroups in nine categories in the D/M group and R/D group which have been identified according to their expression profiles during dehydration and rehydration. T+ indicates significant increase in the total RNA abundance (unchanged polysomal RNA abundance). P+ refers to enhanced translation level (unchanged transcription level). T+/P+ represents increase of total RNA and polysomal RNA, and T+/P- represents increase of total RNA but decrease of polysomal RNA. The increase of polysome occupancy caused by the additive effect of the no significant change on either transcription level or translation level is termed additive effect. The subtractive effect represents the opposite effect. T-, P-, T-/P- represent decrease of total RNA, polysomal RNA or decrease of both total and polysomal RNA.

3.4 Sequence features correlate with translational regulation

To understand which sequence features could be important for translational regulation in *C. plantagineum*, the CDS length, GC content, GC3 content and effective codon numbers (*Nc*) of genes under translational control were investigated in the D/M group and R/D group (Fig. 5). Transcripts in the R/D up-regulated group had a significant shorter CDS length compared with the R/D down-regulated gene set. However, the opposite pattern was observed in the D/M group (Fig. 5a). Significantly lower GC contents were identified in the D/M up-regulated group and the R/D down-regulated, which correlates with increased translation (Fig. 5b). Intriguingly, the D/M up-regulated group had a lower GC3 content and a higher *Nc* than the D/M down-regulated group, while the R/D group had the opposite characteristics (Fig. 5c, d).

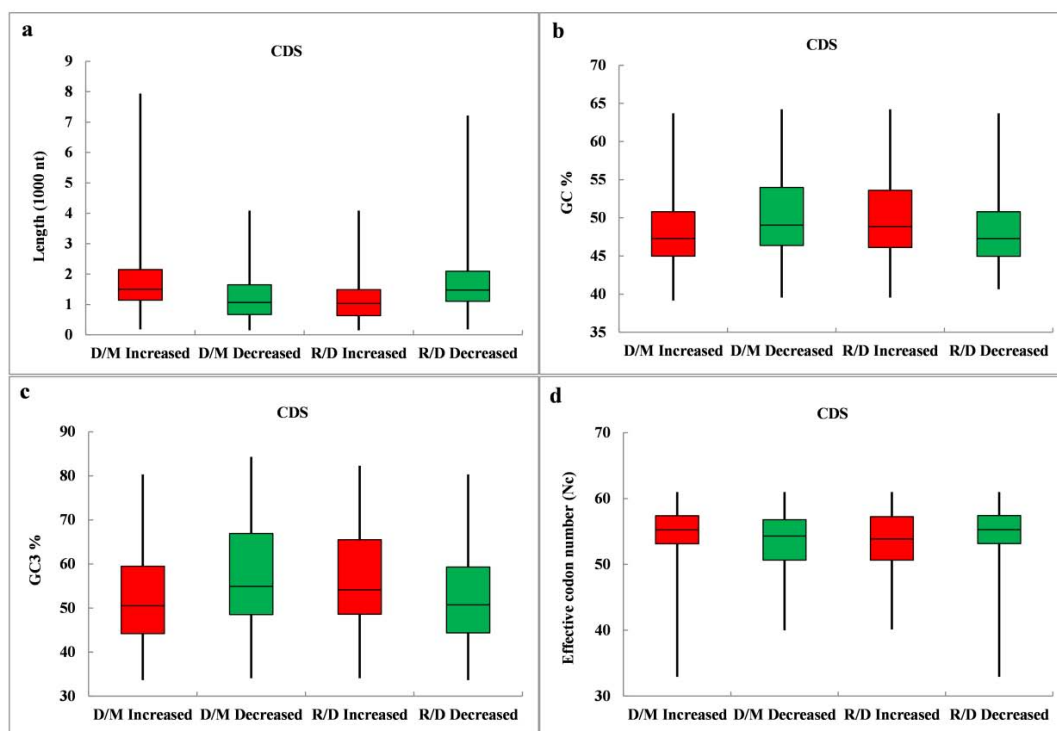


Fig. 5 Coding DNA sequence features of genes under translational control in the D/M group and R/D group. The length (a), GC content (b), GC3 content (c) and effective codon number (N_c) (d) of the CDSs are shown. The red bar represents genes with increased polysome occupancy and the green bar represents genes with decreased polysome occupancy.

We analyzed GC content in the 5'UTR and 3'UTR (50 nt, 100 nt and 200 nt) of genes in the D/M group and R/D group (Fig. 6). The D/M up-regulated group had a lower GC content in the 50 nt region upstream of the ATG start codon than the 100 nt and 200 nt region (Fig. 6a). A significantly higher GC content has been observed in the 200 nt region downstream of the stop codon compared with the 50 nt and 100 nt region (Fig. 6b). The GC content in the D/M up-regulated group (both 5'UTR and 3'UTR) correlates positively with PO changes in the 50 nt and 100nt region (Fig. 6c, d, e, f).

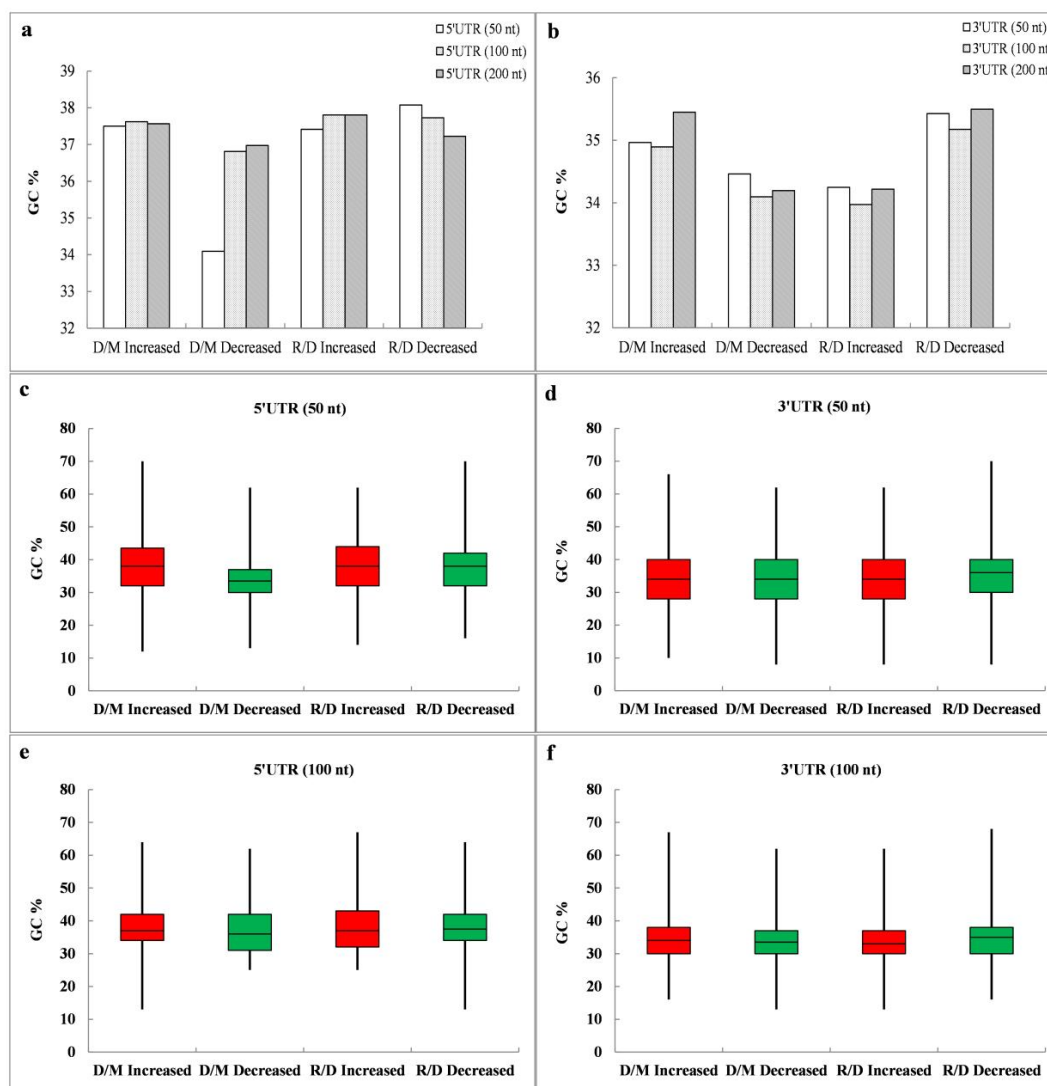


Fig. 6 Sequence features of the untranslated regions of translationally regulated genes in the D/M and R/D group. (a) Average GC content of the 5'UTR (50nt, 100nt and 200nt). (b) Average GC content of 3'UTR (50nt, 100nt and 200nt). The box-graphs show GC content in 50nt 5' UTR (c), GC content in 50nt 3'UTR (d), GC content in 100nt 5'UTR (e) and GC content in 100nt 3'UTR (f), respectively. The red bar represents genes with increased polysome occupancy and the green bar represents genes with decreased polysome occupancy.

A motif analysis of three regions (5'UTR, CDS and 3'UTR) in the D/M group and R/D group revealed four significantly enriched motifs (Fig. 7). The GA (purine) enriched motifs (GAAGAAGA) in the CDS in D/M up-regulated group and R/D up-regulated group were similar to the motif (GAAGAAGAAG) found in *A. thaliana*

(Bai et al. 2017) (Fig. 7a). The motifs (AAGAAA) enriched in 5'UTR region were mainly localized in 100 nt region upstream of the start codon (Fig. 7b).





a		Number of genes with motif	
CDS	Motif logo	D/M Increased (383)	P-value
		271	1.30E-30
	Motif logo	R/D Increased (131)	P-value
		83	8.80E-16
b		Number of genes with motif	
5'UTR (100 nt)	Motif logo	R/D Decreased (433)	P-value
		226	6.10E-07
	Motif logo	D/M Increased (383)	P-value
		172	2.10E-10

Fig. 7 Motif features of genes under translational control in the D/M and R/D group. Significantly enriched motifs are detected from (a) full length DNA coding sequences in the D/M up-regulated group and R/D up-regulated group and (b) 100nt 5'UTRs in the R/D down-regulated group and D/M up-regulated group. *P*-values are calculated by Fisher's exact test.

3.5 GO term and pathway enrichment analyses of genes under translational regulation in D/M group and R/D group

GO term analysis was performed for genes under translational control in the D/M and R/D group. The enriched biological process GO terms included developmental processes, signal transduction, response to abiotic or biotic stimulus, and electron

transport or energy pathways, etc. (Fig. 8). For molecular function GO terms, kinase activity, transcription factor activity, protein binding and transferase activity were enriched (Fig. 8). The enriched cellular components GO terms included plasma membrane, cell wall, Golgi apparatus, cytosol and ribosome, etc. (Fig. 8).

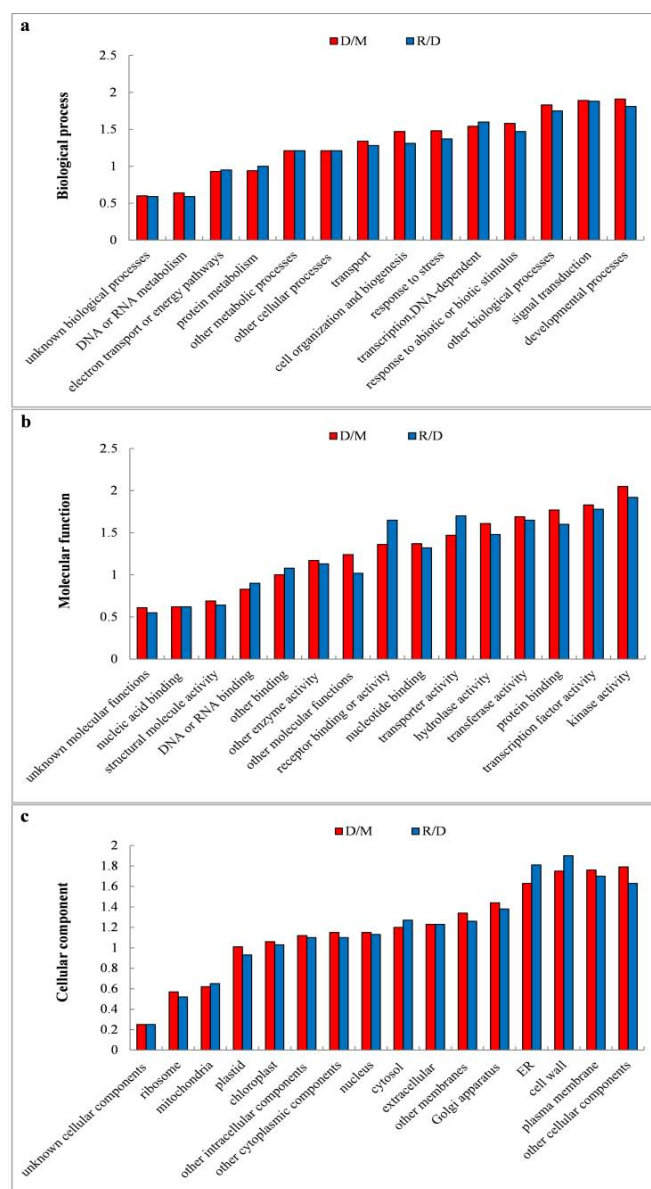


Fig. 8 GO term enrichment analysis of genes under translational regulation in the D/M and R/D group. Differentially expressed genes (\log_2 fold change > 1 and $P < 0.05$) with putative annotation to Arabidopsis were used for GO term analysis. Polysome occupancy was used as the classification source. The red bar represents the D/M group while the blue bar indicates the R/D group.

Pathway enrichment analysis showed that two MapMAN pathways, including major carbohydrate (CHO) metabolism and cell wall were enriched both in the D/M and R/D group. The D/M group specifically involved the polyamine metabolism pathway, while the R/D group affected the minor CHO metabolism, lipid metabolism and hormone metabolism (Table 1).

MapMAN pathway	Polysome occupancy(D/M)		Polysome occupancy(R/D)	
	NF	<i>P-value</i>	NF	<i>P-value</i>
polyamine metabolism	9.29	0.0180	-	-
minor CHO metabolism	-	-	2.75	0.0260
major CHO metabolism	4.41	0.0020	2.7	0.0450
cell wall	3.12	0.0000	2.61	0.0000
lipid metabolism	1.9	0.0180	2.06	0.0066
signalling	1.85	0.0002	1.85	0.0001
hormone metabolism	1.78	0.0170	2.27	0.0007
transport	1.6	0.0096	1.67	0.0042
RNA	1.58	0.0000	1.56	0.0000
cell	1.52	0.0250	1.48	0.0270
development	-	-	1.38	0.0460
stress	1.33	0.0370	-	-
not assigned	0.79	0.0001	0.74	0.0000
protein	0.64	0.0002	0.84	0.0200
DNA	0.21	0.0000	0.17	0.0000

Differentially expressed transcripts with putative annotation to *A. thaliana* were used for analysis. MapMAN was used as the classification source. The detailed scales are as following: >2.0 1.5-2.0 1.0-1.5 0.7-1.0 <0.7

Table 1 MapMan pathway enrichment analysis of genes under translational regulation in the D/M and R/D group.

3.6 Regulation overview of genes under translational control

To visualize metabolic pathways in more detail, genes in the D/M group and R/D group were analyzed using MapMAN software. Totally 132 and 156 differentially expressed genes are involved in D/M group and R/D group, respectively (Fig. 9). Genes primarily enriched for regulation fall into six subgroups including transcription factor, protein modification, protein degradation, receptor kinases, enzymes involved in IAA metabolism and calcium regulation subunit. Among them, 112 genes are up-regulated and 20 genes are down-regulated in the D/M group (Fig. 9a), while in the R/D group 38 genes are up-regulated and 118 genes are down-regulated (Fig. 9b).

3.7 Transcription factors in D/M group and R/D group

Based on the overview of the regulatory pathways, some transcription factors were identified which are under translational control in the D/M group and R/D group. According to the annotation of *A. thaliana*, 30 and 10 transcription factors up-regulated in D/M and R/D group, and 12 and 39 transcription factors down-regulated in D/M and R/D group, respectively (Fig. 10a). The pie graphs show the different transcription factor families and gene numbers in each family (Fig. 10b, c). The zinc finger, WRKY, ARF, TCP and others are the top five up-regulated transcription factor families in the D/M group (Fig. 10b). For the R/D group, 5 zinc finger transcription factors are up-regulated while 10 zinc finger, 5 bHLH, 4 ARF, 3 AP2\ERF and 3 TCP transcription factors are down-regulated (Fig. 10c). Heat maps show the relative polysome occupancy level of up-regulated transcription factors in the D/M group and R/D group during the four stages of dehydration and rehydration in *C. plantagineum* (Fig. 11a, b).

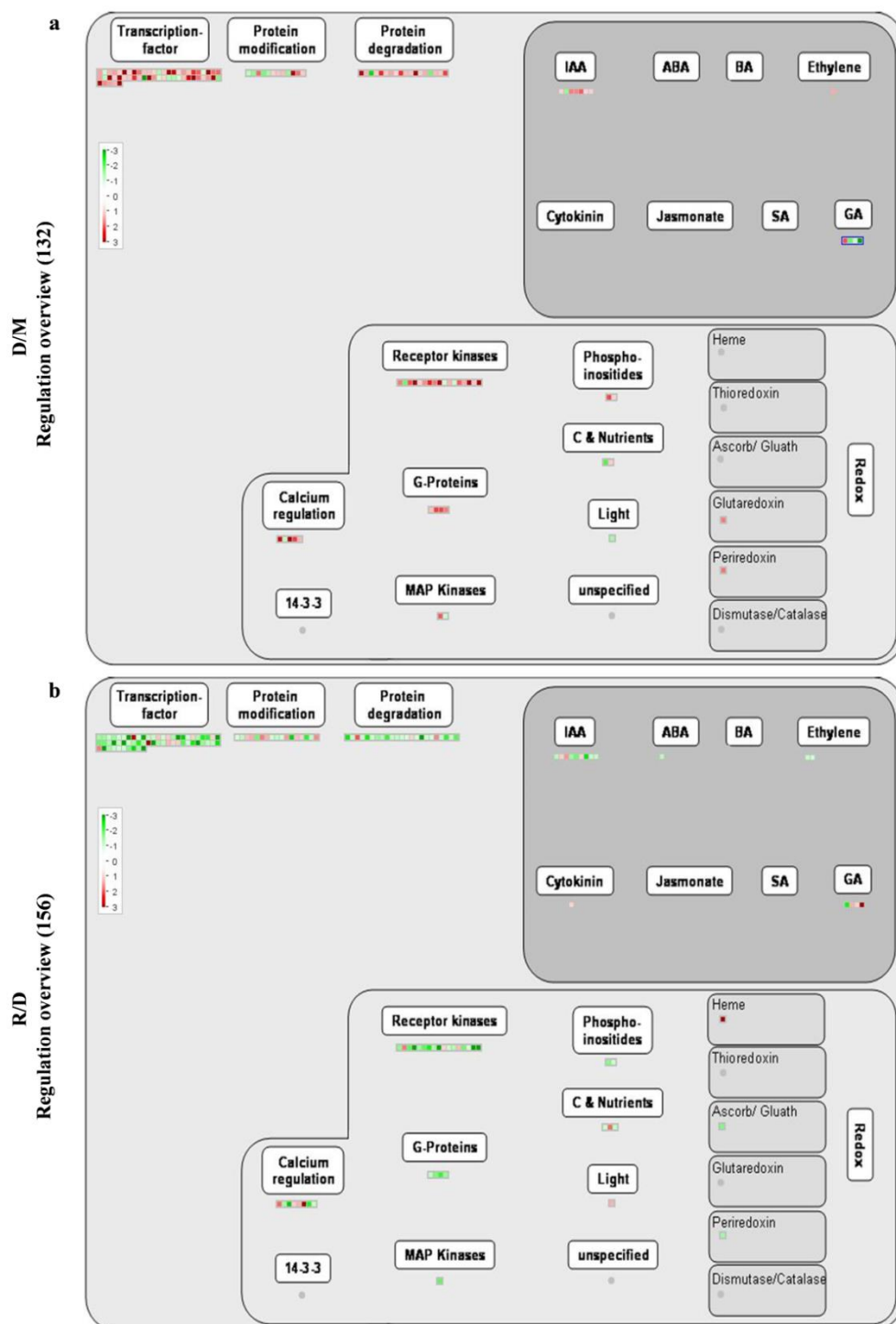


Fig. 9 Overview of genes under translational regulation in the D/M group and R/D group. The overview was generated using MapMAN software (Version 3. 6.0RC1). Totally 132 genes (a) and 156 genes (b) are involved in the regulation overview in the D/M group and R/D group, respectively. Each square indicates a specific gene. Red color represents up-regulation and green color represents down-regulation.

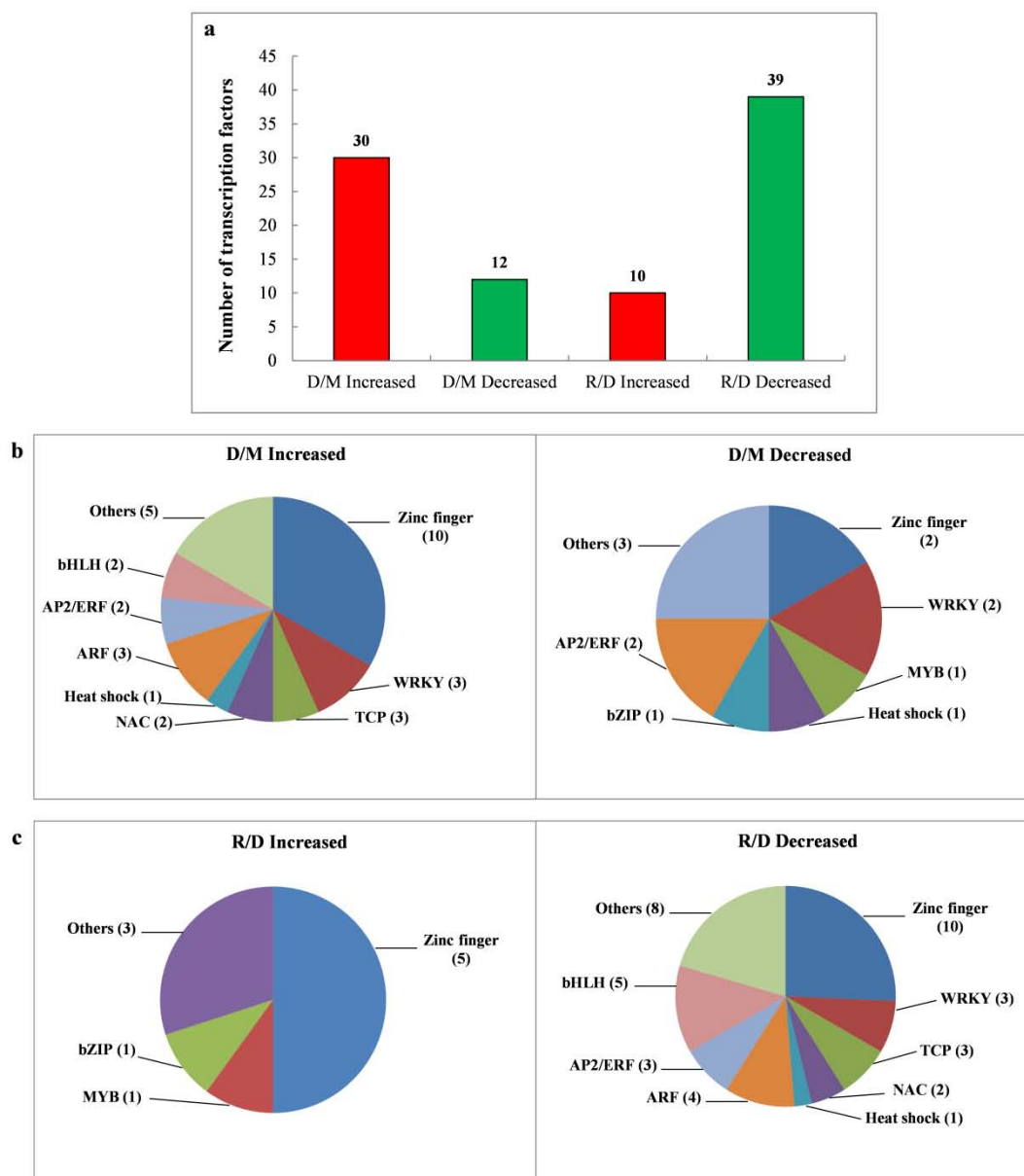


Fig. 10 The transcription factor gene families in the D/M group and R/D group. **(a)** Number of transcription factors under translational control in the D/M group and the R/D group. The red bar means increased polysome occupancy and green bar means decreased polysome occupancy. The up-regulated and down-regulated transcription factor gene families (gene numbers are shown in the brackets) in the D/M group **(b)** and R/D group **(c)** were identified using annotations from *A. thaliana*.

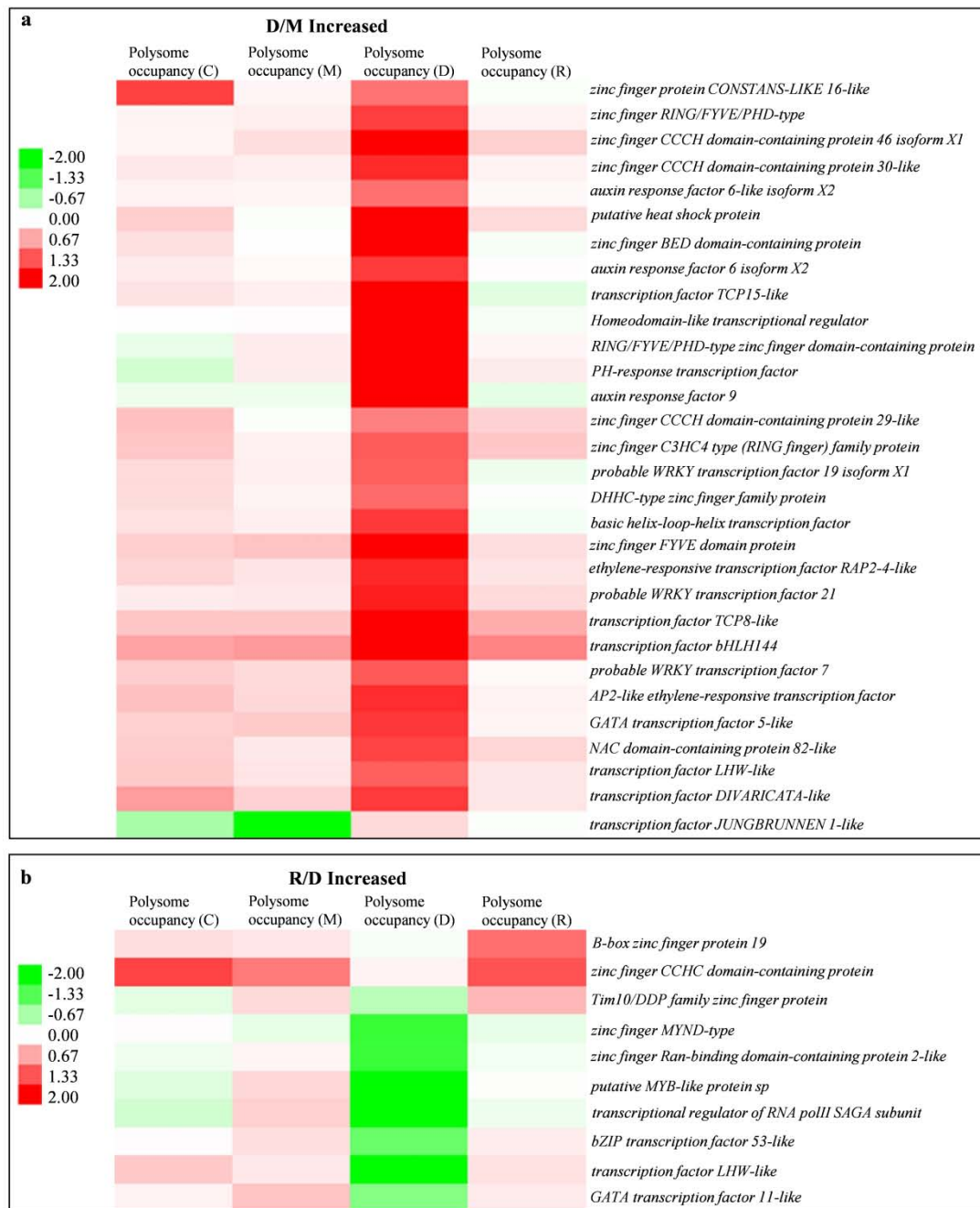


Fig. 11 The polysome occupancy pattern of the transcription factors in the D/M group and R/D group during four stages of dehydration and rehydration in *C. plantagineum*. **(a)** The polysome occupancy levels of the transcription factors with increased PO from partial dehydration to desiccation. **(b)** The polysome occupancy pattern of the transcription factors with increased PO from desiccation to rehydration. The heat map was obtained using Cluster 3.0 software and Java Treeview. The color bar is shown as \log_2 fold change.

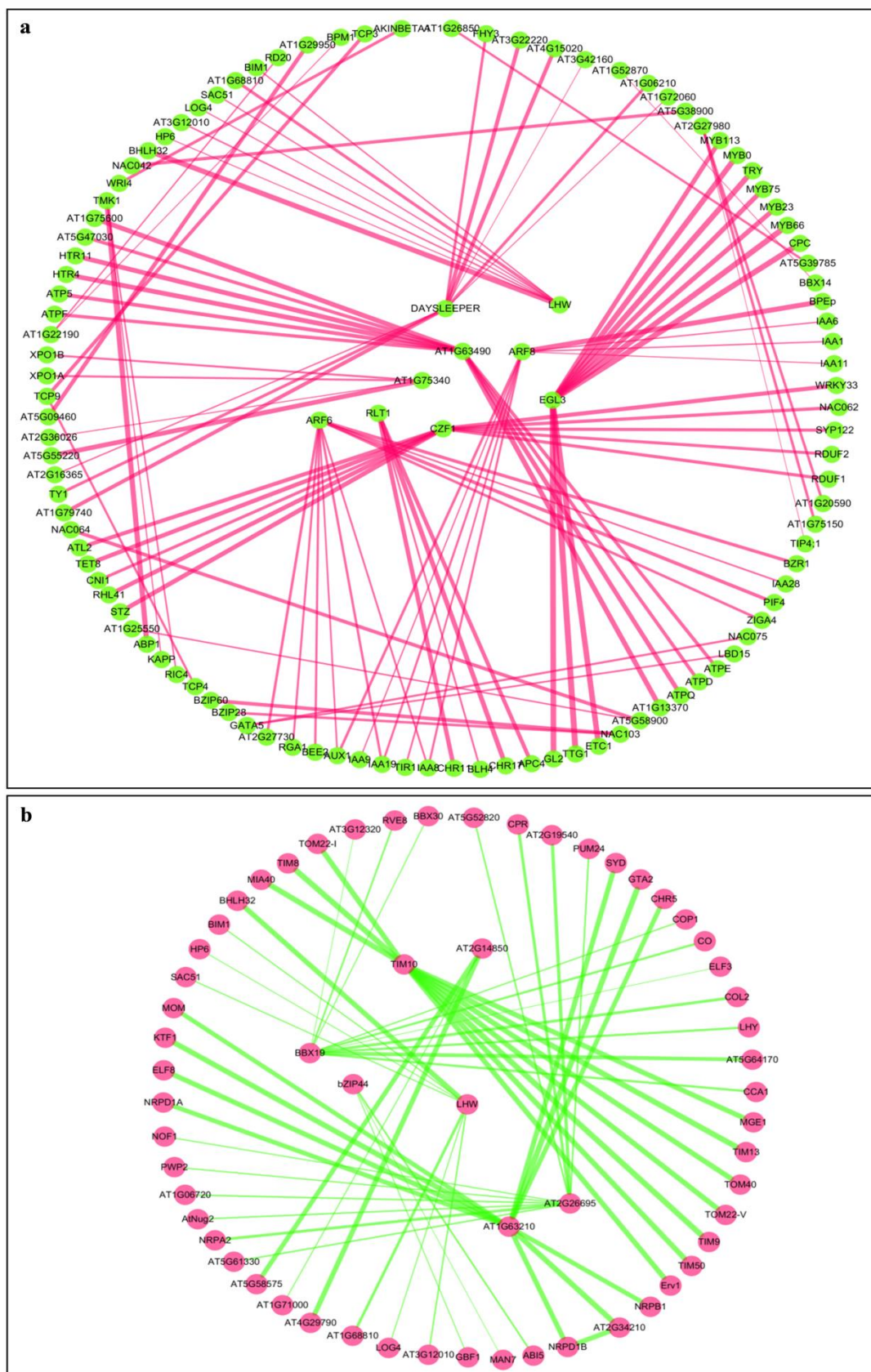


Fig. 12 Interaction network analyses of transcription factors under translational control in the D/M group and R/D group. Networks of transcription factors (**a**) up-regulated in the D/M group (green

node and red edge) and **(b)** up-regulated in R/D group (red node and green edge), respectively. The combined interaction score is indicated by the width of the edge. The annotation of genes in the interaction network can be found in STRING database (<https://string-db.org/>).

To investigate the effect of transcription factors in the D/M group and R/D group during the four stages of dehydration and rehydration in *C. plantagineum*, possible interaction networks were constructed using STRING and Cytoscape software (Fig. 12). Interaction network analysis revealed that 112 nodes and 94 edges were observed for up-regulated transcription factors in the D/M group (Fig. 12a), and 60 nodes and 54 edges for up-regulated transcription factors in the R/D group (Fig. 12b). The results showed that ENHANCER OF GLABRA 3 (EGL3) as a transcription activator interacted with several MYB or MYB-type transcription factors in the D/M up-regulated group. The ARF6 and ARF8 interacted with several indole-3-acetic acid inducible proteins (including IAA 1, IAA 6, IAA 8, IAA 9, IAA 11, IAA 19, and IAA 28) which participated in early auxin response (Guilfoyle and Hagen 2007). In the R/D up-regulated group, transcription factor bZIP44 interacted with ABA insensitive 5 (ABI5), which is involved in ABA signaling (Chang et al. 2019). LONESOME HIGHWAY (LHW) from R/D up-regulated group interacted with histidine phosphotransfer protein 6 (HP6), which acts as a negative regulator in cytokinin signaling (Besnard et al. 2014).

4 Discussion

As a resurrection plant, *C. plantagineum* can survive under extreme dehydrated environmental conditions (Bartels and Hussain 2011). Previous researches reported that early responses to dehydration are often studied in plants dehydrated to 60 % RWC and late responses are analyzed in plants dehydrated to 2 % RWC (1-2 weeks of dehydration). These are crucial physiological stages (Rodriguez et al. 2010; Giarola and Bartels 2015). In this work, the untreated, partially dehydrated (dry 3d, RWC 67%), desiccated (dry 10d, RWC 5%) and rehydrated (re-water 2d, RWC 80%) stages had been chosen to study gene expression profiles (Fig. 1a, b). The leaves of *C. plantagineum* shrank and folded during dehydration, expanded and unfolded after being re-watered (Fig. 1c). Extensive reversible shrinkage of leaves and folding as observed in resurrection plants *C. wilmsii*, *Xerophyta humilis* and *Myrothamnus flabellifolius* is hypothesized to preserve cellular integrity, shade chlorophyll and reduce formation of reactive oxygen species (Farrant 2000; Farrant et al. 2003, 2007).

The abundance of polysomal mRNA may provide a more accurate estimate of gene expression than the abundance of total mRNA, because this takes translational regulation into account (Kawaguchi et al. 2004). To identify genes affected by dehydration and rehydration in *C. plantagineum*, polysomal mRNAs of leaf samples were isolated using sucrose gradient-based fractionation and quantified by RNA sequencing. It has been reported that desiccation tolerant plants (*C. plantagineum* and *Lindernia brevidens*) have higher efficiency for recruiting mRNAs to ribosomes than the desiccation sensitive species (*Lindernia subracemosa*) (Juszczak and Bartels 2017). In *C. plantagineum*, the polysomal mRNA abundance in desiccated leaf tissues was higher than that in untreated tissues, which demonstrates that mRNA actively binds to polysomes during desiccation (Fig. 1d, e). It is known from yeast that mutations in the translation initiation factor binding sites of mRNAs can affect the stability of mRNA, and binding of these translation initiation factors to mRNA can enhance translation efficiency and protect mRNA from degradation (Schwartz and

Parker 1999; Brown et al. 2000; Huch and Nissan 2014). It was reported that mRNA binding to polysomes increases the stability of mRNA and prevents it from degradation in resurrection plants (Juszczak and Bartels 2017). Our data showed 383 genes with increased polysome occupancy in the D/M group, which means that the amount of polysomal mRNA of these genes is higher than total mRNA from partial dehydration to desiccation (Fig. 2). During the rehydration stage, the polysome occupancy of 433 genes decreased while 131 genes had increased polysome occupancy (Fig. 2). This shows that binding of mRNAs to polysomes might protect mRNA from degradation caused by dehydration while during the rehydration stage the protection mechanism is diminished.

The correlation plots showed that the transcriptional and translational dynamics of genes during the dehydration and rehydration, and revealed the key stages of the mRNA binding to polysomes (Fig. 3). This system has been successfully applied to investigate the translational regulation during seed germination in *A. thaliana* (Bai et al. 2017). In *C. plantagineum*, the 22 subgroups in the D/M group and R/D group explained the internal reasons for polysome occupancy changes (Fig. 4). It uncovered that the total mRNA and polysomal mRNA in the D/M up-regulated group mostly decreased, but the extent of the decline of total mRNA was larger than that of polysomal mRNA which caused the increased polysome occupancy (Fig. 4). This indicates that mRNA abundance decreased and the existing mRNAs are more likely to bind to polysomes which might contribute to desiccation tolerance. On the contrary, the abundance of total mRNA and polysomal mRNA increased in the R/D down-regulated group of transcripts and the extent of total mRNA increased more than the polysomal mRNA (Fig. 4). The reason for this phenomenon might be that after re-watering more genes are involved in transcriptional control for the recovery or mRNAs which were bound to polysomes during desiccation have been translated and the proteins are involved in the recovery. Experiments performed in *C. wilmsii* showed rapidly dried plants do not survive if mRNA or protein synthesis is inhibited during rehydration, which demonstrates that mRNAs are stored during dehydration

(Cooper and Farrant 2012).

The sequence features (transcript length, GC content, GC3 content, N_c and enriched motifs) correlated with translational regulation had been investigated in the D/M and R/D group (Fig. 5, 6, 7). It is reported that the translation rate and the translational ratio increased with decreasing mRNA length and decreasing GC content (Valleriani et al. 2011; Qu et al. 2011). The effective number of codons shows codon bias, varying from 20-61 (Hershberg and Petrov 2008, 2009). It has been reported for several species that the translation efficiency is also affected by N_c (Akashi 1994; Duret 2000; Bai et al. 2017). Codon bias is affected by the third base position of a codon and the GC content in this position (GC3) (Crick 1966). Interestingly, in the R/D group, the reduction of the CDS length, N_c and 3'UTR GC content correlated with the up-regulation of translation, while the decrease of the CDS GC content is positively related to the translational up-regulation in the D/M group (Fig. 5, 6). The GA enriched (GAAGAAGA) motif in the D/M group and R/D group is similar to the motif (GAAGAAGAAG) found in *A. thaliana* by Bai et al. (2017), which might play a role in alternative splicing events (Thomas et al. 2012).

GO terms including signal transduction, kinase activity, transcription factor activity, cell wall and ribosome were enriched in the D/M and R/D group (Fig. 8). Pathway analysis results showed that major CHO metabolism, cell wall, signaling, lipid metabolism and hormone metabolism were over-represented in the D/M and R/D group (Table 1). These results indicate that the mRNAs related to these pathways are under translational regulation during dehydration and rehydration which might activate the downstream stress response or protect the plant through accumulating of protective proteins and metabolites. Transcripts encoding enzymes related to carbohydrate metabolism, such as sucrose phosphate synthases and sucrose synthases, are up-regulated during dehydration (Whittaker et al. 2007; Gechev et al. 2013; Ma et al. 2015). As the predominant protective sugar in resurrection plants, sucrose rapidly accumulates upon dehydration through different pathways (Challabathula and Bartels

2013; Yobi et al. 2017).

Transcription factors functioning for plant adaptation to dehydration have been investigated in different plant species, such as *A. thaliana*, *Boea hygrometrica* and *Pyrus betulaefolia* (Wang et al. 2009; Sato et al. 2018; Liu et al. 2019a). Transcription factors were enriched in the D/M and R/D group (Fig. 9). We identified several transcription factor gene families, such as zinc finger, WRKY, NAC and ARF, which are regulated on the translational level during dehydration and rehydration in *C. plantagineum* (Fig. 10, 11). The WRKY and zinc finger gene families have been suggested to play important roles in the regulation of transcriptional reprogramming associated with plant stress responses (Chen et al. 2012b; Perrella et al. 2018). The polysome occupancy patterns and the interaction networks of the transcription factors in Fig. 11 and Fig. 12 provide a basis for further research.

Overall, our data demonstrate changes of regulation of mRNA expression on the translational level during dehydration and rehydration in *C. plantagineum*. The extensive translational regulation and the changes from partial dehydration to desiccation and from desiccation to rehydration are controlled by different mechanisms. The identified sequence features uncover independent regulation mechanisms of translation during dehydration and rehydration in *C. plantagineum*. The discovered genes and their interaction networks, and the related metabolic pathways may help to design a strategy to produce dehydration tolerant crops. However, these analyses are completely dependent on the RNA-seq data, so more proofs are needed for further confirm the findings reported here.

Acknowledgements

The author would like to thank Dr. Valentio Giarola (former member of IMBIO, University of Bonn), Dr. Sylvain Legay and colleagues (Research and Innovation Department, Luxembourg Institute of Science and Technology) for supporting the RNA-seq data analysis.

Supporting data

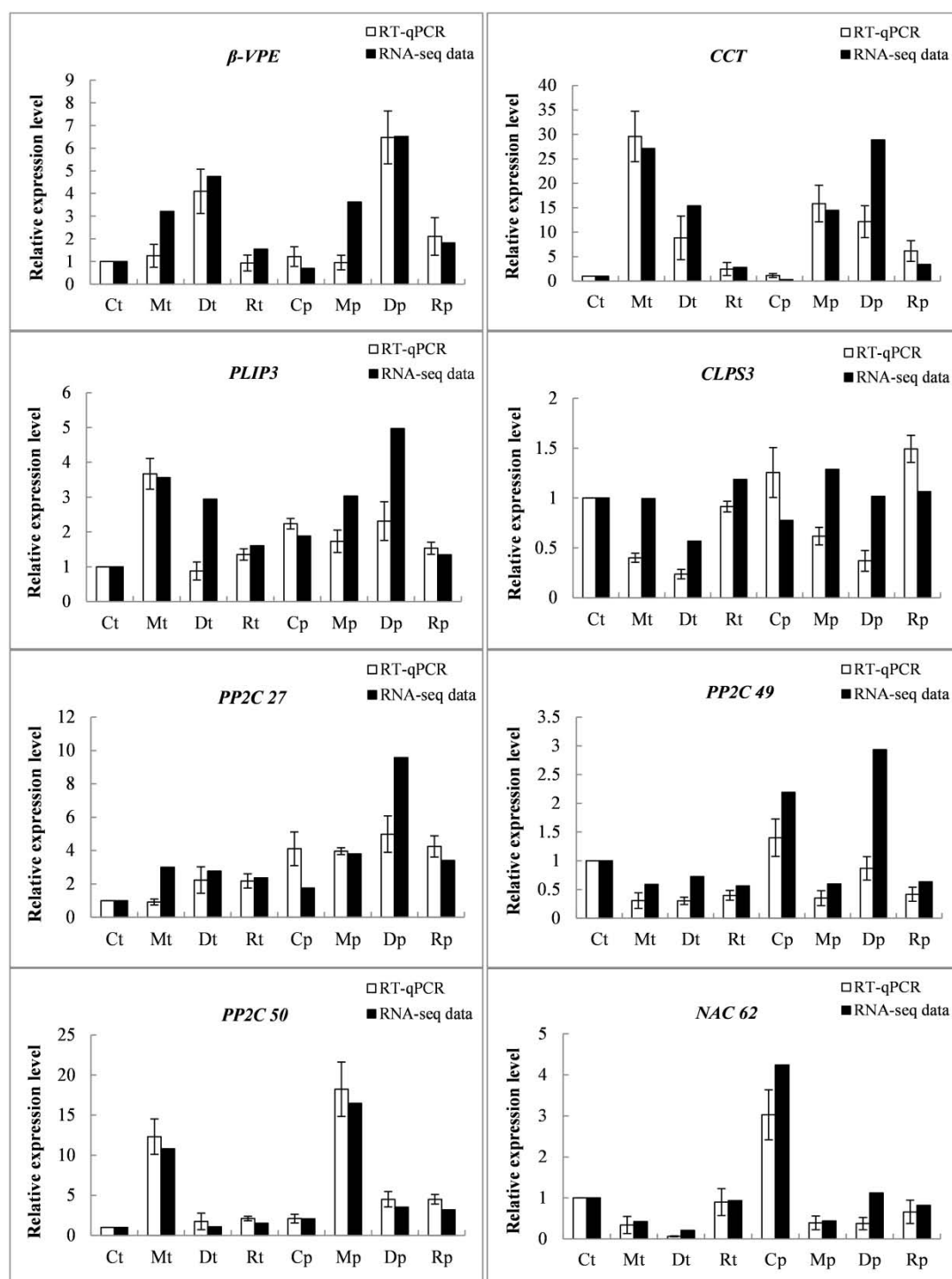


Fig. S1 The relative expression level of eight chosen genes during four stages of dehydration and rehydration cycle in *C. plantagineum*. The white bar represents the data from RT-qPCR while the dark bar shows the data from RNA sequencing.

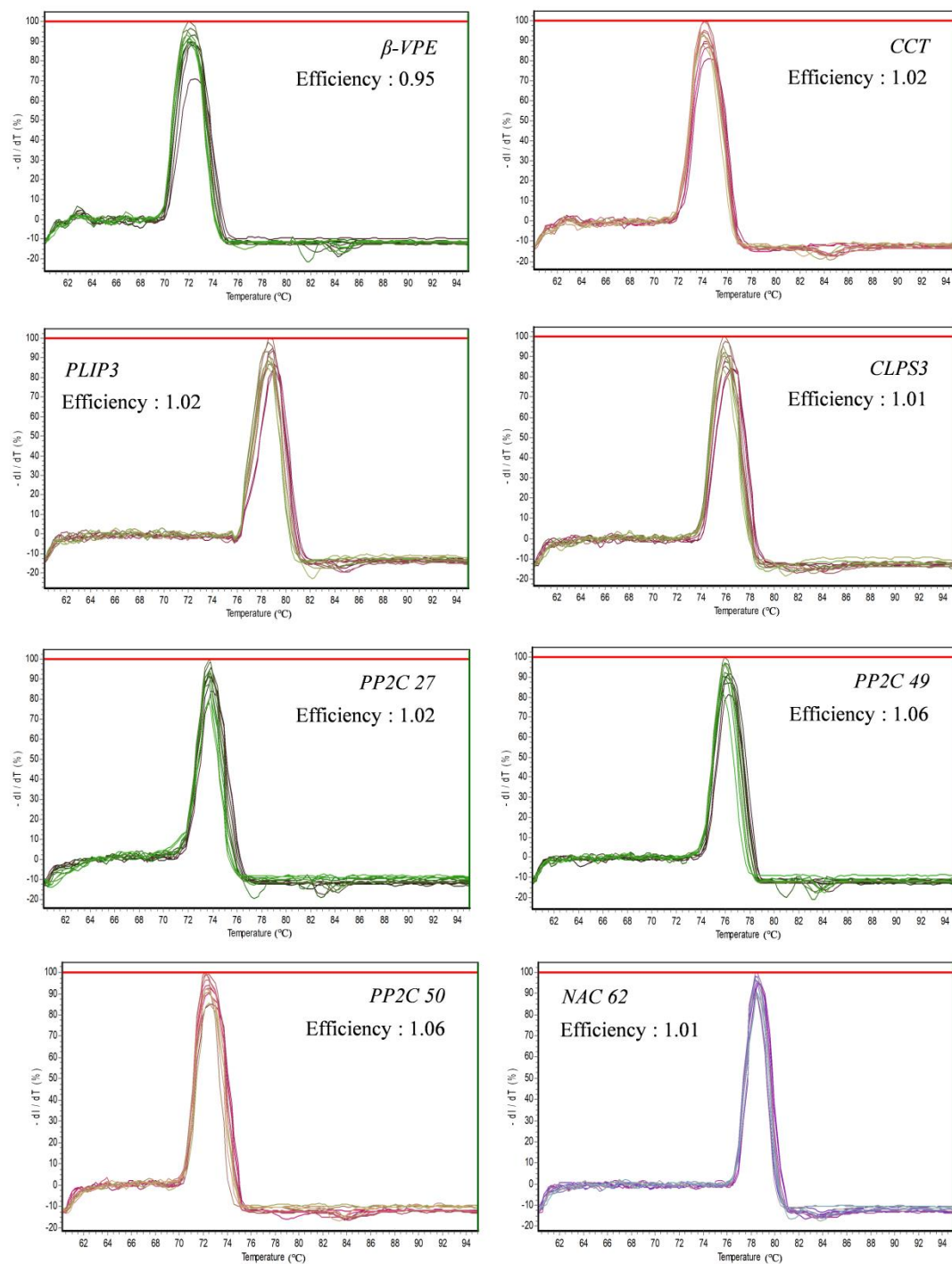


Fig. S2 The dissociation curves of eight chose genes derived from three biological replicates and three technical replicates within each biological experiment showing the specificity of the RT-qPCR by amplifying a single amplicon.

Table S1 The primer sequences of candidate genes and reference genes and amplicon characteristics.

Gene	Description	Primer sequence	Amplicon length (bp)	Amplicon T _m (°C)	Amplific. Efficiency (%)	R ²
β-VPE	vacuolar-processing enzyme beta-isozyme	Forward: CAGTGCATAGTAATACGATAAACCTC Reverse: AGCAAAAAGGCTTCGCMAAC	93	72.1	95	0.999
CCT	phosphorylcholine cytidyltransferase	Forward: TGTGAGTATATACGTTCCAGCCAAG Reverse: CGCTTTCACAACAACCTACACAGAG	77	74.2	102	0.999
PLIP3	plastid lipase 3	Forward: TTGGCGCTTTAGTTGCTTCT Reverse: CCAGCCCAAGCAATTAACCTA	78	78.8	102	0.999
CLPS3	CLP-similar protein 3	Forward: AGCCTCACGTGGTATGAACC Reverse: TGGTACATGGGTTCTGTGAACC	83	76.1	101	0.999
PP2C 27	probable protein phosphatase 2C 27	Forward: GCAGGGGAAAAGTGGAGTTC Reverse: TCAACCCAAAGTTAAAAGAGAAGA	118	73.9	102	0.998
PP2C 49	probable protein phosphatase 2C 49	Forward: TGCTGAAGCTTTTGGCAGTC Reverse: ACGGGGGTTAAACAAAAACT	100	76.1	106	0.997
PP2C 50	probable protein phosphatase 2C 50	Forward: TGAAAACCCACAGAAAAGTTCA Reverse: CAGCCAAAGCAAAAGCAAAAAT	98	72.4	106	0.995
NAC 62	NAC domain-containing protein 62	Forward: GCCTATTCGATTTGGAGCAGAG Reverse: TCGAATTTCTCCAGCAITCTT	99	78.6	101	0.999
EF1a	Elongation factor 1-alpha	Forward: TCGTATCTGCTTTTGGCATTGAGT Reverse: ACGAACAGCAAGCACTCACA	70	76.5	100	0.998
GAPDH	Glyceraldehyde-3-phosphate dehydrogenase	Forward: GGCCTTGATTCGGATCTTCT Reverse: AGCCCAAAATATATCAAGAACTCA	94	75.0	97	0.999

CHAPTER 4

Identification and characterization of CTP:phosphocholine cytidyltransferase CpCCT1 in the resurrection plant *Craterostigma plantagineum*

Xun Liu

Institute of Molecular Physiology and Biotechnology of Plants (IMBIO), University of Bonn,
Kirschallee 1, 53115 Bonn, Germany

Abstract

CTP:phosphocholine cytidyltransferase (CCT) is an important regulatory enzyme in the CDP-choline pathway for *de novo* phosphatidylcholine (PC) synthesis in plants. Here, we cloned the *CpCCT1* gene from the resurrection plant *C. plantagineum* and compared the putative amino acid sequence with the desiccation sensitive plant (*Arabidopsis thaliana*), an animal homolog (*Rattus norvegicus*) and a yeast homolog (*Saccharomyces cerevisiae*). CCTs have a conserved catalytic domain and membrane-binding domain while the N-terminal and C-terminal domains have diverged. The tissue specific expression analysis indicated that *CpCCT1* is expressed in all tissues and it is induced by dehydration. After treatment with 0.5 M NaCl solution, the expression of CpCCT1 was increased both on the transcriptional and translational level in leaves and roots of *C. plantagineum*. Intriguingly, cold stress failed to induce CpCCT1 protein expression although the transcript was increased after treated in 4 °C for 4 h. *CpCCT1* expression in leaf and root samples did increase in response to mannitol and sorbitol treatment, and higher concentrations induced higher amounts of transcript and proteins. Expression of *CpCCT1* transcript in leaves and roots was also increased by treatments with exogenous 100 μM abscisic acid (ABA) and 1 μM indole-3-acetic acid (IAA), whereas no CpCCT1 proteins accumulated during treatments with these hormones. Analysis of promoter activity revealed that *CpCCT1* gene expression is mainly under translational regulation during dehydration. In summary, the characteristics described here could be general features of CCT gene expression in resurrection plants.

1 Introduction

Phosphatidylcholine (PC) is the major phospholipid found in membranes of plant cells except for chloroplastic membranes. Usually it constitutes about 50% of the total phospholipid content of such membranes (Harwood 1988). PC acts as a substrate in desaturation reactions, oil body formation, triacylglycerol (TAG) biosynthesis, and the production of secondary messengers such as diacylglycerol (DAG) and phosphatidic acid (PA) (Ohlrogge and Browse 1995; Gibellini and Smith 2010). This gives PC a central role in response to environment changes and an important starting of the product for the synthesis of other lipids (Harwood and Moore 1989; Jones et al. 1998).

There are two major pathways for *de novo* PC synthesis in eukaryotes, the methylation of phosphatidylethanolamine (PE) and the CDP-choline pathway (Kent 1997; Vance and Vance 2004). In metazoans and angiosperm plants, PC is largely synthesized via the CDP-choline pathway (Ohlrogge and Browse 1995; Cornell and Ridgway 2015). The CDP-choline pathway contains three steps starting from choline, while CCT catalyzes the second step (a rate limiting step) for PC biosynthesis: catalyzing phosphocholine and CTP to form CDP-choline (Kinney et al. 1987; Jackowski and Fagone 2005; Cornell and Ridgway 2015) (Fig. 1 in **CHAPTER 1**). The enzymatic activity of CCT is regulated by the PC content of membranes (Johnson and Cornell 1999; Cornell and Northwood 2000). This enzyme is amphitropic which means that it can interconvert between a soluble inactive form and a membrane-lipid-bound active form (Cornell and Northwood 2000).

It was reported that CCT proteins are separated into four functional domains in mammalian organism, including N-terminal domain, catalytic core domain, membrane-binding regulatory domain, and C-terminal phosphorylation region (Cornell et al. 1995; Cornell and Northwood 2000; Jackowski and Fagone 2005). Recently, research on AtCCT1 has been done in *A. thaliana*. After comparing AtCCT1

to rat CCT1, the result showed homology of the internal domains (catalytic core and membrane-binding regulatory domain) whereas the N-terminal and C-terminal domains are highly divergent (Caldo et al. 2019). Two isoforms (CCT α and CCT β_2) in rat have almost identical membrane-binding domains and very similar catalytic domains, however, the N-terminal and C-terminal regions have also diverged and are structurally disordered (Dennis et al. 2011). In mammalian CCTs, the N-terminal domain contains a 30 residue-segment serving as a cap before the catalytic domain (Cornell and Ridgway 2015). The C-terminal of CCTs contains an amphipathic α -helix in *Drosophila melanogaster*, plants and mammals, and plays a vital role in mediating lipid interactions and CCT enzymatic activity (Kent 1997; Clement et al. 1999; Lykidis and Jackowski 2000; Helmink and Friesen 2004; Caldo et al. 2019). The CCT protein is thought to be in the cytoplasm or the nuclear in different cell types, and may function in vesicle traffic (Wang et al. 1995; Houweling et al. 1996; Kent 1997).

The characteristics of CCTs in plants have been studied some time ago. Four CCT transcripts were firstly isolated from *Brassica napus* roots by complementation of a yeast cct mutant in 1996 (Nishida et al. 1996). CCT transcripts in *A. thaliana* were identified in 1997 through the complementation of a yeast mutant which is deficient in corresponding yeast CCT gene (Choi et al. 1997). The full length CCT coding sequence in pea was isolated and the deduced amino acid was used for comparative analysis with amino acid sequences of rat, yeast and *B. napus* CCT, respectively (Jones et al. 1998). The enzyme activity of AtCCT is controlled on both the transcriptional and post-translational levels (Tasseva et al. 2004; Craddock et al. 2015). Recently, it has been shown that AtCCT1 has a consensus site (Ser-187) for phosphorylation by sucrose nonfermenting 1-related protein kinase 1 (SnRK1 or KIN10/SnRK1.1) (Caldo et al. 2019). The results show that SnRK1 can mediate the phosphorylation of the AtCCT1 enzyme at the site (Ser-187) to inhibit its enzymatic activity (Caldo et al. 2019).

C. plantagineum belongs to the *Linderniaceae* family is an extreme desiccation tolerant plant, which can turn into a quiescent state during desiccation (relative leaf water content around 5%) and recovers rapidly after re-watered (Bartels and Salamini 2001; Phillips et al. 2008). The research on plant CCTs have been done in several desiccation sensitive species, so we were interested to know the structure and characteristic of CCT in the desiccation tolerant plant *C. plantagineum*. Therefore, we cloned *CpCCT1*, analyzed the structure by comparing the amino acid sequences with rat CCT1, AtCCT1 and ScCCT, and monitored expression of CpCCT1 on the transcriptional and translational levels during dehydration, salt stress, cold stress, osmotic stress, ABA and IAA treatments.

2 Materials and methods

2.1 Plant materials and treatments

C. plantagineum plants and callus were grown as previously described by Bartels et al. (1990). The dehydration and rehydration treatments were performed as described in **CHAPTER 2**. The cold treatment was conducted in a 4 degree refrigerator (4°C, dark), while the plants in control group were kept in dark in a controlled growth room (22°C, dark). Detached leaves and roots were incubated in 100 µM abscisic acid (ABA), 1µM indole-3-acetic acid (IAA), 0.5 M NaCl solution, 0.5 M or 0.8 M mannitol solutions and 0.5 M or 0.8 M sorbitol solutions for 4h, 24h and 48h, respectively. The plant leaves and roots were harvested at each time point, frozen and ground in liquid nitrogen. After being freeze-dried samples were stored at -80 °C for further analysis. Three independent biological repetitions were included in each treatment.

2.2 Gene cloning

The 5' region of the *CpCCT1* gene was amplified by PCR from a λ ZAP II cDNA library prepared from leaves (2 h dried) of *C. plantagineum* (Bockel et al. 1998) using vector-specific (ZAP F2) and gene-specific (CpDN37040 R) primers (Table S1). The PCR product was sequenced by cloned into pJET1.2 vector with the CloneJET PCR Cloning Kit (Thermo Fisher Scientific, St Leon-Rot, Germany).

2.3 Phylogenetic analysis and sequence analysis

Putative homologs of *CpCCT1* were identified from *Lindernia brevidens* and *Lindernia subracemosa* transcriptome data and obtained by blast from the NCBI website (www.ncbi.nlm.nih.gov/) using *CpCCT1* predicted protein sequence as the query. The phylogenetic tree was generated after sequence alignment in Mega 7 using the maximum likelihood method with 1000 bootstrap predictions (Hall 2013).

Protein sequence identities were calculated by using sequence manipulation suite (https://www.bioinformatics.org/sms2/ident_sim.html) (Stothard 2000). Sequence alignment was carried out by using DNAMAN 6.0 software and Clustal Omega (<https://www.ebi.ac.uk/Tools/msa/clustalo/>) (Caldo et al. 2019). The predicted amphipathic α -helices were shown in Helix wheel using NetWheels (<http://lbqp.unb.br/NetWheels/>) (Mol et al. 2018).

2.4 RNA isolation and cDNA synthesis

Total RNAs were extracted from freeze-dried leaf and root samples of *C. plantagineum* in each treatment according to Valenzuela-Avenidaño et al. (2005). Reverse transcription PCR was conducted as described by Zhao et al. (2017). The elongation factor 1-alpha (*EF1a*) gene was used as the internal reference gene for both leaf and root samples in *C. plantagineum* (Giarola et al. 2015). Gene specific primers are listed in Table S1. The relative gene expression level in each treatment was deduced using Image-J (<https://imagej.nih.gov/ij/>). Fold changes in different treatments were analyzed by setting untreated or control samples as 1.

2.5 CpCCT1 antibody generation and protein analysis

The full length cDNA with an NcoI site (5' end) and an XhoI site (3' end) was obtained by PCR from the constructed plasmid (*CpCCT1* + pJET 1.2 vector) using specific primers (Table S1). This PCR product with NcoI and XhoI sites was cloned into the pET28a+ empty vector (Novagen, Darmstadt, Germany), and transformed into the *Escherichia coli* expression strain BL21 (DE3) (Amersham Pharmacia Biotech, Piscataway, NJ, USA). Protein induction and purification were carried out as described by Kirch and Röhrig (2010) with some modifications. Since the CpCCT1-His protein was difficult to purify by a nickel-column, CpCCT1-His proteins were collected from SDS-PAGE after incubation in 0.25 M KCl for 5 min. The purified proteins were sent to Seqlab (Sequence Laboratories Göttingen GmbH, Göttingen, Germany; www.seqlab.de) after being freeze-dried to raise a polyclonal

antiserum in rabbits.

Ten micrograms of total proteins extracted from leaves and roots of *C. plantagineum* were separated on 10% polyacrylamide SDS gels and transferred to nitrocellulose membranes (Laemmli 1970; Towbin et al. 1979). The CpCCT1 protein was detected by protein blots using a 1: 5000 dilution of the polyclonal antiserum. The relative protein expression level in each treatment was measured by Image-J (<https://imagej.nih.gov/ij/>). Fold changes in different treatments were analyzed by setting untreated or control samples as 1.

2.6 Protein localization prediction and analysis

The following programs were selected for the CpCCT1 subcellular localization prediction: MultiLoc2 (<http://abi.inf.uni-tuebingen.de/Services/MultiLoc2>), PSORT (<http://psort1.hgc.jp/form.html>), Predotar 1.04 (<https://urgi.versailles.inra.fr/predotar/>), Yloc (<http://abi.inf.uni-tuebingen.de/Services/YLoc/webloc.cgi>), and TargetP 1.1 (<http://www.cbs.dtu.dk/services/TargetP/>). Heat map was performed in the Cluster 3.0 software (<http://bonsai.hgc.jp/~mdehoon/software/cluster/software.htm>) and revealed by Java Treeview software (<http://jtreeview.sourceforge.net/>) (Shi et al. 2014).

The full length *CpCCT1* cDNA with NcoI sites at both ends generated by PCR was fused to the GFP gene (5' end) in the CaMV35S::GFP vector (pGJ280 vector) (Willige et al. 2009). The specific primers were listed in Table S1. The constructed plasmids were transiently transformed into onion cells via particle bombardment (van den Dries et al. 2011). Protein fluorescence in untreated cells and in cells undergoing plasmolysis (0.5M sucrose solution treated for 5 min) were observed using an inverted confocal laser scanning microscope (Nikon Eclipse TE2000-U/D-Eclipse C1; Nikon, Düsseldorf, Germany), setting as excitation wave lengths: 488 nm for GFP, 543 nm for chloroplast auto-fluorescence, and emitted light: 515-530 nm and 570 nm, respectively (Giarola et al. 2016).

2.7 Analysis of interaction network

The interaction network of CpCCT1 protein was constructed using STRING database (<https://string-db.org/>) with high confidence (combined score>0.7) (Szklarczyk et al. 2017). The interaction data collected from STRING database were then analyzed with Cytoscape software (Version 3.7.1) (<http://www.cytoscape.org/>).

2.8 Subcellular fractionation

Subcellular fractionation was performed as described by Serna et al. (2001) with modifications. The untreated and desiccated leaves (1 g freeze-dried) were homogenized with 40 mL pH 7.7 extraction buffer (containing 5 mM EDTA, 0.5 M sucrose, 5 mM DTT, 0.5 M Mes, 30 mM Tris), respectively. The homogenate was filtrated by four layers of nylon and centrifuged at 2300 rpm at 4 °C for 5 min. The pellet (pellet 1) was re-suspended in 2.5 mL extraction buffer while the supernatant was centrifuged at 8000 rpm at 4 °C for 20 min. The pellet (pellet 2) was re-suspended in 1.5 mL extraction buffer and the supernatant was then centrifuged at 30000 rpm at 4 °C for 2 h. The final supernatant was collected in a new tube, and the pellet (pellet 3) was re-suspended in 1 mL pH 7.2 pellet buffer (containing 1 mM DTT, 0.25 M sucrose, 0.5 M MEs, 3 mM Tris). The final supernatant and three pellets were used for protein analysis.

2.9 Yeast complementation assay

The full length *CpCCT1* cDNA with an XhoI site (5' end) and a BamHI site (3' end) was amplified by PCR using specific primers (Table S1), and cloned into the pDR-195 vector provided by Professor Gabriel Schaaf (University of Bonn). The well-constructed plasmid and the pDR-195 empty vector were transformed into wild type (WT) yeast (BY4741, genotype: MATa; his3D1; leu2D0; met15D0; ura3D0 / Euroscarf Y0000) and *cct* mutant yeast cells (Scientific Research and Development GmbH, Oberursel, Germany; <http://www.euroscarf.de>) according to Gietz et al (1995)

with some modifications. Yeast competent cells were prepared as follows: yeast cells were inoculated in 5 mL liquid YPAD medium (4% (w/v) bacto peptone, 2% (w/v) yeast extract, 80 mg/L adenine hemisulfate, 4% (w/v) glucose, pH 5.6) and grew overnight. After a short centrifugation and discarding the liquid, cells were re-suspended in fresh YPAD medium to adjust the $OD_{600nm} = 0.2$. After growing cells to $OD_{600nm} = 0.8-1.0$ (approximately 4-6 h), cells were collected in Falcon tubes by spinning 1 min at 4000 rpm. The cells were re-suspended in 500 μ L pH 7.5 TE/LiAc buffer (10 mM TRIS/HCL, 0.1M LiAc, 1 mM EDTA), and transferred to 1.5mL eppendorf tubes followed by spinning 1 min at 4000 rpm. These wash steps were repeated three times as before and the yeast competent cells were ready to use after re-suspending in 150 μ L TE/LiAc buffer. The transformation mixtures were added in a PCR tube in the following order: 100 μ L pH 7.5 PEG/LiAc buffer (containing 40% PEG, 0.1M LiAc, 1 mM EDTA, 10 mM TRIS/HCL), 16.5 μ L competent cells, 200-500 ng plasmid, 3.5 μ L pre-warmed (95 °C for 3 min) salmon sperm DNA (8 mg/mL). The PCR tubes with transformation mixtures were shaken at 250 rpm for 30 min at room temperature. The mixtures were placed on selective plates (pH 5.8, 182.2 g/L D-sorbitol, 6.7 g/L Difco yeast nitrogen base without amino acids, 20 g/L agar, 40 g/L glucose, 1 \times amino acids solution omit Uracil) after incubation for 20 min at 42 °C.

The yeast genotyping and colony PCR programs were performed with specific primers (Table S1). For the yeast complementation treatments, different chemicals (0.5 M/0.75 M/1 M NaCl and KCl, 0.5 M/1 M mannitol, 5 mM/10 mM/20 mM 3-amino-1,2,4-triazol (3AT)) were added in the selective plates. 5 μ L yeast cell dilutions were spotted on different plates.

2.10 Promoter analysis

Genomic DNA was extracted from *C. plantagineum* leaves as described by Rogers and Bendich (1985). *CpCCT1* 5' upstream sequence (promoter + 5'UTR) was

obtained with the CpCCT1 promoter F (with a HindIII site) and CpCCT1 promoter R primers (Table S1). The promoter sequence (1197 bp) fused with pBT10GUS empty vector was used for promoter activity analysis. Putative promoter *cis*-elements were identified using the New PLACE database scan tool (<https://www.dna.affrc.go.jp/PLACE/?action=newplace>) (Higo et al. 1999). Relative promoter activities were analyzed by using the method of transient transformation in *C. plantagineum* and *A. thaliana* according to van den Dries et al. (2011).

3 Results

3.1 Quantification of *CpCCT1* transcripts and molecular phylogeny of *CCT* genes

The *CpCCT1* gene has been found in our previous research on polysomal profiling analysis in *C. plantagineum* (**CHAPTER 2**). RT-qPCR had been performed to verify the RNA-seq data, in which the expression levels of *CpCCT1* transcripts were analyzed in total mRNA and polysomal mRNA during dehydration and rehydration (untreated, partial dehydrated, desiccated and rehydrated) (**CHAPTER 2**).

As shown in Fig. 1a, the total mRNA abundance of *CpCCT1* significantly increased in partial dehydration stage (30 fold higher than untreated stage). The expression level decreased from partial dehydration to desiccation, but the transcript abundance was still 9 fold higher in desiccated tissues than in untreated tissues. The change pattern of *CpCCT1* polysomal mRNA abundance was similar as the total mRNA (Fig. 1a).

Fig. 1b shows the polysome occupancy (the ratio between the polysomal mRNA abundance and the total mRNA abundance) of *CpCCT1* during the dehydration and rehydration cycle. The polysome occupancy increased from partial dehydration to desiccation. The results indicate that *CpCCT1* is a dehydration stress response gene, and *CpCCT1* is under translational control during dehydration.

Based on these results (from **CHAPTER 2**), we cloned the coding sequence of *CpCCT1* from a cDNA library to gain more insight into the role of this gene. Fig. 1c shows the coding sequence (849 nt), the predicted amino acid sequence (282 amino acids) and the predicted secondary structure (including 16 helical structures and 7 extended strand structures) of CpCCT1.

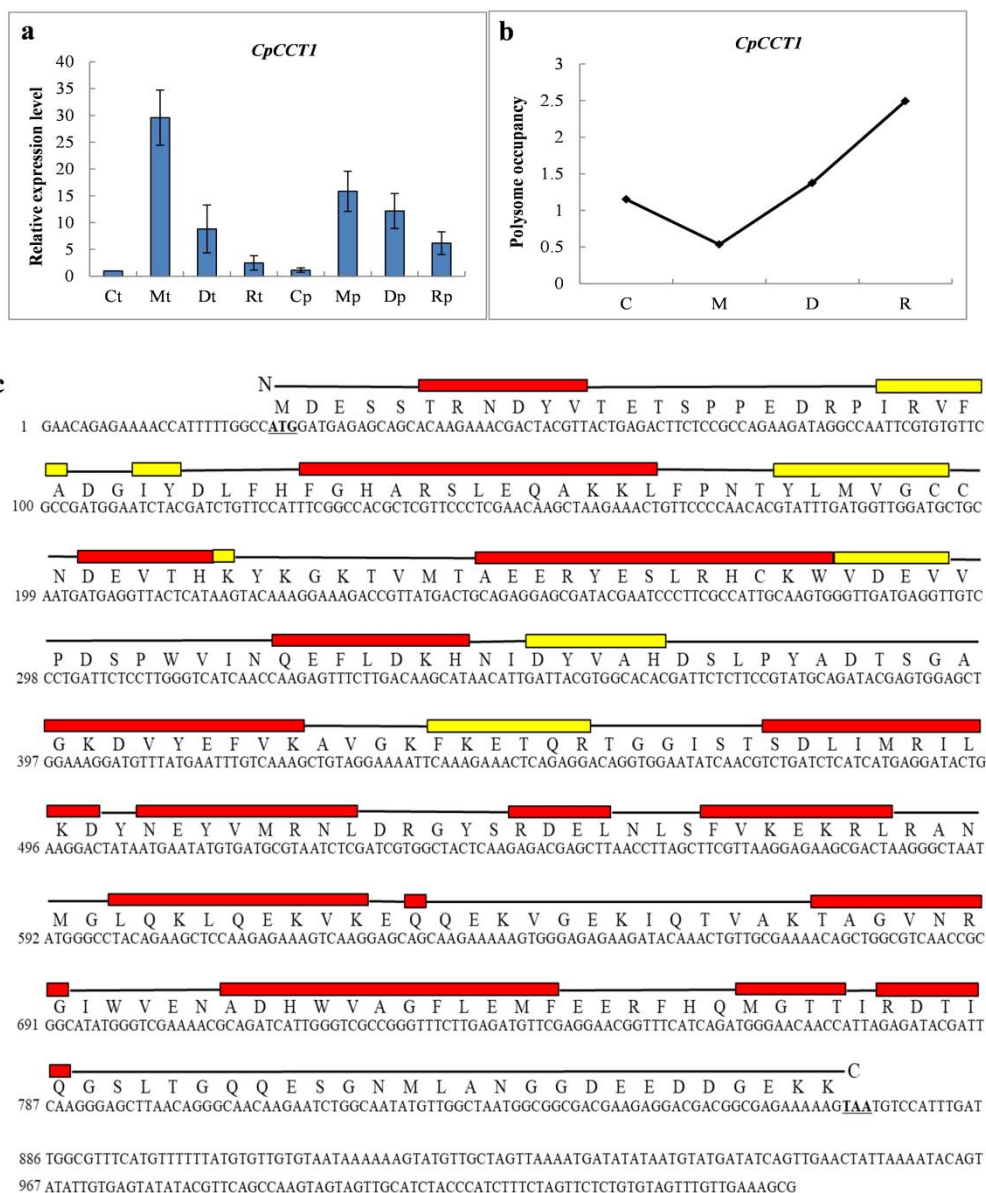


Fig. 1 The expression pattern and sequence characteristic of *CpCCT1*. The relative expression level in total mRNA and polysomal mRNA (a) and polysome occupancy (b) of *CpCCT1* during the dehydration and rehydration cycle. (c) The nucleotide sequence, predicted amino acid sequence and predicted secondary structure of *CpCCT1* (red represents predicted helical structure and yellow refers to predicted extended beta-strand).

In the phylogenetic tree, homologous genes of CCT from eudicots, monocots, spikemosses, mosses, green algae, bacteria, yeast and animal contained conserved domains and formed several separate clusters (Fig. 2).

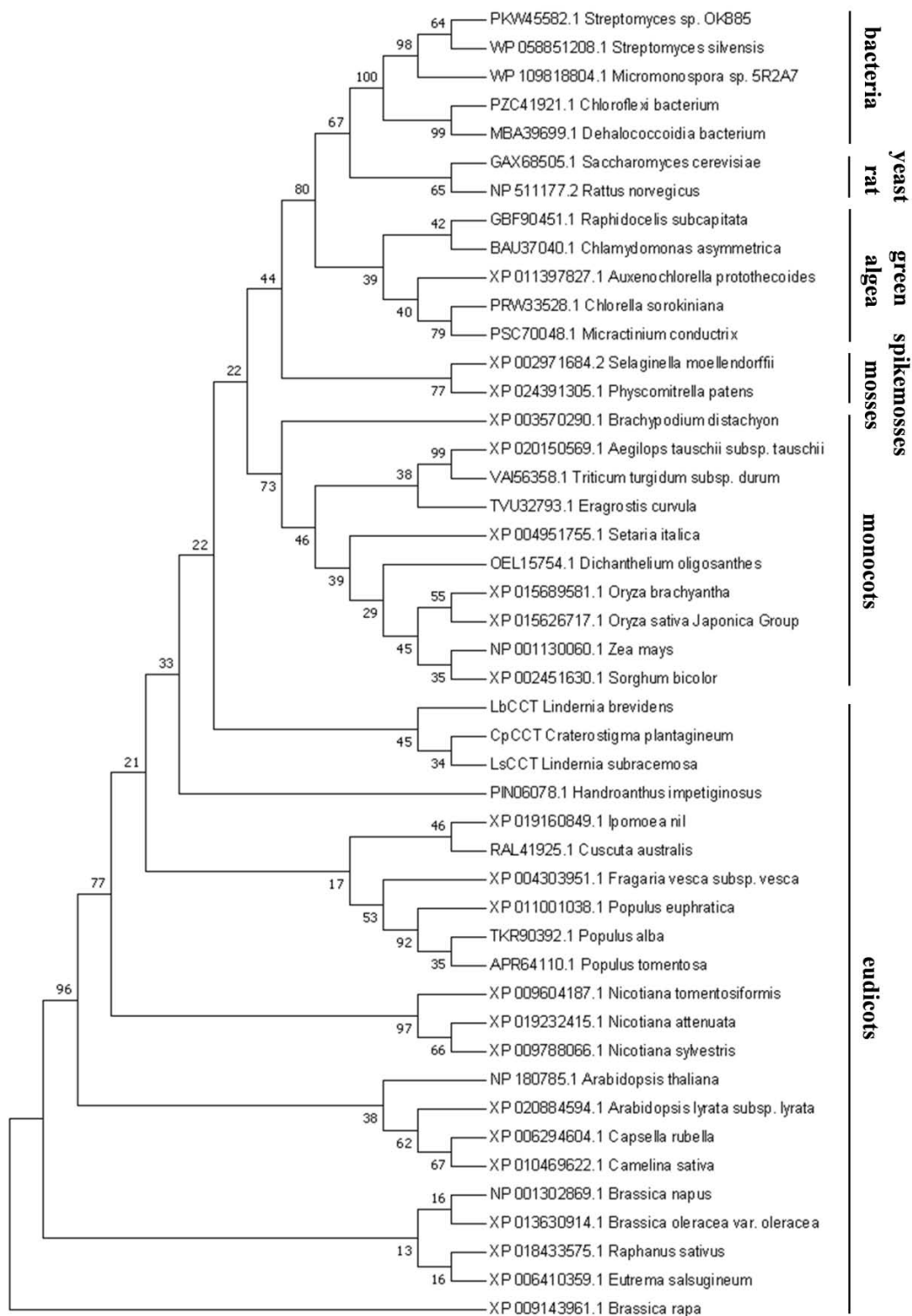


Fig. 2 Phylogenetic tree of CCT proteins from different species. The analysis was executed by Mega 7 using the maximum likelihood method with 1000 bootstrap. The protein sequences of CCT homologs were obtained from transcriptomes of *L. brevidens* and *L. subracemosa* and NCBI database.

Homologs of CpCCT1 were also identified in the closely related species *L. brevidens* and *L. subracemosa* and were termed LbCCT and LsCCT, respectively. The predicted protein sequences of CCT from these three species showed 78.2% (CpCCT1 vs. LbCCT), 39.6% (CpCCT1 vs. LsCCT) and 44.0% (LbCCT vs. LsCCT) identity and 90.0% (CpCCT1 vs. LbCCT), 95.4% (CpCCT1 vs. LsCCT) and 96.0% (LbCCT vs. LsCCT) similarity between each other, with the C-terminal region being the most divergent region (Fig. 3).

		HXGH	
CpCCT1	MDESSTRNDYVTETSPEDRPIRVFADGIYDLFHFHGARS		40
LbCCT	MGESIVRNGDVVETSPFLDRPIRVYADGIYDLFHFHGARS		40
LsCCT	MGESSTRNDYVTETSPEDRPIRVYADGIYDLFHFHGARS		40
CpCCT1	LEQAKKLF PNTYLLVGCNDEVTHKYKGTVMTAERYES		80
LbCCT	LEQAKKLF PNTCLLVGCNDEVTHKYKGTVMTAERYES		80
LsCCT	LEQAKKLF PNTYLLVGCNDEVTHKYKGTVMTAERYES		80
CpCCT1	LRHCKWVDEVVPEPSPWVINOEFLDKRNIDYVAHDSL PYAD		120
LbCCT	LRHCKWVDEVIPDAPWVINOEFLDKRNIDYVAHDALPYAD		120
LsCCT	LRHCKWVDEVVPEPSPWVINOEFLDKRNIDYVAHDALPYAD		120
CpCCT1	TSGAGKDVEYEFVKAAGKFKETQRTDGGISTSDIIMRILKDY		160
LbCCT	TSGAGKDVEYEFVKAAGKFKETKRTDGGISTSDIIMRIVKDY		160
LsCCT	TSGAGKDVEYEFVKAAGKFKETQRTDGGISTSDIIMRIVKDY		160
CpCCT1	NEYVMRNLDRGYSRDELNLSFVKEKRLRANMGLKQLQEKV		200
LbCCT	NEYVMRNLDRGYSRDELNLSFVKEKRLRANMGLKQLQEKV		200
LsCCT	NEYVMRNLDRGYSRDELNLSFVKEKRLRANMGLKQLQEKV		200
CpCCT1	KEHQEKVGEKIQTVAKTAGVNRGIWVENADHWVAGFLEMF		240
LbCCT	KEHQEKVGEKIQTVAKTAGVHRNMWVENADRWVAGFLEMF		240
LsCCT	KEHQEKVGEKIQTVAKTAGVHNNIWVENADRWVAGFLEMF		240
CpCCT1	EERFHQMGTAIRDRICERLTGQQESGRMLINGDDEE...		276
LbCCT	EERFHQMGTAIRDRICERLTGQQ.SSRMLINGDEDD...		275
LsCCT	EERFHQMGTAIRDRICERLTGQQ.SGRMLINGDDDDSYYE		279
CpCCT1	DDGEK.....		282
LbCCT	DDDDYYESEEYDEDDYDSDEK.....		302
LsCCT	SEEEYHDEEEDDEYHDSGKIGGLVIDMCCADMVDVGD		319

Fig. 3 Alignment of CpCCT1, LbCCT and LsCCT protein sequences. The black color represents identical amino acids and the red frame represents a HXGH motif.

3.2 Prediction of CpCCT1 functional domains

To examine whether the *CCT* gene in the desiccation tolerant plant (*C. plantagineum*) has a similar structure as the *CCT* gene in the desiccation sensitive

plant (*A. thaliana*), in an animal homolog (*R. norvegicus*), and in a yeast homolog (*S. cerevisiae*), the amino acid sequences were aligned. As shown in Fig. 4a and Fig. 4b, the sequences are separated into four functional regions (N-terminal region, core catalytic domain, membrane-binding domain and C-terminal region); the different regions are indicated by colored lines.

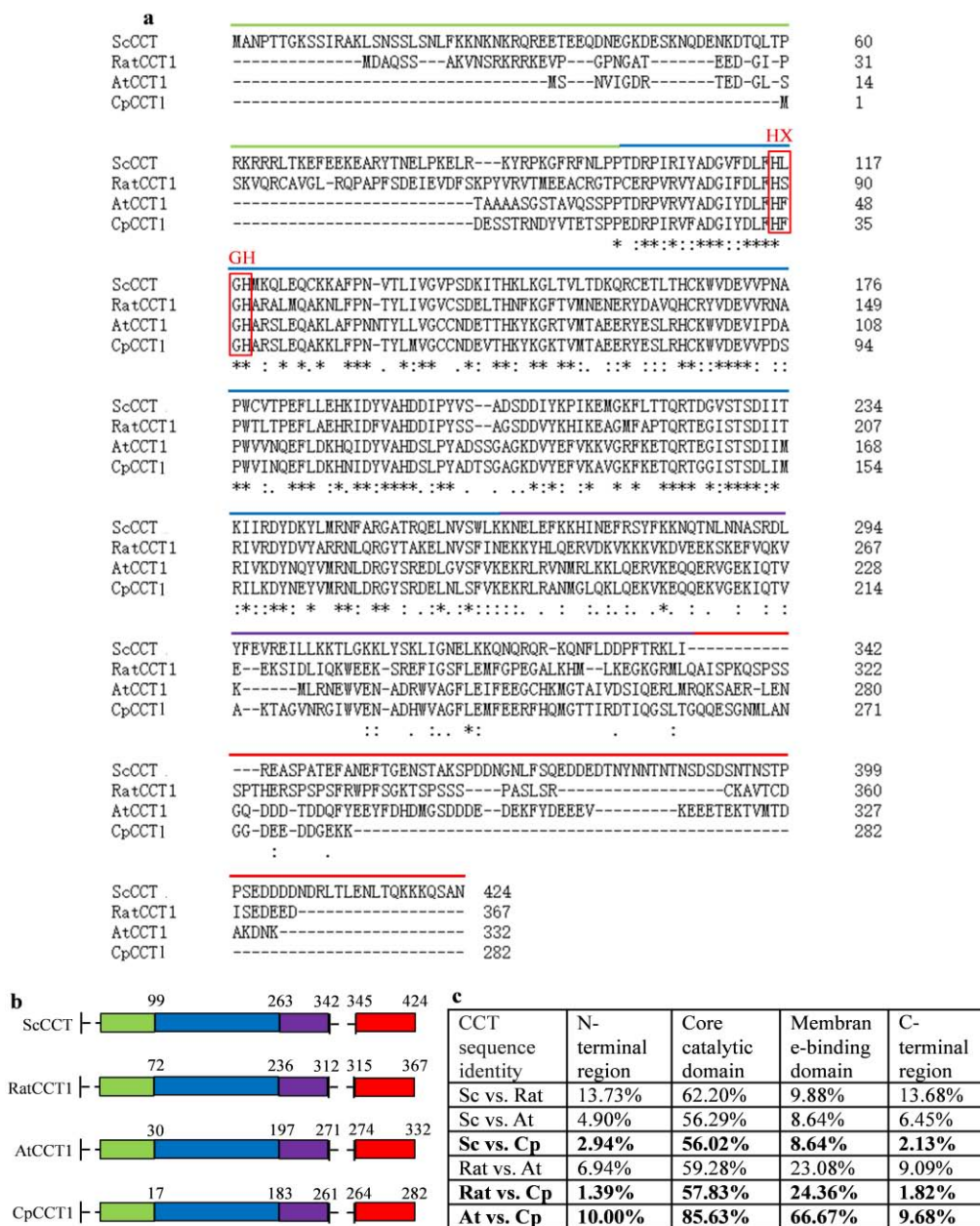


Fig. 4 Sequence alignment of ScCCT, Rat CCT1, AtCCT1 and CpCCT1 using Clustal Omega. (a) The different functional domains are indicated by different color lines above the amino acids (light green: N-terminal region, blue: core catalytic domain, purple: membrane-binding domain, red:

C-terminal region). The red frame represents a HXGH motif in the catalytic domain. **(b)** The length of different functional domains (light green: N-terminal region, blue: core catalytic domain, purple: membrane-binding domain, red: C-terminal region). **(c)** The sequence identity of different regions in different comparisons, including ScCCT vs. Rat CCT1, ScCCT vs. AtCCT1, ScCCT vs. CpCCT1, Rat CCT1 vs. AtCCT1, Rat CCT1 vs CpCCT1, and AtCCT1 vs. CpCCT1.

The results of sequence identity analysis showed 57.83% and 24.36% identity between rat CCT1 and CpCCT1 in the catalytic and membrane-binding domains, while the N-terminal and C-terminal domains are highly divergent (N-terminal region: 1.39%, C-terminal region: 1.82%). The sequence identities in the N-terminal region (2.94%), catalytic domain (56.02%) and C-terminal region (2.13%) between ScCCT and CpCCT1 are similar to the identities of the corresponding domains between rat CCT1 and CpCCT1. However, the sequence homology in membrane-binding domain is relatively low (8.64% identity) between ScCCT and CpCCT1 compared to the identity between rat CCT1 and CpCCT1 (24.36%). The sequences between the two plants have a high homology in the catalytic domain (85.63% identity) and membrane-binding domain (66.67% identity), whereas the terminal domains are also divergent (N terminal region: 10.00%, C terminal region: 9.68%) between AtCCT1 and CpCCT1 (Fig. 4c).

It was reported that several segments in the membrane-binding domain of CCTs are similar in rat CCT and AtCCT; these segments can form amphipathic helices upon interaction with the membranes (Lee et al. 2014, Caldo et al. 2019). The corresponding regions of amphipathic α -helices in the membrane-binding domain of CpCCT1 were identified through sequence alignment. The residues 183-220 of CpCCT1 can form amphipathic helices which have a hydrophobic face composed of leucine (L), isoleucine (I) and valine (V) residues (Fig. 5a). The autoinhibitory motif covering residues 222-242 of CpCCT1 form another α -helix. The leucine (L), valine (V), phenylalanine (F), tryptophan (W) and isoleucine (I) residues from CpCCT1 also constitute a hydrophobic face (Fig. 5b).

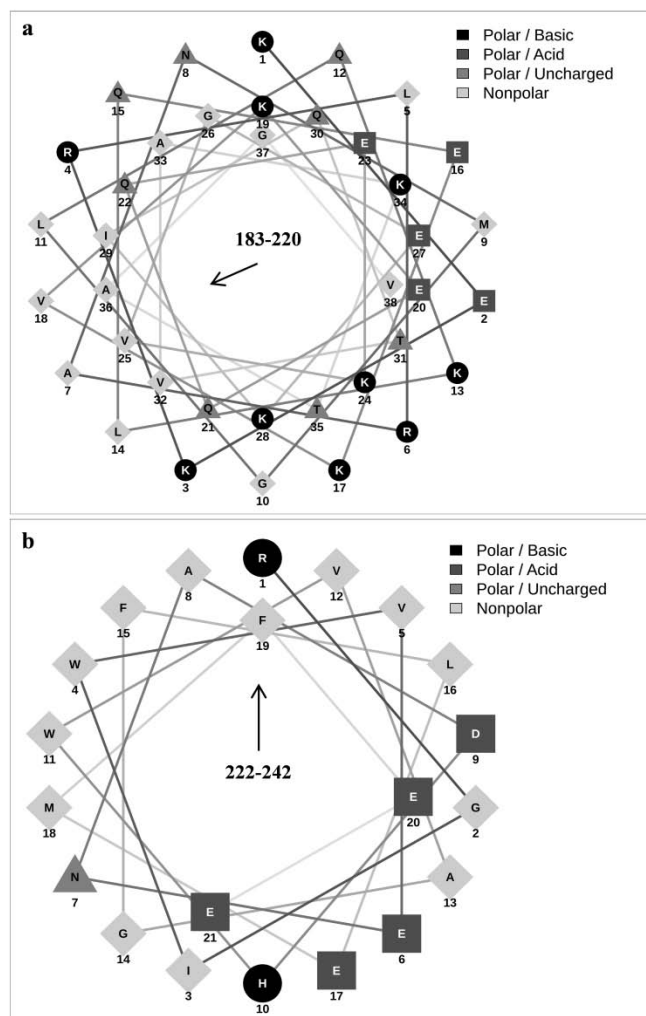


Fig. 5 Helix wheels representing 2 parts of the membrane-binding domain of CpCCT1 were identified through alignments with rat CCT1 and AtCCT1. The hydrophobic faces of the two segments: (a) residues 183-220, (b) residues 222-242 are shown in light gray (rhombus) on the left side and upward side, respectively.

3.3 Localization of CpCCT1

According to the subcellular localization predictions, the CpCCT1 protein is most likely to be localized in cytoplasm and nucleus (Fig. 6).

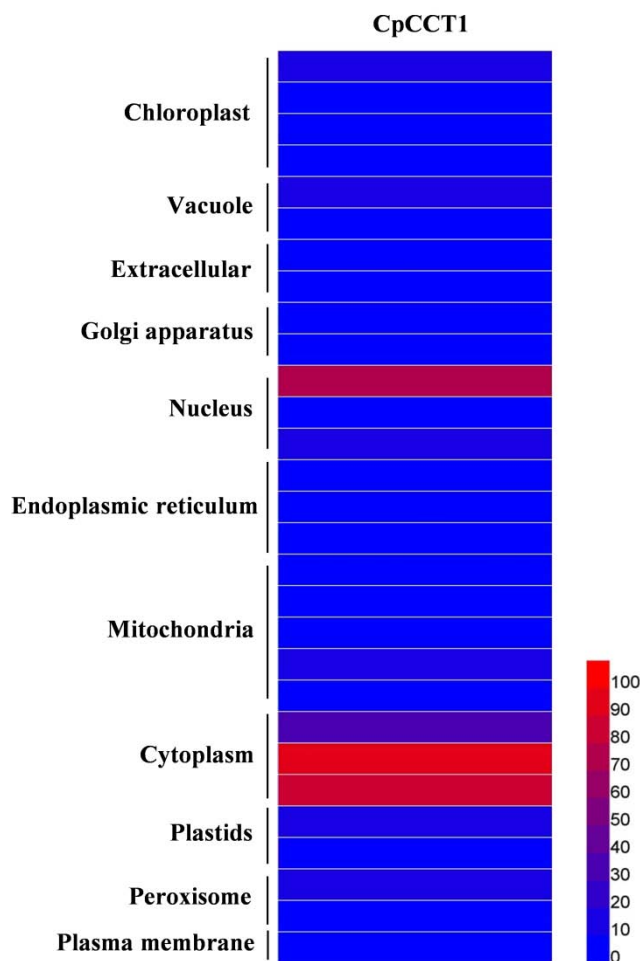


Fig. 6 Heat map of subcellular localization prediction of the CpCCT1 protein. Red color means 100% possibility, and blue color represents 0% possibility. The values were obtained from different localization prediction programs (see details in Materials and methods).

To verify this prediction, onion cells were transformed with constructs overexpressing the full-length CpCCT1-GFP and GFP alone (data not shown). The fluorescence analysis (both in untreated tissues and after plasmolysis) show that the CpCCT1-GFP protein is localized in the cytoplasm (Fig. 7a), which coincides with the prediction (Fig. 6). The localization of CpCCT1 protein in cells of *C. plantagineum* leaves (desiccated) was analyzed by subcellular fractionation. As shown with immunoblot, the CpCCT1 protein is detected in all the four fractions, but it is enriched in the membrane fraction (Fig. 7b). The percentage of the CpCCT1 distribution in *C. plantagineum* leaves is analyzed by setting the total subcellular

fractions as 100% (Fig. 7d). To check the tissue specific expression of CpCCT1, *C. plantagineum* leaf, root, callus, flower, and stem samples of untreated and desiccated tissues were collected. The immunoblot results showed that the CpCCT1 protein exists in all the five types of tissues after dehydration stress, while it only exists in callus in the untreated state. The majority of CpCCT1 protein was enriched in leaf and root samples under desiccation stress (Fig. 7c). As shown in Fig. 7e, the relative protein expression level of CpCCT1 in *C. plantagineum* was measured by setting the untreated state as 1.

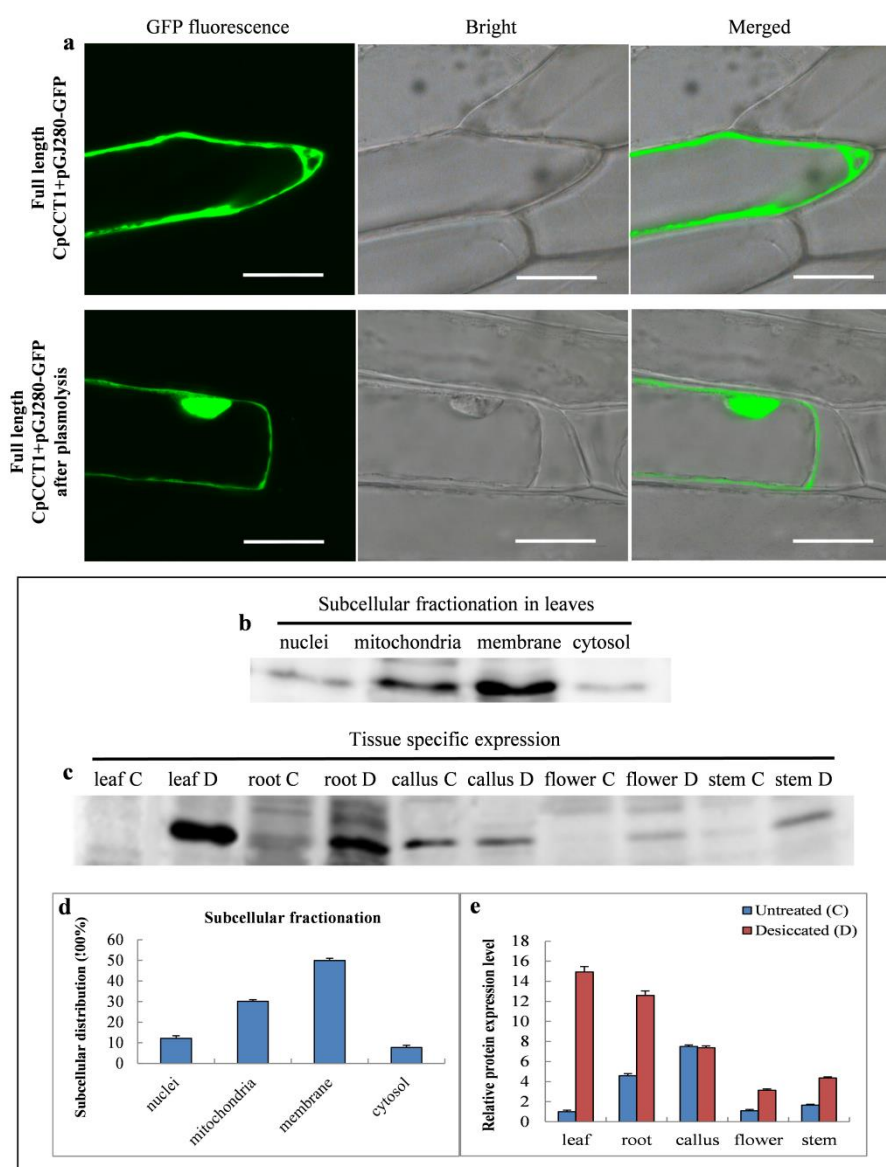


Fig. 7 Localization of the CpCCT1 protein. (a) Cellular localization of CpCCT1. Images of

transformed onion cells were taken around 16 h after particle bombardment. GFP fluorescence, bright field and merged images are shown (Bars correspond to 50 μm). (b) Subcellular fractionation results of CpCCT1 in *C. plantagineum*. Polyclonal antibodies were used to detect the CpCCT1 protein; equal amount of proteins were loaded for each fraction. (c) Tissue specific expression of CpCCT1 in *C. plantagineum*, including leaf, root, callus, flower and stem samples under untreated state (C) and desiccation state (D). (d) The percentage of subcellular distribution of CpCCT1. Data were analyzed by setting the total subcellular fractions as 100% using Image-J software. (e) The relative expression level of the CpCCT1 protein in different tissues. Data were analyzed by setting the level of untreated leaf sample as 1 using the Image-J software.

3.4 Transcript changes of *CpCCT1* during different treatments

Transcript levels of the *CpCCT1* gene were determined in *C. plantagineum* leaves and roots after dehydration and treated with 0.5 M NaCl and cold. Fig. 8a shows the transcript abundance of *CpCCT1* in leaf and root samples during different time points of the treatments. The expression pattern of *CpCCT1* was detected by semi-quantitative PCR and coincided with the one detected by RT-qPCR before in leaves during dehydration and rehydration (Fig. 8b). The transcript abundance of *CpCCT1* in leaves increased after treated with 0.5 M NaCl solution and cold stress (Fig. 8c, d). Intriguingly, the *CpCCT1* transcripts in leaf samples gradually decreased after cold stress for 24 h and 48 h, and eventually the transcript levels were lower than those in the control samples (Fig. 8d). *CpCCT1* transcripts of root samples also increased during dehydration and decreased after 2 d re-watering (Fig. 8e). After incubation in 0.5 M NaCl, *CpCCT1* transcripts in roots gradually accumulated during the whole treatment process (Fig. 8f). For root samples treated by cold stress, *CpCCT1* transcript levels showed a slight increase at 4 h, then gradually decreased at 24 h and 48 h of cold treatment (Fig. 8g).

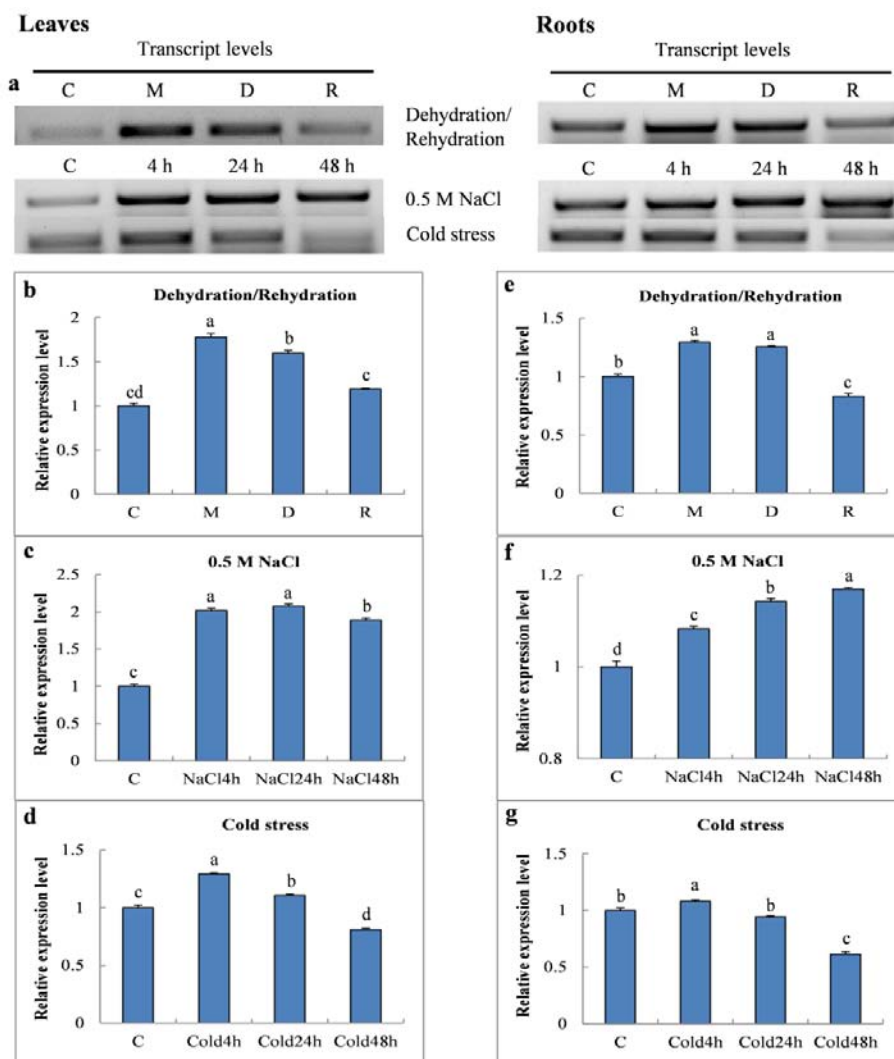


Fig. 8 (a) Transcript levels of *CpCCT1* in *C. plantagineum* leaves and roots during dehydration, salt and cold stresses. Transcript abundance of *CpCCT1* in leaves under dehydration stress (b), salt stress (c) and cold stress (d) and roots under dehydration stress (e), salt stress (f) and cold stress (g) were measured by semi-quantitative PCR. Fold changes of each sample at different time points were analyzed by setting the level of the control samples as 1 using the Image-J software (b-g). *EF1 α* was used as an internal control. Values in (b-g) were calculated from three independent biological repetitions (mean \pm SE). The vertical bars with different lower-case letters are significantly different from each other at $P < 0.05$ (one-way ANOVA).

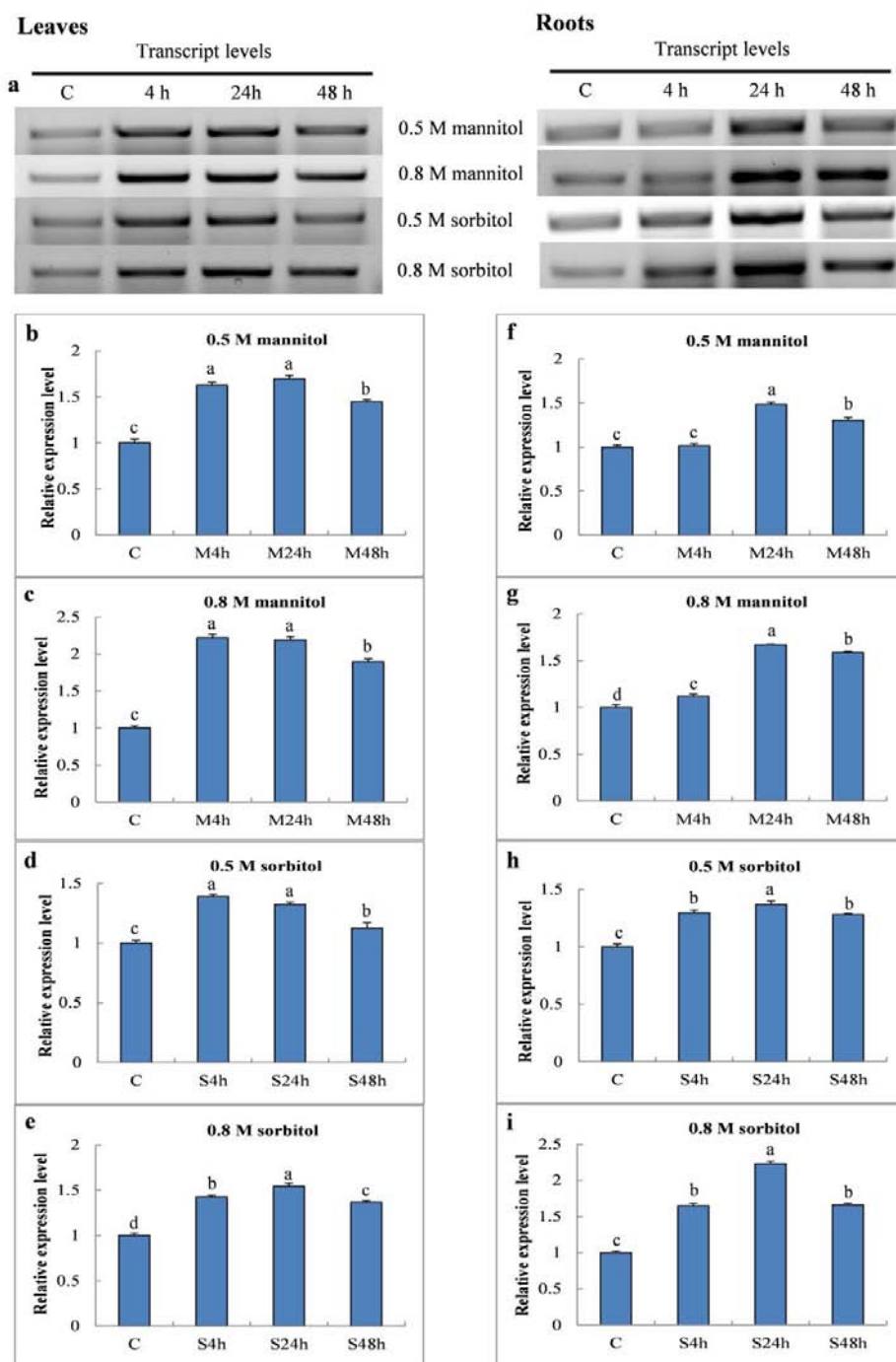


Fig. 9 (a) Transcript levels of *CpCCT1* in *C. plantagineum* leaves and roots under different type of osmotic stresses. Transcript abundance of *CpCCT1* in leaves treated with 0.5 M mannitol (b), 0.8 M mannitol (c), 0.5 M sorbitol (d) and 0.8 M sorbitol (e), and roots treated with 0.5 M mannitol (f), 0.8 M mannitol (g), 0.5 M sorbitol (h) and 0.8 M sorbitol (i) were measured by semi-quantitative PCR. Fold changes of each sample at different time points were analyzed by setting the level of the control samples as 1 using the Image-J software (b-i). *EF1 α* was used as an

internal control. Values in (b-i) were calculated from three independent biological repetitions (mean \pm SE). The vertical bars with different lower-case letters are significantly different from each other at $P < 0.05$ (one-way ANOVA).

The effect of osmotic stresses on *CpCCT1* expression was investigated using detached leaves and roots incubated in 0.5 M or 0.8 M mannitol and 0.5 M or 0.8 M sorbitol solutions for 4 h, 24 h and 48 h, respectively (Fig. 9a). The transcripts of *CpCCT1* were transiently induced during all the osmotic stress treatments. The transcript levels of leaf samples treated with 0.8 M mannitol and 0.5 M sorbitol solutions reached a transcription peak at 4 h whereas the other samples in leaves and roots had a transcription peak at 24 h. Interestingly, *CpCCT1* transcripts were reduced in all samples subjected to osmotic stresses for 48 h compared to the transcripts at 24 h, but the transcript levels were still slightly higher than those of the control samples (Fig. 9b-i).

To investigate whether *CpCCT1* is responsive to the plant hormone (ABA and/or IAA), RNA was isolated from leaves and roots of plants treated with 100 μ M ABA or 1 μ M IAA for 4 h, 24 h and 48 h, respectively. Gene expression was analysed by semi-quantitative PCR in all samples (Fig. 10a). Both ABA and IAA led to induction of *CpCCT1* transcripts in leaves and roots (Fig. 10b-d). The *CpCCT1* transcripts of ABA-treated leaves rapidly increased at 4 h and stayed at that level, while the *CpCCT1* transcripts of leaves treated with IAA were kept at the same level until 24h and significantly accumulated at 48 h (Fig. 10b, c). Root samples treated with ABA had a similar expression pattern of *CpCCT1* as the leaf samples (Fig. 10d). Transcripts of *CpCCT1* only slightly accumulated in root samples treated with 1 μ M IAA (Fig. 10e).

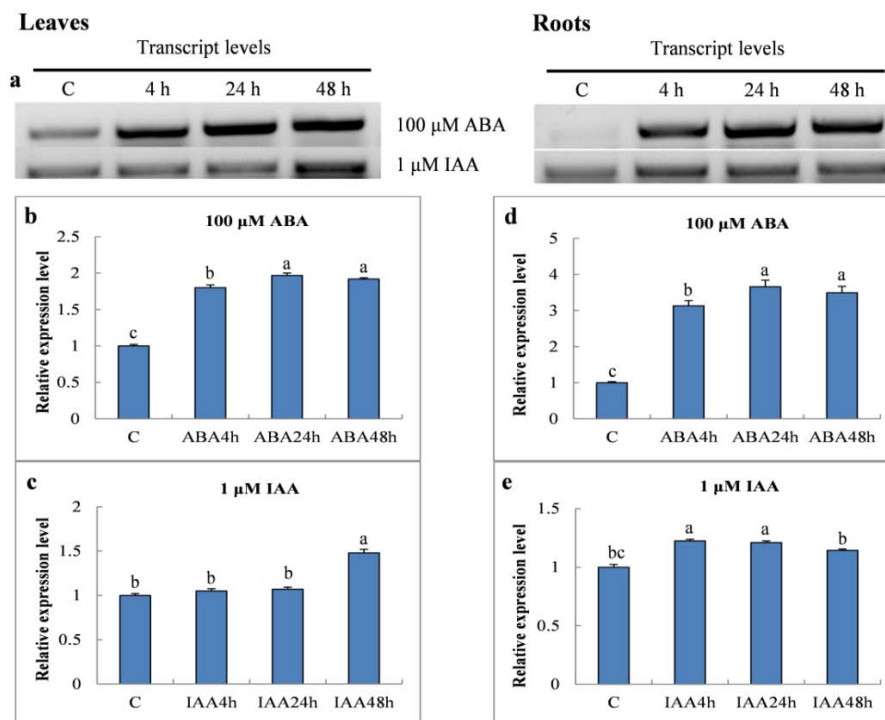


Fig. 10 (a) Transcript levels of *CpCCT1* in *C. plantagineum* leaves and roots during exogenous plant hormone treatments. Transcript abundance of *CpCCT1* in leaves treated with 100 μ M ABA (**b**) and 1 μ M IAA (**c**), and roots treated with 100 μ M ABA (**d**) and 1 μ M IAA (**e**) were measured by semi-quantitative PCR. Fold changes of each sample at different time points were analyzed by setting the level of the control samples as 1 using the Image-J software (**b-e**). *EF1 α* was used as an internal control. Values in (**b-e**) were calculated from three independent biological repetitions (mean \pm SE). The vertical bars with different lower-case letters are significantly different from each other at $P < 0.05$ (one-way ANOVA).

3.5 Expression patterns of CpCCT1 protein under different treatments

To analyze accumulation of the CpCCT1 protein in *C. plantagineum* during different treatments, antibodies were raised against the recombinant CpCCT1 protein. Fig. 11 shows the specificity of the antibodies, which could detect CpCCT1-His proteins in *E.coli* cells with a molecular weight of 37 kDa. The antibodies detected CpCCT1 proteins in *C. plantagineum* with an apparent molecular weight of 35 kDa, which is similar as the expected value.

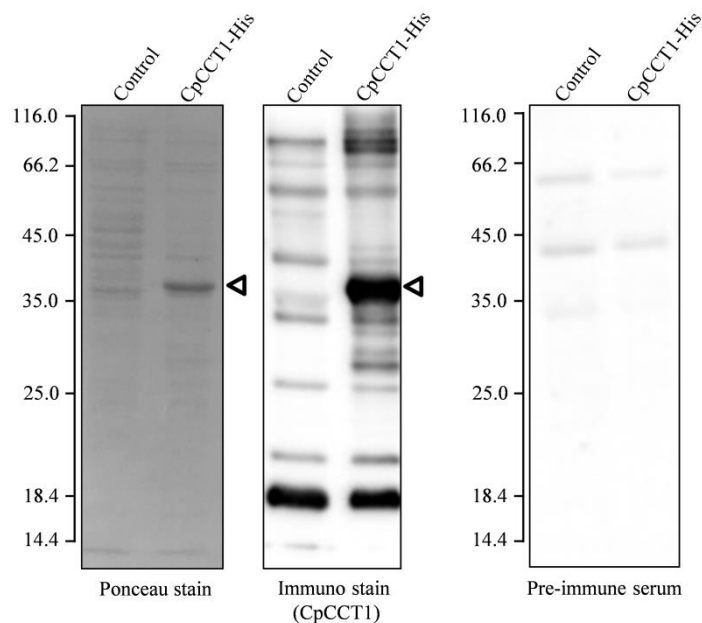


Fig. 11 The specificity of the polyclonal antiserum used to detect CpCCT1 was analyzed by protein blots. Protein blots of overexpressing BL21 *E. coli* cells carried the empty pET28a(+) vector (control) or the CpCCT1+pET28a(+) vector (CpCCT1-His) were induced with 1 mM IPTG for 7 h. Total proteins were separated by 15% (w/v) SDS-PAGE firstly, then blotted to a nitrocellulose membrane for protein immune detection. The membrane was incubated in Ponceau for 5 min before incubated with CpCCT1 polyclonal antiserum or pre-immune serum. The black triangle represents CpCCT1 protein.

Immunological analysis was conducted using protein samples from all the treatments mentioned above to investigate whether *CpCCT1* transcript levels correlated with CpCCT1 protein levels (Fig. 12a, Fig. 13a). However, the CpCCT1 proteins were not detectable in leaf and root samples treated with cold stress, 100 μ M ABA or 1 μ M IAA for 4 h, 24 h and 48 h. In the dehydration and rehydration cycle, CpCCT1 proteins accumulated from partial dehydration, reached a peak in desiccated tissue and declined during rehydration in leaves (Fig. 12b). CpCCT1 protein levels correlate with transcript accumulation in dehydrated roots (Fig. 12d). CpCCT1 proteins only accumulated at 48 h after 0.5 M NaCl treatment both in leaves and roots (Fig. 12c, e). The immunological analysis showed that mannitol and sorbitol-treated samples at 48 h had significantly higher accumulation of CpCCT1 proteins compared

with control samples both in leaves and roots; but there were no obvious differences between control samples and mannitol or sorbitol-treated samples at 4 h or 24 h (Fig. 13a). 0.8 M mannitol and 0.8 M sorbitol treatments induced higher amounts of CpCCT1 proteins at 48 h than the same treatments with solutions of lower concentrations (0.5 M), respectively (Fig. 13b-e).

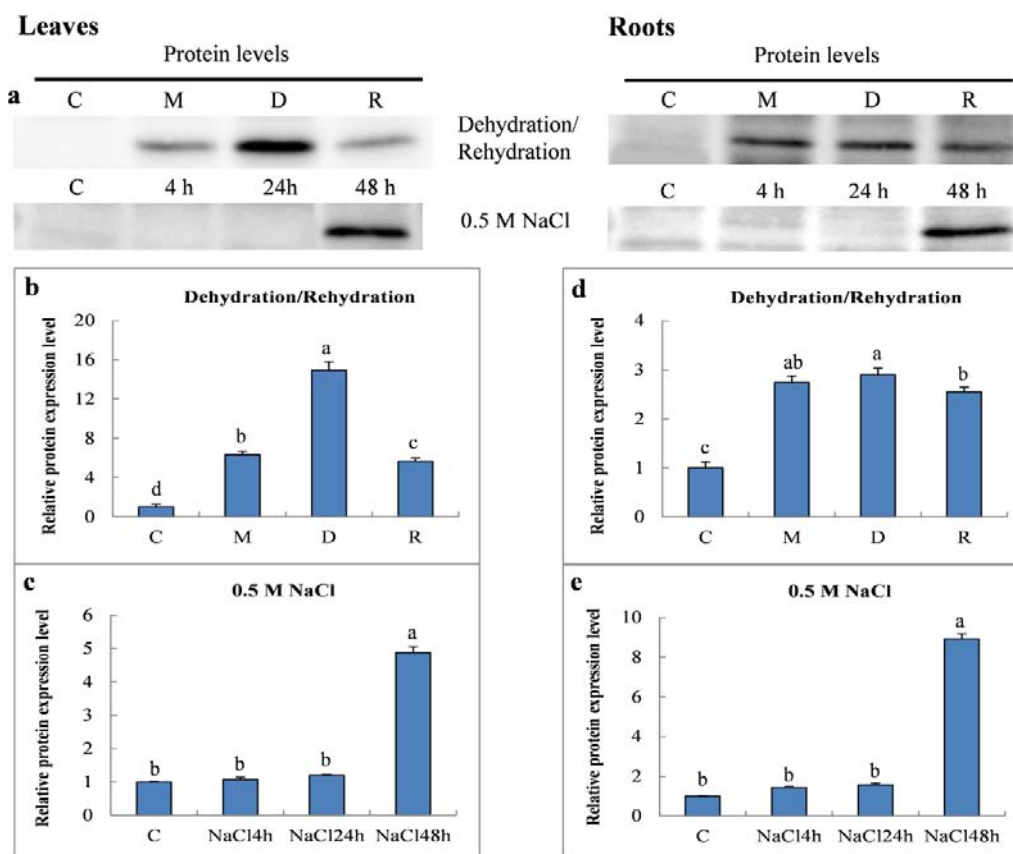


Fig. 12 (a) Expression abundance of the CpCCT1 protein in *C. plantagineum* leaves and roots during dehydration stress and salt stress. Expression levels of the CpCCT1 protein in leaves under dehydration stress (b) and salt stress (c), and roots under dehydration stress (d) and salt stress (e) were measured by Western blot. Equal loading of proteins was monitored by staining the membrane with Ponceau S (data not shown). Fold changes of each sample at different time points were analyzed by setting the level of the control samples as 1 (b-e). Values in (b-e) were calculated from three independent biological repetitions (mean \pm SE). The vertical bars with different lower-case letters are significantly different from each other at $P < 0.05$ (one-way ANOVA).

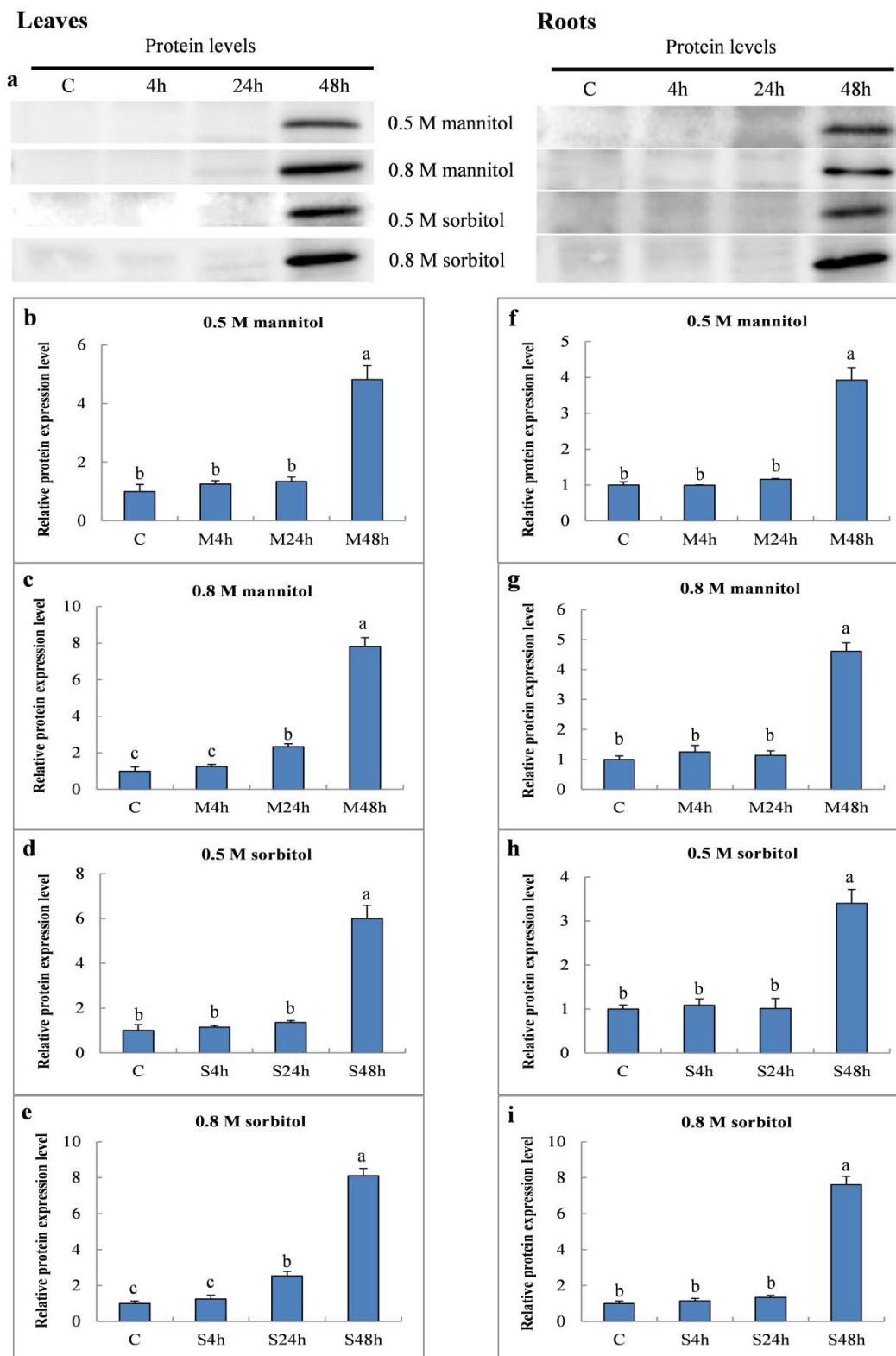


Fig. 13 (a) Expression abundance of the CpCCT1 protein in *C. plantagineum* leaves and roots under different osmotic stresses. Expression levels of the CpCCT1 protein in leaves treated with 0.5 M mannitol (b), 0.8 M mannitol (c), 0.5 M sorbitol (d) and 0.8 M sorbitol (e), and roots treated

with 0.5 M mannitol (**f**), 0.8 M mannitol (**g**), 0.5 M sorbitol (**h**) and 0.8 M sorbitol (**i**) were measured by Western blot. Equal loading of proteins were monitored by staining the membrane with Ponceau S (data not shown). Fold changes of each sample at different time points were analyzed by setting the level of control samples as 1 (**b-i**). Values in (**b-i**) were calculated from three independent biological repetitions (mean \pm SE). The vertical bars with different lower-case letters are significantly different from each other at $P < 0.05$ (one-way ANOVA).

3.6 Yeast complementation assay

To elucidate the possible function of the newly identified gene *CpCCT1*, we performed a complementation assay of the yeast *cct* mutant (provided by Scientific Research and Development GmbH, Oberursel, Germany) with the plant cDNA *CpCCT1*. Firstly, the yeast genotyping has been performed for WT yeast (BY4741, genotype: MATa; his3D1; leu2D0; met15D0; ura3D0 / Euroscarf Y0000) and *cct* mutant yeast cells (Fig. 14a). The results showed that the mutant yeast is a *cct* mutant type, while the WT type contains yeast *CCT* gene (Fig. 14a). The full length *CpCCT1* cDNA was cloned into a pDR-195 vector with specific primers and the constructed vector was transformed into WT yeast and *cct* mutant yeast cells. The yeast colony PCR was performed to verify the successful transformation (Fig. 14b).

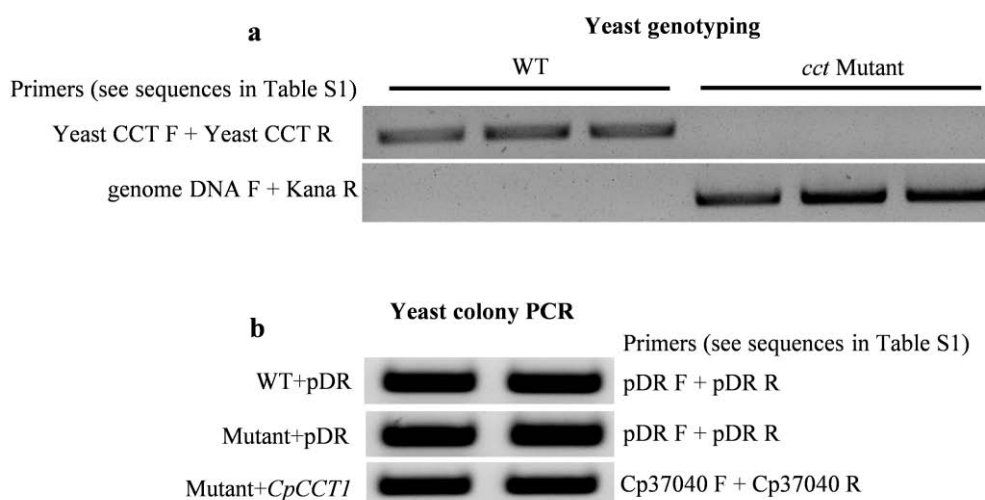


Fig. 14 The genotyping PCR for wild type (WT) and *cct* mutant yeast cells (**a**), and yeast colony

PCR for transformed yeast cells **(b)**. The specific primers were used for different PCR programs (see details in Table S1).

To inspect the possible complementary effect of full length *CpCCT1* cDNA in *cct* mutant yeast cells, transformed yeast cells were treated in different conditions, including different concentration of NaCl, KCl, mannitol, and 3-amino-1,2,4-triazole (3-AT), and different pH values (see the specific treatment methods in Materials and methods). As shown in Fig. 15, the growth state of *cct* mutant+*CpCCT1*, WT+pDR empty vector (as a positive control) and *cct* mutant+pDR empty vector (as a negative control) yeast cells was monitored on the same YPAD plate for each treatment. The results showed that the three types of yeast cells grew slower under NaCl and KCl treatments than those under control conditions (Fig. 15a). The growth state of yeast cells was also affected by different concentrations of NaCl and KCl (Fig. 15a). Namely, the higher concentration caused slower growth of all the three types of yeasts. The effect of the NaCl and KCl treatments also could partly be replaced by each other (Fig. 15a).

In Fig. 15b, the growth of three types of yeast cells was significantly receded in the presence of 0.5 M mannitol or 1 M mannitol, while the growth state of three types of yeast cells treated with 3-AT or different pH values was slightly better than that under control condition (Fig. 15b). In addition, the relative growth state was measured using Image-J software and calculated by setting the growth state of the positive control yeast (WT+pDR empty vector) as 1 (Fig. 15c, d). However, no significant functional complementation was observed in all the treatments tested and described above (Fig. 15).

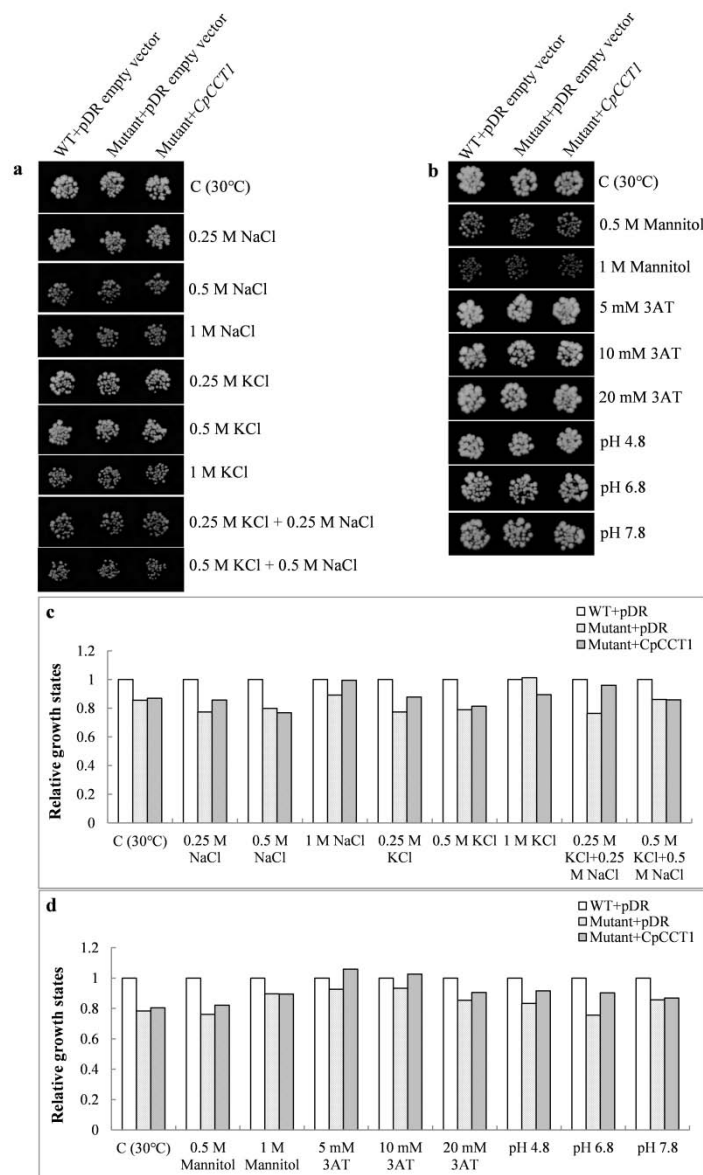


Fig. 15 Functional complementation of *S. cerevisiae cct* mutant with *C. plantagineum CpCCT1* cDNAs. Growth states were checked in parallel on selective plates (YPAD medium omit Uracil) under different treatment conditions: **(a)** different concentrations of NaCl and KCl treatments; **(b)** different concentrations of mannitol, 3AT and different pH. Four serial 1:10 dilutions of yeast cell suspensions starting from OD₆₀₀=0.1 were tested for each construct (data only show the growth state of the fourth dilution). The wild type yeast+pDR empty vector was used as a positive reference, and the yeast mutant+pDR empty vector was used as a negative control. **(c, d)** The relative growth state was analyzed by setting the growth state of WT+pDR empty vector as 1 using the Image-J software.

3.7 *CpCCT1* promoter activity in response to dehydration

To study the promoter activity of the *CpCCT1* gene in response to dehydration, the promoter region (1197 bp) was cloned and fused to GUS as a reporter gene. Several putative *cis*-acting elements which were associated with dehydration-induced gene expression are present in the promoter region of *CpCCT1* (Fig. 16a). Two ABA-responsive elements (ABREs) and three drought-responsive elements (DREs) were observed. The promoter activity was evaluated by monitoring GUS accumulation in dehydrated leaf tissues after transient transformation. The results showed that the *CpCCT1* promoter responds to dehydration both in *C. plantagineum* and *A. thaliana* (Fig. 16b). However, the *CpCCT1* promoter activity was lower (around 50%) than the activity of the stress inducible *Cp13-62* promoter which had been studied previously (Giarola et al. 2018).

a Putative *cis*-acting regulatory elements in *CpCCT1* promoter region

<i>cis</i> -element	sequence	position
ABRE	ACGT	-145, -1099
DRE	CCGAC	-718, -751, -944
MYBCORE	CNGTTR	-744, -979, -1183

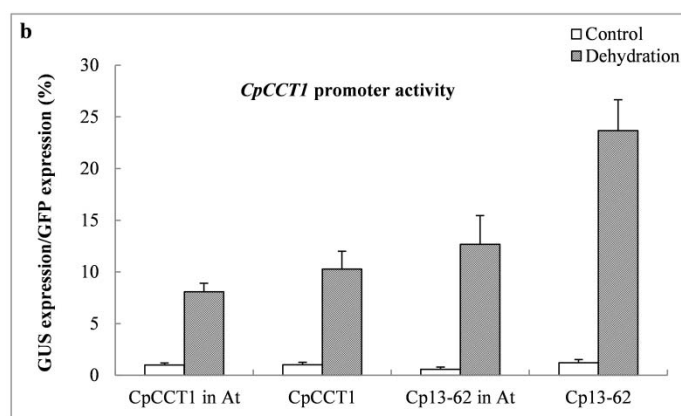


Fig. 16 Putative *cis*-acting regulatory elements in the *CpCCT1* promoter region and the *CpCCT1* promoter activity in response to dehydration in *C. plantagineum* and *A. thaliana*. (a) The table shows *cis*-elements and their positions in the *CpCCT1* promoter. N represents any nucleotide and

R represents adenine or guanine. (b) The wild-type *CpCCT1* promoter fragment was fused to the GUS reporter gene and tested their activities under dehydration in the leaf tissues of *C. plantagineum* and *A. thaliana* using a transient expression assay. The values were calculated from four independent experiments (mean \pm SE) for each treatment.

3.8 CpCCT1 interaction network prediction

To further investigate the possible function of CpCCT1 in *C. plantagineum*, the interaction network was constructed using STRING and Cytoscape software based on the data from *A. thaliana*. Interaction network analysis revealed that 10 nodes and 19 edges were observed for CpCCT1 (Fig. 17). The results showed that CpCCT1 could interact with choline/ethanolamine phosphotransferase 1 and 2 which can catalyze phosphatidylcholine and phosphatidylethanolamine biosynthesis (Liu et al. 2015), and interact with PEAMT1 (Phosphoethanolamine methyltransferase 1) which can catalyze three methylation steps and is required for root system development and epidermal cell integrity (Craddock et al. 2015).

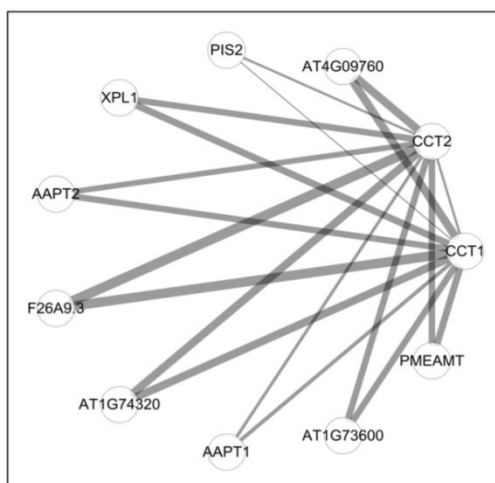


Fig. 17 Prediction of the interaction network of CpCCT1. The network was constructed using STRING and Cytoscape software based on the data from *A. thaliana*. Interaction combined scores are indicated by the width of the edge. The annotation of genes in this predicted network can be found in STRING database (<https://string-db.org/>).

4 Discussion

Plant PC biosynthesis involves a series of reactions consuming carbon and energy, and CCT enzymes catalyze a key regulatory step in PC formation (Inatsugi et al. 2009). According to our previous research on polysomal profiling analysis in *C. plantagineum*, the *CpCCT1* transcripts were induced after dehydration treatment and it was under translational regulation from the partial dehydration phase to desiccation (Fig. 1a, b). In order to further study the function of *CpCCT1* in the resurrection plant *C. plantagineum*, the full coding sequence of *CpCCT1* gene was cloned in this study.

Mammalian CCTs and AtCCT has four functional domains named the N-terminal signal domain (important for nuclear transport), catalytic core domain, membrane-binding regulatory domain, and C-terminal phosphorylation domain (Cornell et al. 1995; Cornell and Northwood 2000; Caldo et al. 2019). The sequence analysis showed that CpCCT1 and its homologs (e.g. LbCCT from *L. brevidens*, LsCCT from *L. subracemosa*, AtCCT1, ScCCT and rat CCT1) had almost conserved catalytic domains and membrane-binding domains while the N-terminal and C-terminal domains differed, except for the homology of membrane-binding domain between CpCCT1 and ScCCT was relatively lower (8.64% identity) (Fig. 2-4). The catalytic domain was highly conserved between CpCCT1 and rat CCT1 with a sequence identity of 57.8%, which was similar as the value (59.3%) between AtCCT1 and rat CCT1 reported previously (Fig. 4b) (Caldo et al. 2019). We also compared the catalytic domain between desiccation tolerant plant and desiccation sensitive plant, namely between CpCCT1 and AtCCT1. The result showed a higher conservation of CCT catalytic domain among plants compared to rat or yeast, with a sequence identity of 85.6% (Fig. 4b). This feature in different CCT sequences had been reported for different species (Cornell et al. 1995; Choi et al. 1997; Jones et al. 1998; Caldo et al. 2019).

The CCT sequences were predicted in *L. brevidens* and *L. subracemosa*, which

are closely related species of *C. plantagineum*. *C. plantagineum* and *L. brevidens* are the desiccation tolerant species whereas *L. subracemosa* is the desiccation sensitive plant within the *Linderniaceae* family, which are good sources of plants for comparative studies (Giarola et al. 2018). The LbCCT and LsCCT predicted protein sequences were compared with CpCCT1, which showed a sequence identity of 78.2% between CpCCT1 and LbCCT, and a sequence identity of 39.6% between CpCCT1 and LsCCT (Fig. 3). The results indicated that the CCT sequences are more conserved between desiccation tolerant species compared with the desiccation sensitive species within the *Linderniaceae* family.

A HXGH motif contained in the catalytic domain was implicated in binding CTP and stabilizing the transition states, which is the characteristic of the cytidyltransferase superfamily (Bork et al. 1995; Veitch et al. 1996, 1998; Helmink et al. 2003). In our sequence alignment results, the plants CCT including CpCCT1, LbCCT, LsCCT and AtCCT1 contained the same sequence: HFGH in the HXGH motif, while the rat CCT1 and ScCCT had different sequences: HSGH and HLGH, respectively (Fig. 3, Fig. 4a). The membrane-binding domain in rat CCT1 could modulate CCT activity through weakly and reversibly binding to membranes by amphitrophism (Cornell 2016). An auto-inhibitory motif contained in the membrane-binding domain could form an α -helix, and interact with another helix which is located at the bottom part of the catalytic domain (Lee et al. 2014). The amphipathic helices shown in rat CCT1 and AtCCT1 are also predicted in CpCCT1 (Fig. 5) (Lee et al. 2014; Caldo et al. 2019).

Previous data indicated that CCT could function to generate CDP-choline in both cytoplasmic and nuclear compartments (Cornell and Ridgway 2015). CCT was thought to traffic in vesicles, so its cellular localization might be cytoplasmic or nuclear in different type of cells (Wang et al. 1995; Houweling et al. 1996; Kent 1997). In this study, our prediction of cellular localization also showed that CpCCT1 was most likely to be localized in the cytoplasm and nucleus (Fig. 6). Consistent with the

prediction, the localization of the full-length CpCCT1-GFP in transformed onion cells showed that the CpCCT1-GFP proteins are localized in cytoplasm in untreated cells and in plasmolyzed cells (Fig. 7a). Nevertheless, the subcellular fractionation results indicated that CpCCT1 proteins existed in all the four fractions (Fig. 7b, d). Research on transgenic *A. thaliana* expressing AtCCT1-sGFP under the control of *ProCCT1* and *Pro35S* showed that the AtCCT1-sGFP was detected in the cell nuclei of flower buds, carpels, sepals, and roots, which demonstrated that the AtCCT1 was located in nucleus (Hayakawa et al. 2015). However, the PSORT or the cNLS Mapper used in the previous searches failed to identify a putative nucleus-localizing signal of CCT (Nakai and Kanehisa 1992; Kosugi et al. 2009). According to the above results, the localization of CCT in different types of cells remains an open question. In addition, the immunoblots for analyzing tissue specific expression showed that CpCCT1 proteins existed in leaf, root, callus, flower, and stem tissues after dehydration, and also in untreated callus (Fig. 7c, e). The results suggested that *CpCCT1* might be a non-tissue-specific gene while it is a dehydration-induced gene.

Considering the importance of PC synthesis in cellular function and the key step mediated by the CCT enzyme in PC synthesis, we analyzed the expression of CpCCT1 both on the transcriptional and translational level during different treatments in the resurrection plant *C. plantagineum* (Fig. 8-10, 12-13). The results showed that the *CpCCT1* transcripts accumulated after dehydration, salt stress and cold stress in leaf and root samples (Fig. 8). Similarly, the CpCCT1 proteins also accumulated in *C. plantagineum* leaves and roots during dehydration and salt stress, while cold stress did not induce the CpCCT1 proteins even though the transcripts increased after treatment at 4 °C for 4 h (Fig. 7d, g, Fig. 12). It has been reported that the cellular PC contents increased during cold acclimation by up-regulating PC biosynthesis in *A. thaliana* (Inatsugi et al. 2009). When *A. thaliana* plants were treated at 2 °C for 12 h, the level of *AtCCT2* transcripts in the rosettes increased and were around 6-fold higher than those of the control samples whereas no significant change occurred on the level of *AtCCT1* transcripts during 7 d of 2 °C treatment (Inatsugi et al. 2002). However, the

immunoblot analyses in *cct1* or *cct2* mutant plants revealed that AtCCT2 or AtCCT1 proteins increased after exposure to 2 °C for 7 d, respectively, which coincides with the increased enzyme activity (Inatsugi et al. 2009).

To test osmotic stress, high concentrations (0.5 M and 0.8 M) of mannitol were prepared and used in the CpCCT1 expression analyses. The expression of the glycine-rich protein 1 (CpGRP1) and cell wall-associated protein kinase 1 (CpWAK1) and CpWAK2 had been reported to be induced in response to mannitol treatment (Giarola et al. 2016). The 0.5 M and 0.8 M mannitol treatments significantly induced the transcript abundance of *CpCCT1* in leaves after 4 h, then the *CpCCT1* transcript level gradually decreased after 24 h or 48 h (Fig. 9a, b, c). Interestingly, the CpCCT1 protein level in leaves was induced at 48 h after treated with 0.5 M and 0.8 M mannitol (Fig. 13a, b, c). The detached leaves were also incubated in 0.5 M and 0.8 M sorbitol (the isomer of mannitol) solutions. The expression pattern of CpCCT1 in leaves treated with sorbitol was similar as that in mannitol treatments (Fig. 9, 13). The 0.8 M mannitol and 0.8 M sorbitol treatments induced higher transcript and protein abundance in leaves than the 0.5 M mannitol and 0.5 M sorbitol treatments (Fig. 9, 13). At the same time, roots of *C. plantagineum* were treated in the same way as leaves. The expression pattern of CpCCT1 in roots was similar to that of leaf samples, except for the *CpCCT1* transcript in roots was induced to reach a peak after 24 h of osmotic stress, which is later than the leaf samples (Fig. 9, 13). The results suggested that the accumulation of CpCCT1 proteins at 48 h after mannitol and sorbitol treatments are probably attributed to the transient up-regulation of the *CpCCT1* transcripts.

It is known that ABA is a mediator of abiotic stress responses (Leung and Giraudat 1998). In *C. plantagineum*, many desiccation-related genes accumulate in response to exogenous ABA application (Bartels et al. 1990; van den Dries et al. 2011; Giarola et al. 2016). The transcript level of *CpCCT1* increased after 4 h of ABA treatment and reached a peak after 24 h, then slightly decreased after 48 h in leaves

and roots under 100 μM ABA treatment (Fig. 10a, b, d). However, no CpCCT1 protein was detected in ABA treated samples. The results might indicate that CpCCT1 is probably involved in ABA-related pathways. IAA as a widely known plant hormone was reported to negatively affect CCT enzyme activity in pea (*Pisum sativum*) (Price-Jones and Harwood 1986). However, in the roots and stems of pea (*Pisum sativum*), transcripts of CCT were induced by treatment with 0.1 μM IAA (Jones et al. 1998). Our results are in agreement with the reported results in pea. The transcript abundance of *CpCCT1* was induced in detached leaves and roots after 1 μM IAA treatments for 4 h and 48 h, respectively (Fig. 10c, e). The results indicated that *C. plantagineum* roots might be more sensitive to IAA. There was no CpCCT1 protein detected in leaves or roots after treated with 1 μM IAA, which agreed with the reported results in pea to some extent (Price-Jones and Harwood 1986).

The yeast complementation assay for plant CCTs had been successfully completed in *B. napus* and *A. thaliana* (Nishida et al. 1996; Choi et al. 1997). In our results, we found that the yeast growth state changed under different treatments, whereas no significant enzyme activity complementation was observed in the whole experiment (Fig. 15). It suggests that the CCT from *C. plantagineum* failed to restore the enzyme activity in the yeast *cct* mutant. Comparing to the previous successful cases, different types of yeast had been used in the complementary assay with *B. napus* and *A. thaliana* CCTs (Nishida et al. 1996; Choi et al. 1997). As shown in Fig. 15, the growth state of the yeast *cct* mutant was almost the same as that of WT yeast in all the treatment conditions, which made it hard to discover the complementation caused by the CpCCT1. The results suggested that we might not find out the suitable treatment condition. Furthermore, according to the alignment results (Fig. 4), although the sequence identity of the catalytic domain between ScCCT and CpCCT1 is 56.02%, the N-terminal region, membrane-binding domain and C-terminal region between ScCCT and CpCCT1 are very divergent (Fig. 4c). The divergent sequence between ScCCT and CpCCT1 might also be a reason for the inapparent result of enzyme activity complementation with CpCCT1.

The dehydration responsive element binding (DREB) transcription factor was reported to regulate many dehydration-inducible genes through binding to DRE *cis*-elements in the promoters (Lata and Prasad 2011). Many ABA-dependent drought-related genes containing a conserved ABRE *cis*-element with ACGT core are mainly regulated by the basic-domain leucine zipper (bZIP) transcription factor (Uno et al. 2000; Fujita et al. 2009). The DRE and ABRE *cis*-elements were identified and analyzed in the promoter region of *LEA-like 11-24* and *CpGRP1* in *C. plantagineum* (van den Dries et al. 2011; Giarola et al. 2016). In this study, the *CpCCT1* promoter containing putative DRE and ABRE *cis*-elements showed activities in response to dehydration both in *C. plantagineum* and *A. thaliana*, but the *CpCCT1* promoter activity only reached around 50% of *Cp13-62* promoter activity (Fig. 16b). The relative lower *CpCCT1* promoter activity together with the highest transcripts level in partially dehydrated samples (Fig. 8) and the highest protein level in desiccated samples (Fig. 12) might suggest a translational regulation of *CpCCT1* gene expression during dehydration stress, which verified our initial results from RT-qPCR (Fig. 1b).

The phosphorylation of mammalian CCTs mainly localized in the C-terminal phosphorylation domain, which has an effect on regulation of enzyme activity (Cornell et al. 1995). A more recently study showed this part was missing in plant CCTs, instead, the phosphorylation of AtCCT1 occurred in the catalytic domain at Ser-187 by SnRK1 (Caldo et al. 2019). Our future work will focus on the enzyme regulatory mechanisms of CCTs in the resurrection plant *C. plantagineum* through heterologous overexpression and purification.

Supporting data

Table S1 Primers used in this study.

5' and 3' end clone	Sequence (5' to 3')	Restrict. site
ZAP F2	CAGGAAACAGCTATGAACC	-
CpDN37040 R	CATGAAACGCCAATCAAATG	-
Protein overexpression	Sequence (5' to 3')	Restrict. site
CpORF37040 F1	AGAAAACCTCGCGCCAAGAAC	-
Cp37040 XhoI R	ATGGCTCGAGCTTTTCTCGCCGTCGTCCTCTT	XhoI
Protein localization	Sequence (5' to 3')	Restrict. site
CpORF37040 F1	AGAAAACCTCGCGCCAAGAAC	-
Cp37040 NcoI R1	TGGACCCATGGTTTTCTCGCCGTCGTCCTCTT	NcoI
Yeast complementation assay	Sequence (5' to 3')	Restrict. site
Cp37040 XhoI F	AGGAGACTCGAGATGGATGAGAGCAGCA	XhoI
Cp37040 BamHI R	TGGTGCGGATCCTTTTTCTCGCCGTCGT	BamHI
RT-PCR	Sequence (5' to 3')	Restrict. site
Cp37040 F	TGCAGATACGAGTGGAGCTG	-
Cp37040 R	CCAGATTCTTGTTGCCCTGT	-
CpEF1 α F	AGTCAAGTCCGTCGAAATGC	-
CpEF1 α R	CACTTGGCACCCTTCTTAGC	-
Promoter::GUS fusions	Sequence (5' to 3')	Restrict. site
CpCCT1 promoter F	CCTAACCAAGCTTTTGATCAGTTAGG	HindIII
CpCCT1 promoter R	AACAGGGCGACGAATTACAG	-
Yeast genotyping	Sequence (5' to 3')	Restrict. site
Yeast CCT F	ACCCAATAAGCGAAATGTGC	-
Yeast CCT R	ATGTGGCCAAGATGGAAAAG	-
genome DNA F	ACCCAATAAGCGAAATGTGC	-
Kana R	CATCGGGCTTCCCATACAATCG	-
Yeast colony PCR	Sequence (5' to 3')	Restrict. site
pDR F	ACACACATTCAAAGAAAGAAAAA	-
pDR R	TTTCGTAAATTTCTGGCAAGG	-

CHAPTER 5

General discussion

Desiccation as one of the most formidable obstacles affects the successful adaptation to continental environments (Farrant and Moore 2011). Desiccation tolerance is considered as the key solution for terrestrial plants for survival on land (Farrant and Moore 2011). Desiccation tolerance acquisition involves protection mechanisms for membranes, chloroplasts, and macromolecules (Dinakar and Bartels 2013; Gechev et al. 2012). *C. plantagineum* as an extreme desiccation tolerant resurrection plant belongs to the *Linderniaceae* family, which can survive extreme dehydration and achieve full recovery after re-watering (Gaff 1971; Bartels and Salamini 2001). Some genes and mechanisms related to this vegetative desiccation tolerance in *C. plantagineum* have been reported over time. In this work, genes under translational regulation in different physiological conditions were identified through RNA sequencing (**CHAPTER 3**). One gene was selected for detailed studies. The gene encodes the rate limiting enzyme CTP:phosphocholine cytidyltransferase (CCT) for PC synthesis (**CHAPTER 4**). Stress memory responses can lead to increased stress tolerance in plants (Ramírez et al. 2015). *C. plantagineum* was exposed to multiple dehydration/rehydration treatments to check the putative memory responses in a desiccation tolerant plant (**CHAPTER 2**).

1 The responses to reiterated dehydration in plants

The memory for a previously experienced environmental cue may last several days or even months. This can affect the later stress responses or development of plants (Hilker and Schmölling 2019). In agreement with previous reports, the dehydration stress-induced memory responses identified in *C. plantagineum* can persist for up to six days after the stress stimulation has disappeared (Fig. 10 in **CHAPTER 2**).

The stress memory responses affected by a previous stress event were reflected on the physiology and biochemistry level through rapidly adjusting the structural and functional adaptation, including minimizing the water loss rate, ROS homeostasis, and alteration of photosynthetic rate (Fleta-Soriano and Munné-Bosch 2016). Among them, minimizing water loss was reported to be a key factor for survival of plants through keeping the stomata partially closed during a subsequent dehydration stress (Hu et al. 2012; Shi et al. 2012; Virilouvet and Fromm 2015). Ding et al. (2012) reported that *A. thaliana* plants which had encountered the second, third and fourth dehydration stress had a significantly lower water loss rate than the first stress event. A similar phenomenon was observed in the leaves of *C. plantagineum*: the water loss rate decreased from the first dehydration stress event to the fourth stress event (Fig. 1 in **CHAPTER 2**). During dehydration, the excessive production of ROS could induce oxidative stress, then give rise to lipid peroxidation and even cause damage of the nucleic acids and proteins damage (Mittler et al. 2004; Liu and Chan 2015). Reddy et al. (2004) reported that photosynthesis is one of the most sensitive processes affected by abiotic stresses. The dehydration stress memory found in *Aptenia cordifolia* plants by Fleta-Soriano et al. (2015) showed that the level of lipid hydroperoxides and ratios of chlorophyll a/b increased in the double stressed plants. In this study, the metabolite changes observed in leaf samples of *C. plantagineum* showed that SOD activity gradually increased, H₂O₂ content decreased while total chlorophyll content and MDA content were retained at a similar level during reiterated dehydration stress treatments (Fig. 2 in **CHAPTER 2**).

The responses to reiterated dehydration in plants are not only reflected on the physiological and biochemical level but also on the transcriptional and translational level. Researches showed that transcriptional responses to a subsequent stress could be altered by a previous stress treatment or multiple consecutive stress/recovery treatments (Ding et al. 2012; Liu et al. 2014, 2016; Hu et al. 2016). The accumulation of transcripts and proteins of stress-related genes during repetitive exposures to dehydration suggested that stress memory responses existed in the desiccation tolerant

plant *C. plantagineum* on the molecular level (Fig. 4, 5, 6, 7, and 9 in **CHAPTER 2**). The dehydration stress memory responses observed here is probable a general feature of a plant memory in resurrection plants. Campos and Reinberg (2009) reported that changes of gene expression patterns were usually correlated with changes of the chromatin status. The changes in DNA methylation, histone modifications, RNA molecules, prions, and chromatin structures could contribute to epigenetic inheritance of the memory in plants, which plays an important role in the control of gene expression and presents epigenetic mechanisms of a stress memory (Campos and Reinberg 2009).

The dehydration stress memory in *C. plantagineum* plants may cause cross-protection to other environmental conditions besides dehydration, which are referred to as cross memory. Due to the irregular and variable growth environments, cross stress tolerance is extremely important in overcoming unpredictable and diverse stresses happened during the whole life span of plants (Walter et al. 2013). Munne-Bosch and Alegre (2013) reported that cross stress memory is regulated by a complex network involving the interaction of multiple external and internal factors. There is plenty of evidence that cross memory could happen between cold and drought stress, between drought and heat stress, or even between biotic stress and abiotic stress in different plant species, including *A. thaliana*, strawberry, *P. nigra*, spring wheat, *etc.* (Shinozaki and Yamaguchi-Shinozaki 2000; Kreyling et al. 2012; Rajashekar and Panda 2014; Li et al. 2015; Wang et al. 2015).

Like the resurrection plant *C. plantagineum*, the seeds of most angiosperm plants are tolerant to desiccation (Giarola et al. 2017). Currently, seed priming is reported as an efficient and low-cost approach to increase crop yield, which could not only promote seed germination and improve plant growth state, but also increase the tolerance of abiotic stresses (Sher et al. 2019). Even though seed priming is different from plant priming, it stimulated us to address the question whether the desiccation tolerant resurrection plant *C. plantagineum* could gain tolerance to biotic and/or

abiotic stress except for dehydration stress, through the similar treatments as seed priming. Desiccated *C. plantagineum* plants probably can be treated with hydropriming, osmopriming, solid matrix priming, biopriming, nutripriming, hormonal priming, and thermopriming methods which have already been used for seed priming. If untreated *C. plantagineum* plants are treated in different ways and then stress memory responses are induced to a second treatment; the phenomenon should be called cross stress memory. However, if we use desiccated *C. plantagineum* plants to do such experiments, it may induce different responses compared to the untreated plants. This hypothesis might contribute to uncover a new sight of plant priming or plant stress memory.

2 Regulation of expression of genes related to desiccation tolerance and recovery in *C. plantagineum*

It has been reported that gene expression was regulated on several different levels, of which the regulation on the translational level is an important response mechanism, which governs protein production in response to various environmental conditions in plants (Hershey et al. 2012; Chassé et al. 2016). Currently, polysome profiling has become a powerful technique to analyze the translational regulation of gene expression under a specific condition (Kawaguchi et al. 2004; Panda et al. 2017).

Polysome profiling was done with RNA obtained from sucrose gradient-based polysome mRNA isolation. This has been used to deduce the translational state of a specific mRNA in a specific tissue (Chassé et al. 2016; Smit et al. 2018). In this work, the polysome profiling and the total mRNA profiling of samples from untreated, partially dehydrated, desiccated and rehydrated stages were used to analyze gene expression profiles in *C. plantagineum* (**CHAPTER 3**). Combined with the total mRNA profiling, we could calculate the polysome occupancy, which represents the ratio between polysomal mRNA abundance and total mRNA abundance of a specific mRNA. This was used to deduce the translational efficiency of a specific mRNA (Bai

et al. 2017). According to the changes of polysome occupancy in different stages of hydration of *C. plantagineum*, we identified more genes with increased polysome occupancy from partial dehydration to desiccation than from desiccation to rehydration (Fig. 2 in **CHAPTER 3**). The increased polysome occupancy for a specific gene during a specific stage suggests that the amount of polysomal mRNA was higher than that of total mRNA, and also indicated that this gene was under translational regulation. The patterns of polysome occupancy changes in *C. plantagineum* suggest that if more mRNAs bind to polysomes it might prevent mRNA degradation caused by extreme water loss while the protection mechanisms receded during the rehydration stage (Fig. 1, 2 in **CHAPTER 3**).

The translation rate and the translational ratio could increase with the decreasing of mRNA length and GC content (Valleriani et al. 2011; Qu et al. 2011). The effective number of codons (N_c) and the GC content of the third base position (GC3) are also correlated with translational regulation (Crick, 1966; Akashi 1994; Duret 2000; Bai et al. 2017). The sequence features investigated in the stages from partial dehydration to desiccation and from desiccation to rehydration showed that the transcript length, GC content, GC3 content, N_c and enriched motifs are involved in the translational regulation in the resurrection plant *C. plantagineum* (Fig. 5, 6 in **CHAPTER 3**). Several transcription factor gene families found in this work together with their putative interaction networks might have important functions in plant adaptation under dehydration stress (Fig. 9, 12 in **CHAPTER 3**). Although this analytical work is entirely based on the RNA-seq data, it can still provide some references for future research.

3 The function, regulation and structure of CTP:phosphocholine cytidyltransferase (CCT) in plants

The metabolic map of PC biosynthesis in *Arabidopsis* drawn by Liu et al. (2019) showed that CCT was a rate limiting enzyme catalyzing phosphocholine which is

converted to CDP-choline. PC as a main structural component of cell membranes in plants has an important role in keeping the integrity and functionality of cell membranes and can participate in stress defenses (Chen et al. 2018; Sun et al. 2020). The cell membrane integrity was reported to be one of the factors most strongly affected by various stresses (Willing and Leopold 1983). Considering all these factors, the expression of CpCCT1 was investigated in this work on the transcriptional and translational level under different treatment conditions in the resurrection plant *C. plantagineum* (**CHAPTER 4**). In agreement with the results from previous research, the expression of CpCCT1 in leaf and root samples was increased both on the transcriptional and translational level under dehydration stress, salt and osmotic stress, but it failed to respond to cold stress, exogenous 100 μ M ABA and 1 μ M IAA treatments on the translational level (Price-Jones and Harwood 1986; Jones et al. 1998; Inatsugi et al. 2002) (Fig. 8, 9, 10, 12, 13 in **CHAPTER 4**).

The structure of CCT has been uncovered by Caldo et al. (2019) in *A. thaliana* through the comparison with rat CCT. AtCCT has four domains, named as N-terminal signal domain (variegated), catalytic core domain (conserved), membrane-binding regulatory domain (conserved), and C-terminal phosphorylation domain (variegated) (Caldo et al. 2019). Compared with AtCCT1, rat CCT1 and ScCCT, the CpCCT1 also has a conserved catalytic domain and membrane-binding domain while the N-terminal and C-terminal domains of CpCCT1 are very diverse (Fig. 4 in **CHAPTER 4**). The relatively lower sequence identity between ScCCT and CpCCT1 might be the reason for the inapparent result of enzyme activity complementation with CpCCT1 in *cct* mutant yeast (Fig. 4, 15 in **CHAPTER 4**). According to the predicted CCT sequences in *L. brevidens* and *L. subracemosa*, CCT sequences are more conserved between desiccation tolerant species compared with the desiccation sensitive species in *Linderniaceae* family (Fig. 2, 3 in **CHAPTER 4**). These structural features might contribute to future research on the enzyme regulatory mechanisms of CCT in the resurrection plants.

REFERENCES

- Akashi H (1994) Synonymous codon usage in *Drosophila melanogaster*: natural selection and translational accuracy. *Genetics* 136:927-935
- Alam MN, Zhang L, Yang L, Islam MR, Liu Y, Luo H, Yang P, Wang Q, Chan Z (2018) Transcriptomic profiling of tall fescue in response to heat stress and improved thermotolerance by melatonin and 24-epibrassinolide. *BMC Genomics* 19:224
- Alpert P, Oliver M (2002) Drying without dying. In: Black M, Pritchard HW (ed) *Desiccation and Survival in Plants: drying without dying*. CABI Publishing, Wallingford, pp 4-43
- Alvarez-Venegas R, Abdallat AA, Guo M, Alfano JR, Avramova Z (2007) Epigenetic control of a transcription factor at the cross section of two antagonistic pathways. *Epigenetics* 2:106-113
- Apel K, Hirt H (2004) Reactive oxygen species: metabolism, oxidative stress, and signal transduction. *Annu Rev Plant Biol* 55:373-399
- Arava Y, Wang Y, Storey JD, Liu CL, Brown PO, Herschlag D (2003) Genomewide analysis of mRNA translation profiles in *Saccharomyces cerevisiae*. *Proc Natl Acad Sci USA* 100:3889-3894
- Avramova Z (2015) Transcriptional ‘memory’ of a stress: transient chromatin and memory (epigenetic) marks at stress-response genes. *Plant J* 83:149-159
- Azzam ME, Algranati ID (1973) Mechanism of puromycin action: fate of ribosomes after release of nascent protein chains from polysomes. *Proc Natl Acad Sci USA* 70:3866-3869
- Bai B, Novák O, Ljung K, Hanson J, Bentsink L (2018) Combined transcriptome and translome analyses reveal a role for tryptophan-dependent auxin biosynthesis in the control of *DOG1*-dependent seed dormancy. *New Phytol* 217:1077-1085
- Bai B, Peviani A, Horst S, Gamm M, Snel B, Bentsink L, Hanson J (2017) Extensive translational regulation during seed germination revealed by polysomal profiling. *New Phytol* 214:233-244
- Bailey TL, Boden M, Buske FA, Frith M, Grant CE, Clementi L, Ren J, Li WW, Noble WS (2009) MEME SUITE: tools for motif discovery and searching. *Nucleic Acids Res* 37:W202-W208
- Bajji M, Kinet JM, Lutts S (2002) The use of the electrolyte leakage method for assessing cell

REFERENCES

- membrane stability as a water stress tolerance test in durum wheat. *Plant Growth Regul* 36:61-70
- Barkan A (1993) Nuclear mutants of maize with defects in chloroplast polysome assembly have altered chloroplast RNA metabolism. *Plant Cell* 5:389-402
- Barkan A (1998) Approaches to investigating nuclear genes that function in chloroplast biogenesis in land plants. *Method Enzymol* 297:38-57
- Bartels D, Hussain SS (2011) Resurrection plants: physiology and molecular biology. In: Lüttge U, Beck E, Bartels D (ed) *Plant desiccation tolerance*. Springer, Heidelberg, pp 339-364
- Bartels D, Salamini F (2001) Desiccation tolerance in the resurrection plant *Craterostigma plantagineum*. A contribution to the study of drought tolerance at the molecular level. *Plant Physiol* 127:1346-1353
- Bartels D, Schneider K, Terstappen G, Piatkowski D, Salamini F (1990) Molecular cloning of abscisic acid-modulated genes which are induced during desiccation of the resurrection plant *Craterostigma plantagineum*. *Planta* 181:27-34
- Bartels D (2005) Desiccation tolerance studied in the resurrection plant *Craterostigma plantagineum*. *Integr Comp Biol* 45:696-701
- Basbous-Serhal I, Soubigou-Taconnat L, Bailly C, Leymarie J (2015) Germination potential of dormant and nondormant *Arabidopsis* seeds is driven by distinct recruitment of messenger RNAs to polysomes. *Plant Physiol* 168:1049-1065
- Beck EH, Fettig S, Knake C, Hartig K, Bhattarai T (2007) Specific and unspecific responses of plants to cold and drought stress. *J Biosci* 32:501-510
- Benjamini Y, Hochberg Y (1995) Controlling the false discovery rate: a practical and powerful approach to multiple testing. *J R Stat Soc B* 57:289-300
- Bernacchia G, Salamini F, Bartels D (1996) Molecular characterization of the rehydration process in the resurrection plant *Craterostigma plantagineum*. *Plant Physiol* 111:1043-1050
- Berry S, Dean C (2015) Environmental perception and epigenetic memory: mechanistic insight through FLC. *Plant J* 83:133-148
- Besnard F, Rozier F, Vernoux T (2014) The AHP6 cytokinin signaling inhibitor mediates an auxin-cytokinin crosstalk that regulates the timing of organ initiation at the shoot apical meristem. *Plant Signal Behav* 9:e28788

REFERENCES

- Bewley JD, Krochko JE (1982) Desiccation tolerance. In: Lange OL, Nobel PS, Osmond BC, Ziegler H (ed) *Physiological plant ecology II*. Springer, Berlin, Heidelberg, pp 325-378
- Bewley JD (1979) Physiological aspects of desiccation tolerance. *Annu Rev Plant Biol* 30:195-238
- Bianchi G, Gamba A, Murelli C, Salamini F, Bartels D (1991) Novel carbohydrate metabolism in the resurrection plant *Craterostigma plantagineum*. *Plant J* 1:355-359
- Blum A (2017) Osmotic adjustment is a prime drought stress adaptive engine in support of plant production. *Plant Cell Environ* 40:4-10
- Blum A, Ebercon A (1981) Cell membrane stability as a measure of drought and heat tolerance in wheat 1. *Crop Sci* 21:43-47
- Bockel C, Salamini F, Bartels D (1998) Isolation and characterization of genes expressed during early events of the dehydration process in the resurrection plant *Craterostigma plantagineum*. *J Plant Physiol* 152:158-166
- Bonasio R, Tu S, Reinberg D (2010) Molecular signals of epigenetic states. *Science* 330:612-616
- Bork P, Holm L, Koonin EV, Sander C (1995) The cytidylyltransferase superfamily: Identification of the nucleotide-binding site and fold prediction. *Proteins* 22:259-266
- Brown JT, Yang X, Johnson AW (2000) Inhibition of mRNA turnover in yeast by an *xrn1* mutation enhances the requirement for eIF4E binding to eIF4G and for proper capping of transcripts by Ceg1p. *Genetics* 155:31-42
- Bruce TJ, Matthes MC, Napier JA, Pickett JA (2007) Stressful “memories” of plants: evidence and possible mechanisms. *Plant Sci* 173:603-608
- Caldo KMP, Xu Y, Falarz L, Jayawardhane K, Acedo JZ, Chen G (2019) Arabidopsis CTP: phosphocholine cytidylyltransferase 1 is phosphorylated and inhibited by sucrose nonfermenting 1-related protein kinase 1 (SnRK1). *J Biol Chem* 294:15862-15874
- Campos EI, Reinberg D (2009) Histones: annotating chromatin. *Annu Rev Genet* 43:559-599
- Candan N, Cakmak I, Ozturk L (2018) Zinc-biofortified seeds improved seedling growth under zinc deficiency and drought stress in durum wheat. *J Plant Nutr Soil Sci* 181:388-395
- Challabathula D, Bartels D (2013) Desiccation tolerance in resurrection plants: new insights from transcriptome, proteome and metabolome analysis. *Front Plant Sci* 4:482
- Challabathula D, Djilianov D, Bartels D (2012) Photosynthesis in desiccation tolerant plants:

REFERENCES

- energy metabolism and antioxidative stress defense. *Plant Sci* 182:29-41
- Challabathula D, Zhang Q, Bartels D (2018) Protection of photosynthesis in desiccation-tolerant resurrection plants. *J Plant Physiol* 227:84-92
- Chang HC, Tsai MC, Wu SS, Chang F (2019) Regulation of *ABI5* expression by ABF3 during salt stress responses in *Arabidopsis thaliana*. *Bot Stud* 60:16
- Chassé H, Boulben S, Costache V, Cormier P, Morales J (2016) Analysis of translation using polysome profiling. *Nucleic Acids Res* 45:e15
- Chen K, Arora R (2012) Priming memory invokes seed stress-tolerance. *Environ Exp Bot* 94:33-45
- Chen K, Fessehaie A, Arora R (2012a) Selection of reference genes for normalizing gene expression during seed priming and germination using qPCR in *Zea mays* and *Spinacia oleracea*. *Plant Mol Biol Rep* 30:478-487
- Chen L, Song Y, Li S, Zhang L, Zou C, Yu D (2012b) The role of WRKY transcription factors in plant abiotic stresses. *BBA-Gene Regul Mech* 1819:120-128
- Chen Y, Li B, Cen K, Lu Y, Zhang S, Wang C (2018) Diverse effect of phosphatidylcholine biosynthetic genes on phospholipid homeostasis, cell autophagy and fungal developments in *Metarhizium robertsii*. *Environ Microbiol* 20:293-304
- Chinnusamy V, Zhu JK (2009) Epigenetic regulation of stress responses in plants. *Curr Opin Plant Biol* 12:133-139
- Choi SB, Lee KW, Cho SH (1997) Cloning of CTP:phosphocholine cytidyltransferase cDNA from *Arabidopsis thaliana*. *Mol Cells* 7:58-63
- Clement JM, Kent C (1999) CTP: phosphocholine cytidyltransferase: insights into regulatory mechanisms and novel functions. *Biochem Biophys Res Commun* 257:643-650
- Colaneri AC, Jones AM (2013) Genome-wide quantitative identification of DNA differentially methylated sites in *Arabidopsis* seedlings growing at different water potential. *PloS ONE* 8:e59878
- Cooper K, Farrant JM (2002) Recovery of the resurrection plant *Craterostigma wilmsii* from desiccation: protection versus repair. *J Exp Bot* 53:1805-1813
- Cornell RB (2016) Membrane lipid compositional sensing by the inducible amphipathic helix of CCT. *BBA Mol Cell Biol L* 1861:847-861

REFERENCES

- Cornell RB, Kalmar GB, Kay RJ, Johnson MA, Sanghera JS, Pelech SL (1995) Functions of the C-terminal domain of CTP: phosphocholine cytidyltransferase. Effects of C terminal deletions on enzyme activity, intracellular localization and phosphorylation potential. *Biochem J* 310:699-708
- Cornell RB, Northwood IC (2000) Regulation of CTP: phosphocholine cytidyltransferase by amphitropism and relocalization. *Trends Biochem Sci* 25:441-447
- Cornell RB, Ridgway ND (2015) CTP: phosphocholine cytidyltransferase: Function, regulation, and structure of an amphitropic enzyme required for membrane biogenesis. *Prog Lipid Res* 59:147-171
- Craddock CP, Adams N, Bryant FM, Kurup S, Eastmond PJ (2015) PHOSPHATIDIC ACID PHOSPHOHYDROLASE regulates phosphatidylcholine biosynthesis in Arabidopsis by phosphatidic acid-mediated activation of CTP:PHOSPHOCHOLINE CYTIDYLYLTRANSFERASE activity. *Plant Cell* 27:1251-1264
- Crick FHC (1966) Codon-anticodon pairing: the wobble hypothesis. *J Mol Biol* 19:548-55
- Crowe JH, Hoekstra FA, Crowe LM (1992) Anhydrobiosis. *Annu Rev Physiol* 54:579-599
- Cruz de Carvalho R, Branquinho C, Marques da Silva J (2011) Physiological consequences of desiccation in the aquatic bryophyte *Fontinalis antipyretica*. *Planta* 234:195-205
- Cruz de Carvalho R, Catal áM, Branquinho C, Marques da Silva J, Barreno E (2017) Dehydration rate determines the degree of membrane damage and desiccation tolerance in bryophytes. *Physiol plantarum* 159:277-289
- Cui Z, Houweling M (2002) Phosphatidylcholine and cell death. *BBA Mol Cell Biol L* 1585:87-96
- Cushman JC, Oliver MJ (2011) Understanding vegetative desiccation tolerance using integrated functional genomics approaches within a comparative evolutionary framework. In: Lüttge U, Beck E, Bartels D (ed) *Plant desiccation tolerance. Ecological studies (analysis and synthesis)*. Springer, Berlin, Heidelberg, pp 307-338
- de Freitas Guedes FA, Menezes-Silva PE, DaMatta FM, Alves-Ferreira M (2019) Using transcriptomics to assess plant stress memory. *Theor Exp Plant Phys* 31:47-58
- Dennis MK, Taneva SG, Cornell RB (2011) The intrinsically disordered nuclear localization signal and phosphorylation segments distinguish the membrane affinity of two cytidyltransferase isoforms. *J Biol Chem* 286:12349-12360

REFERENCES

- Ding Y, Fromm M, Avramova Z (2012) Multiple exposures to drought 'train' transcriptional responses in *Arabidopsis*. *Nat Commun* 3:740
- Ding Y, Liu N, Virlouvet L, Riethoven JJ, Fromm M, Avramova Z (2013) Four distinct types of dehydration stress memory genes in *Arabidopsis thaliana*. *BMC Plant Biol* 13:229
- Ding Y, Virlouvet L, Liu N, Riethoven J, Fromm M, Avramova Z (2014) Dehydration stress memory genes of *Zea mays*; comparison with *Arabidopsis thaliana*. *BMC Plant Biol* 14:141
- Duret L (2000) tRNA gene number and codon usage in the *C. elegans* genome are co-adapted for optimal translation of highly expressed genes. *Trends Genet* 16:287-289
- Eisvand HR, Tavakkol-Afshari R, Sharifzadeh F, Maddah Arefi H, Hesamzadeh Hejazi SM (2010) Effects of hormonal priming and drought stress on activity and isozyme profiles of antioxidant enzymes in deteriorated seed of tall wheatgrass (*Agropyron elongatum* Host). *Seed Sci Technol* 38:280-297
- Exton JH (1994) Phosphatidylcholine breakdown and signal transduction. *BBA Mol Cell Biol L* 1212:26-42
- Farrant JM (2000) A comparison of mechanisms of desiccation tolerance among three angiosperm resurrection plant species. *Plant Ecology* 151:29-39
- Farrant JM, Brandt WB, Lindsey GG (2007) An overview of mechanisms of desiccation tolerance in selected angiosperm resurrection plants. *Plant Stress* 1:72-84
- Farrant JM, Vander Willigen C, Loffell DA, Bartsch S, Whittaker A (2003) An investigation into the role of light during desiccation of three angiosperm resurrection plants. *Plant Cell Environ* 26:1275-1286
- Farrant JM, Moore JP (2011) Programming desiccation-tolerance: from plants to seeds to resurrection plants. *Curr Opin Plant Biol* 14:340-345
- Finkelstein R (2013) Abscisic acid synthesis and response. *Arabidopsis Book* 11:e0166
- Fleta-Soriano E, Munné-Bosch S (2016) Stress memory and the inevitable effects of drought: a physiological perspective. *Front Plant Sci* 7:143
- Fleta-Soriano E, Pinto 'Marijuan M, Munne 'Bosch S (2015) Evidence of drought stress memory in the facultative CAM, *Aptenia cordifolia*: possible role of phytohormones. *PLoS ONE* 10:e0135391
- Friedrich T, Faivre L, Bärlle I, Schubert D (2019) Chromatin-based mechanisms of temperature

REFERENCES

- memory in plants. *Plant Cell Environ* 42:762-770
- Fujita Y, Nakashima K, Yoshida T et al (2009) Three SnRK2 protein kinases are the main positive regulators of abscisic acid signaling in response to water stress in *Arabidopsis*. *Plant Cell Physiol* 50:2123-2132
- Gaff DF (1971) Desiccation-tolerant flowering plants in southern Africa. *Science* 174:1033-1034
- Gechev T, Dinakar C, Benina M, Toneva V, Bartels D (2012) Molecular mechanisms of desiccation tolerance in resurrection plants. *Cell Mol Life Sci* 69:3175-3186
- Gechev TS, Benina M, Obata T et al (2013) Molecular mechanisms of desiccation tolerance in the resurrection glacial relic *Haberlea rhodopensis*. *Cell Mol Life Sci* 70:689-709
- Giarola V, Bartels D (2015) What can we learn from the transcriptome of the resurrection plant *Craterostigma plantagineum*?. *Planta* 242:427-434
- Giarola V, Challabathula D, Bartels D (2015) Quantification of expression of dehydrin isoforms in the desiccation tolerant plant *Craterostigma plantagineum* using specifically designed reference genes. *Plant Sci* 236:103-115
- Giarola V, Hou Q, Bartels D (2017) Angiosperm plant desiccation tolerance: hints from transcriptomics and genome sequencing. *Trends Plant Sci* 22:705-717
- Giarola V, Jung NU, Singh A, Satpathy P, Bartels D (2018) Analysis of *pcC13-62* promoters predicts a link between *cis*-element variations and desiccation tolerance in Linderniaceae. *J Exp Bot* 69:3773-3784
- Giarola V, Krey S, von den Driesch B, Bartels D (2016) The *Craterostigma plantagineum* glycine-rich protein CpGRP1 interacts with a cell wall-associated protein kinase 1 (CpWAK1) and accumulates in leaf cell walls during dehydration. *New Phytol* 210:535-550
- Gibellini F, Smith TK (2010) The Kennedy pathway-*De novo* synthesis of phosphatidylethanolamine and phosphatidylcholine. *IUBMB Life* 62:414-428
- Gietz RD, Schiestl RH, Willems AR, Woods RA (1995) Studies on the transformation of intact yeast cells by the LiAc/SS-DNA/PEG procedure. *Yeast* 11:355-360
- Goh CH, Nam HG, Park YS (2003) Stress memory in plants: a negative regulation of stomatal response and transient induction of *rd22* gene to light in abscisic acid-entrained *Arabidopsis* plants. *Plant J* 36:240-255
- Guilfoyle TJ, Hagen, G (2007) Auxin response factors. *Curr Opin Plant Biol* 10:453-460

REFERENCES

- Hall BG (2013) Building phylogenetic trees from molecular data with MEGA. *Mol Biol Evol* 30:1229-1235
- Hanchi M, Thibaud MC, L'égeret B et al (2018) The phosphate fast-responsive genes *PECP1* and *PPsPase1* affect phosphocholine and phosphoethanolamine content. *Plant Physiol* 176:2943-2962
- Harwood J, Moore Jr TS (1989) Lipid metabolism in plants. *Crit Rev Plant Sci* 8:1-43
- Harwood JL (1988) Fatty acid metabolism. *Ann Review Plant Physiol Plant Mol Biol* 39:101-138
- Hayakawa Y, Duan Z, Yadake M, Tsukano J, Yamaoka Y, Inatsugi R, Fujiki Y, Oikawa A, Saito K, Nishida I (2015) Epigenetic floral homeotic mutation in pD991-AP3-derived T-DNA-tagged lines for CTP: Phosphorylcholine cytidyltransferase (CCT) genes: The homeotic mutation of the *cct1-1* allele is enhanced by the *cct2* allele and alleviated by CCT1 overexpression. *J Plant Biol* 58:183-192
- Helmink BA, Braker JD, Kent C, Friesen JA (2003) Identification of lysine 122 and arginine 196 as important functional residues of rat CTP: phosphocholine cytidyltransferase alpha. *Biochemistry* 42:5043-5051
- Helmink BA, Friesen JA (2004) Characterization of a lipid activated CTP: phosphocholine cytidyltransferase from *Drosophila melanogaster*. *BBA Mol Cell Biol L* 1683:78-88
- Herms DA, Mattson WJ (1992) The dilemma of plants: to grow or defend. *Q Rev Biol* 67:283-335
- Hershberg R, Petrov DA (2008) Selection on codon bias. *Annu Rev Genet* 42:287-299
- Hershberg R, Petrov DA (2009) General rules for optimal codon choice. *PLoS Genet* 5:e1000556
- Hershey JWB, Sonenberg N, Mathews MB (2012) Principles of translational control: an overview. *CSH Perspect Biol* 4:a011528
- Higo K, Ugawa Y, Iwamoto M, Korenaga T (1999) Plant cis-acting regulatory DNA elements (PLACE) database: 1999. *Nucleic Acids Res* 27:297-300
- Hilker M, Schmülling T (2019) Stress priming, memory, and signalling in plants. *Plant Cell Environ* 42:753-761
- Hilker M, Schwachtje J, Baier M, Balazadeh S, Bäurle I, Geiselhardt S, Hinch DK, Kunze R, Mueller-Roeber B, Rillig MC, Rolff J (2016) Priming and memory of stress responses in organisms lacking a nervous system. *Biol Rev* 91:1118-1133
- Hodges DM, DeLong JM, Forney CF, Prange RK (1999) Improving the thiobarbituric

REFERENCES

- acid-reactive-substances assay for estimating lipid peroxidation in plant tissues containing anthocyanin and other interfering compounds. *Planta* 207:604-611
- Hoekstra FA, Golovina EA, Buitink J (2001) Mechanisms of plant desiccation tolerance. *Trends Plant Sci* 6:431-438
- Houweling M, Cui Z, Anfuso CD, Bussiere M, Chen MH, Vance DE (1996) CTP: phosphocholine cytidyltransferase is both a nuclear and cytoplasmic protein in primary hepatocytes. *Eur J Cell Biol* 69:55-63
- Hu L, Li H, Pang H, Fu J (2012) Responses of antioxidant gene, protein and enzymes to salinity stress in two genotypes of perennial ryegrass (*Lolium perenne*) differing in salt tolerance. *J Plant Physiol* 169:146-156
- Hu L, Wang Z, Du H, Huang B (2010) Differential accumulation of dehydrins in response to water stress for hybrid and common bermudagrass genotypes differing in drought tolerance. *J Plant Physiol* 167:103-109
- Hu T, Jin Y, Li H, Amombo E, Fu J (2016) Stress memory induced transcriptional and metabolic changes of perennial ryegrass (*Lolium perenne*) in response to salt stress. *Physiol Plant* 156:54-69
- Huch S, Nissan T (2014) Interrelations between translation and general mRNA degradation in yeast. *WIREs RNA* 5:747-763
- Hussain M, Farooq M, Sattar A, Ijaz M, Sher A, Ul-Allah S (2018) Mitigating the adverse effects of drought stress through seed priming and seed quality on wheat (*Triticum aestivum* L.) productivity. *Pak J Agr Sci* 55:313-319
- Inatsugi R, Kawai H, Yamaoka Y, Yu Y, Sekiguchi A, Nakamura M, Nishida I (2009) Isozyme-specific modes of activation of CTP: phosphorylcholine cytidyltransferase in *Arabidopsis thaliana* at low temperature. *Plant Cell Physiol* 50:1727-1735
- Inatsugi R, Nakamura M, Nishida I (2002) Phosphatidylcholine biosynthesis at low temperature: differential expression of CTP: phosphorylcholine cytidyltransferase isogenes in *Arabidopsis thaliana*. *Plant Cell Physiol* 43:1342-1350
- Ingolia NT, Ghaemmaghami S, Newman JR, Weissman JS (2009) Genome-wide analysis in vivo of translation with nucleotide resolution using ribosome profiling. *Science* 324:218-223
- Ingram J, Bartels D (1996) The molecular basis of dehydration tolerance in plants. *Annu Rev*

REFERENCES

- Plant Biol 47:377-403
- Jackowski S, Fagone P (2005) CTP: phosphocholine cytidyltransferase: paving the way from gene to membrane. J Biol Chem 280:853-856
- Jackson AO, Larkins BA (1976) Influence of ionic strength, pH, and chelation of divalent metals on isolation of polyribosomes from tobacco leaves. Plant Physiol 57:5-10
- Janmohammadi M, Dezfuli PM, Sharifzadeh F (2008) Seed invigoration techniques to improve germination and early growth of inbred line of maize under salinity and drought stress. Gen Appl Plant Physiol 34:215-226
- Jiang R, Yu X, Xie J, Zhao Y, Li F, Yang M (2018) Recent changes in daily climate extremes in a serious water shortage metropolitan region, a case study in Jing-Jin-Ji of China. Theor Appl Climatol 134:565-584
- Jisha KC, Vijayakumari K, Puthur JT (2013) Seed priming for abiotic stress tolerance: an overview. Acta Physiol Plant 35:1381-1396
- Johnson JE, Cornell RB (1999) Amphitropic proteins: regulation by reversible membrane interactions. Mol Membr Biol 16:217-235
- Jones PL, Willey DL, Gacesa P, Harwood JL (1998) Isolation, characterisation and expression of a cDNA for pea cholinephosphate cytidyltransferase. Plant Mol Biol 37:179-185
- Juntawong P, Girke T, Bazin J, Bailey-Serres J (2014) Translational dynamics revealed by genome-wide profiling of ribosome footprints in Arabidopsis. Proc Natl Acad Sci USA 111:E203-E212
- Juszczak I, Bartels D (2017) LEA gene expression, RNA stability and pigment accumulation in three closely related Linderniaceae species differing in desiccation tolerance. Plant Sci 255:59-71
- Kaur S, Gupta A, Kaur N (2002) Effect of osmo- and hydropriming of chickpea seeds on seedling growth and carbohydrate metabolism under water deficit stress. Plant Growth Regul 37:17-22
- Kawaguchi R, Girke T, Bray EA, Bailey-Serres J (2004) Differential mRNA translation contributes to gene regulation under non-stress and dehydration stress conditions in *Arabidopsis thaliana*. Plant J 38:823-839
- Kawaguchi R, Williams AJ, Bray EA, Bailey-Serres J (2003) Water-deficit-induced translational control in *Nicotiana tabacum*. Plant Cell Environ 26:221-229

REFERENCES

- Kent C (1997) CTP: phosphocholine cytidylyltransferase. *Biochim Biophys Acta Lipids Lipid Metabol* 1348:79-90
- Khan MN, Zhang J, Luo T, Liu J, Rizwan M, Fahad S, Xu Z, Hu L (2019) Seed priming with melatonin coping drought stress in rapeseed by regulating reactive oxygen species detoxification: Antioxidant defense system, osmotic adjustment, stomatal traits and chloroplast ultrastructure perseveration. *Ind Crop Prod* 140:111597
- Kim TH (2012) Plant stress surveillance monitored by ABA and disease signaling interactions. *Mol Cells* 33:1-7
- Kim JM, To TK, Ishida J, Matsui A, Kimura H, Seki M (2012) Transition of chromatin status during the process of recovery from drought stress in *Arabidopsis thaliana*. *Plant Cell Physiol* 53:847-856
- Kinney AJ, Clarkson DT, Loughman BC (1987) The regulation of phosphatidylcholine biosynthesis in rye (*Secale cereale*) roots. Stimulation of the nucleotide pathway by low temperature. *Biochem J* 242:755-759
- Kinoshita T, Seki M (2014) Epigenetic memory for stress response and adaptation in plants. *Plant Cell Physiol* 55:1859-1863
- Kirch HH, Röhrig H (2010) Affinity purification and determination of enzymatic activity of recombinantly expressed aldehyde dehydrogenases. *Methods Mol Biol* 639:282-291
- Koressaar T, Remm M (2007) Enhancements and modifications of primer design program Primer3. *Bioinformatics* 23:1289-1291
- Koster KL, Balsamo RA, Espinoza C, Oliver MJ (2010) Desiccation sensitivity and tolerance in the moss *Physcomitrella patens*: assessing limits and damage. *Plant Growth Regul* 62:293-302
- Kosugi S, Hasebe M, Tomita M, Yanagawa H (2009) Systematic identification of yeast cell cycle-dependent nucleocytoplasmic shuting proteins by prediction of composite motifs. *Proc Natl Acad Sci USA* 106:10171-10176
- Kotchoni SO, Kuhns C, Ditzer A, KIRCH HH, Bartels D (2006) Over-expression of different *aldehyde dehydrogenase* genes in *Arabidopsis thaliana* confers tolerance to abiotic stress and protects plants against lipid peroxidation and oxidative stress. *Plant Cell Environ* 29:1033-1048

REFERENCES

- Kozłowski TT, Pallardy SG (2002) Acclimation and adaptive responses of woody plants to environmental stresses. *Bot Rev* 68:270-334
- Kreyling J, Wiesenberg GLB, Thiel D, Wohlfart C, Huber G, Walter J, Jentsch A, Konnert M, Beierkuhnlein C (2012) Cold hardiness of *Pinus nigra* Arnold as influenced by geographic origin, warming, and extreme summer drought. *Environ Exp Bot* 78:99-108
- Krishnan K, Ren Z, Losada L, Nierman WC, Lu LJ, Askew DS (2014) Polysome profiling reveals broad translome remodeling during endoplasmic reticulum (ER) stress in the pathogenic fungus *Aspergillus fumigatus*. *BMC Genomics* 15:159
- Laemmli UK (1970) Cleavage of structural proteins during the assembly of the head of bacteriophage T4. *Nature* 227:680-685
- Lata C, Prasad M (2011) Role of DREBs in regulation of abiotic stress responses in plants. *J Exp Bot* 62:4731-4748
- Layat E, Leymarie J, El-Maarouf-Bouteau H, Caius J, Langlade N, Bailly C (2014) Translome profiling in dormant and nondormant sunflower (*Helianthus annuus*) seeds highlights post-transcriptional regulation of germination. *New Phytol* 204:864-872
- Lee J, Taneva SG, Holland BW, Tieleman DP, Cornell RB (2014) Structural basis for autoinhibition of CTP:phosphocholine cytidyltransferase (CCT), the regulatory enzyme in phosphatidylcholine synthesis, by its membrane-binding amphipathic helix. *J Biol Chem* 289:1742-1755
- Leung J, Giraudat J (1998) Abscisic acid signal transduction. *Annu Rev Plant Physiol Plant Mol Biol* 49:199-222
- Levitt J (1980) Responses of plants to environmental stresses. Academic Press, New York
- Li B, Dewey CN (2011) RSEM: accurate transcript quantification from RNA-Seq data with or without a reference genome. *BMC Bioinformatics* 12:323
- Li RH, Guo PG, Michael B, Stefania G, Salvatore C (2006) Evaluation of chlorophyll content and fluorescence parameters as indicators of drought tolerance in barley. *Agr Sci China* 5:751-757
- Li X, Cai J, Liu F, Dai T, Cao W, Jiang D (2014) Cold priming drives the sub-cellular antioxidant systems to protect photosynthetic electron transport against subsequent low temperature stress in winter wheat. *Plant Physiol Biochem* 82:34-43

REFERENCES

- Li X, Topbjerg HB, Jiang D, Liu F (2015) Drought priming at vegetative stage improves the antioxidant capacity and photosynthesis performance of wheat exposed to a short-term low temperature stress at jointing stage. *Plant Soil* 393:307-318
- Li X, Liu F (2016) Drought stress memory and drought stress tolerance in plants: biochemical and molecular basis. In: Hossain MA (ed) *Drought stress tolerance in plants 1*. Springer, Cham, pp 17-44
- Lin SY, Chen PW, Chuang MH, Juntawong P, Bailey-Serres J, Jauh GY (2014) Profiling of transcriptomes of in vivo-grown pollen tubes reveals genes with roles in micropylar guidance during pollination in *Arabidopsis*. *Plant Cell* 26:602-618
- Lin YC, Liu YC, Nakamura Y (2015) The choline/ethanolamine kinase family in *Arabidopsis*: essential role of CEK4 in phospholipid biosynthesis and embryo development. *Plant Cell* 27:1497-1511
- Liu MJ, Wu SH, Chen HM, Wu SH (2012) Widespread translational control contributes to the regulation of *Arabidopsis* photomorphogenesis. *Mol Syst Biol* 8:566
- Liu MJ, Wu SH, Wu JF, Lin WD, Wu YC, Tsai TY, Tsai HL, Wu SH (2013) Translational landscape of photomorphogenic *Arabidopsis*. *Plant Cell* 25:3699-3710
- Liu N, Ding Y, Fromm M, Avramova Z (2014) Different gene-specific mechanisms determine the 'revised-response' memory transcription patterns of a subset of *A. thaliana* dehydration stress responding genes. *Nucleic Acids Res* 42:5556-5566
- Liu N, Staswick PE, Avramova Z (2016) Memory responses of jasmonic acid-associated *Arabidopsis* genes to a repeated dehydration stress. *Plant Cell Environ* 39:2515-2529
- Liu X, Chan Z (2015) Application of potassium polyacrylate increases soil water status and improves growth of bermudagrass (*Cynodon dactylon*) under drought stress condition. *Sci Hortic-Amsterdam* 197:705-711
- Liu Y, Yang T, Lin Z et al (2019a) A WRKY Transcription Factor PbrWRKY53 from *Pyrus betulaefolia* is involved in drought tolerance and AsA accumulation. *Plant Biotechnol J* 17:1770-1787
- Liu YC, Gunawan F, Yunus IS, Nakamura Y (2018) *Arabidopsis* serine decarboxylase 1 (SDC1) in phospholipid and amino acid metabolism. *Front Plant Sci* 9:972
- Liu YC, Lin YC, Kanehara K, Nakamura Y (2019b) A methyltransferase trio essential for

REFERENCES

- phosphatidylcholine biosynthesis and growth. *Plant Physiol* 179:433-445
- Liu Y, Wang G, Wang X (2015) Role of aminoalcoholphosphotransferases 1 and 2 in phospholipid homeostasis in *Arabidopsis*. *Plant Cell* 27:1512-1528
- Livak KJ, Schmittgen TD (2001) Analysis of relative gene expression data using real-time quantitative PCR and the $2^{-\Delta\Delta CT}$ method. *Methods* 25:402-408
- Love MI, Huber W, Anders S (2014) Moderated estimation of fold change and dispersion for RNA-seq data with DESeq2. *Genome Biol* 15:550
- Lu S, Chen C, Wang Z, Guo Z, Li H (2009) Physiological responses of somaclonal variants of triploid bermudagrass (*Cynodon transvaalensis* × *Cynodon dactylon*) to drought stress. *Plant Cell Rep* 28:517-526
- Lykidis A, Jackowski S (2000) Regulation of mammalian cell membrane biosynthesis. *Prog Nucleic Acid Re* 65:361-393
- Ma C, Wang H, Macnish AJ, Estrada-Melo AC, Lin J, Chang Y, Reid MS, Jiang CZ (2015) Transcriptomic analysis reveals numerous diverse protein kinases and transcription factors involved in desiccation tolerance in the resurrection plant *Myrothamnus flabellifolia*. *Hortic Res* 2:15034
- Michel D, Furini A, Salamini F, Bartels D (1994) Structure and regulation of an ABA- and desiccation-responsive gene from the resurrection plant *Craterostigma plantagineum*. *Plant Mol Biol* 24:549-560
- Missihoun TD (2011) Characterisation of selected *Arabidopsis* aldehyde dehydrogenase genes: role in plant stress physiology and regulation of gene expression. Dissertation, University of Bonn
- Mittler R (2002) Oxidative stress, antioxidants and stress tolerance. *Trends Plant Sci* 7:405-410
- Mittler R, Vanderauwera S, Gollery M, Van Breusegem F (2004) Reactive oxygen gene network of plants. *Trends Plant Sci* 9:490-498
- Mol AR, Castro MS, Fontes W (2018) NetWheels: A web application to create high quality peptide helical wheel and net projections. *BioRxiv* 416347
- Moore JP, Le NT, Brandt WF, Driouich A, Farrant JM (2009) Towards a systems-based understanding of plant desiccation tolerance. *Trends Plant Sci* 14:110-117
- Munne-Bosch S, Alegre L (2013) Cross-stress tolerance and stress “memory” in plants. *Environ*

REFERENCES

- Exp Bot 94:1-88
- Mustroph A, Juntawong P, Bailey-Serres J (2009) Isolation of plant polysomal mRNA by differential centrifugation and ribosome immunopurification methods. In: Belostotsky D (ed) Plant systems biology. Methods in molecular biology™ (methods and protocols). Humana Press, New York, pp 109-126
- Nakai K, Kanehisa M (1992) A knowledge base for predicting protein localization sites in eukaryotic cells. Genomics 14:897-911
- Neves DM, da Hora Almeida LA, Santana-Vieira DDS, Freschi L, Ferreira CF, dos Santos Soares Filho W, Costa MGC, Micheli F, Filho MAC, da Silva Gesteira A (2017) Recurrent water deficit causes epigenetic and hormonal changes in citrus plants. Sci Rep 7:13684
- Niinemets Ü, Kahru A, Mander Ü, Nõges P, Nõges T, Tuvikene A, Vasemägi A (2017) Interacting environmental and chemical stresses under global change in temperate aquatic ecosystems: stress responses, adaptation, and scaling. Reg Environ Change 17:2061-2077
- Nishida I, Swinhoe R, Slabas AR, Murata N (1996) Cloning of *Brassica napus* CTP: phosphocholine cytidyltransferase cDNAs by complementation in a yeast cct mutant. Plant Mol Biol 31:205-211
- Ohlrogge J, Browse J (1995) Lipid biosynthesis. Plant Cell 7:957-970
- Oliver MJ, Bewley JD (1996) Desiccation-tolerance of plant tissues: a mechanistic overview. Horticult Rev 18:171-213
- Oliver MJ, Cushman JC, Koster KL (2010) Dehydration tolerance in plants. In: Sunkar R (ed) Plant stress tolerance. Methods in molecular biology (methods and protocols). Humana Press, New York, pp 3-24
- Oliver MJ, Jain R, Balbuena TS, Agrawal G, Gasulla F, Thelen JJ (2011a) Proteome analysis of leaves of the desiccation-tolerant grass, *Sporobolus stapfianus*, in response to dehydration. Phytochemistry 72:1273-1284
- Oliver MJ, Guo L, Alexander DC, Ryals JA, Wone BWM, Cushman JC (2011b) A sister group metabolomics contrast using untargeted global metabolomics analysis delineates the biochemical regulation underlying desiccation tolerance in *Sporobolus stapfianus*. Plant Cell 23:1231-1248
- Oliver MJ, Tuba Z, Mishler BD (2000) The evolution of vegetative desiccation tolerance in land

REFERENCES

- plants. *Plant Ecol* 151:85-100
- Otto SP (2007) The evolutionary consequences of polyploidy. *Cell* 131:452-462
- Panda AC, Abdelmohsen K, Martindale JL et al (2016) Novel RNA-binding activity of MYF5 enhances *Ccnd1/Cyclin D1* mRNA translation during myogenesis. *Nucleic Acids Res* 44:2393-2408
- Panda AC, Martindale JL, Gorospe M (2017) Polysome fractionation to analyze mRNA distribution profiles. *Bio Protoc* 7:e2126
- Paparella S, Araújo SS, Rossi G, Wijayasinghe M, Carbonera D, Balestrazzi A (2015) Seed priming: state of the art and new perspectives. *Plant Cell Rep* 34:1281-1293
- Perrella G, Davidson MLH, O'Donnell L, Nastase AM, Herzyk P, Breton G, Pruneda-Paz JL, Kay SA, Chory J, Kaiserli E (2018) ZINC-FINGER interactions mediate transcriptional regulation of hypocotyl growth in Arabidopsis. *Proc Natl Acad Sci USA* 115:E4503-E4511
- Phillips JR, Fischer E, Baron M, Van Den Dries N, Facchinelli F, Kutzer M, Rahmzadeh R, Remus D, Bartels D (2008) *Lindernia brevidens*: a novel desiccation-tolerant vascular plant, endemic to ancient tropical rainforests. *Plant J* 54:938-948
- Piccirillo CA, Bjur E, Topisirovic I, Sonenberg N, Larsson O (2014) Translational control of immune responses: from transcripts to translomes. *Nat Immunol* 15:503-511
- Pintó-Marijuan M, Cotado A, Fleta-Soriano E, Munné-Bosch S (2017) Drought stress memory in the photosynthetic mechanisms of an invasive CAM species, *Aptenia cordifolia*. *Photosynth Res* 131:241-253
- Porembski S (2011) Evolution, diversity and habitats of poikilohydrous plants. In: Luttge U, Beck E, Bartels D (ed) *Plant desiccation tolerance*. Springer, Berlin, pp 139-156
- Pradet-Balade B, Boulmé F, Beug H, Müllner EW, Garcia-Sanz JA (2001) Translation control: bridging the gap between genomics and proteomics?. *Trends Biochem Sci* 26:225-229
- Price-Jones MJ, Harwood JL (1986) The control of CTP: choline-phosphate cytidylyltransferase activity in pea (*Pisum sativum* L.). *Biochem J* 240:837-842
- Proctor MC, Oliver MJ, Wood AJ, Alpert P, Stark LR, Cleavitt NL, Mishler BD (2007) Desiccation-tolerance in bryophytes: a review. *Bryologist* 110:595-622
- Provart NJ, Zhu T (2003) A browser-based functional classification SuperViewer for Arabidopsis genomics. *Curr Comput Mol Biol* 2003:271-272

REFERENCES

- Qu XH, Wen JD, Lancaster L, Noller HF, Bustamante C, Tinoco I (2011) The ribosome uses two active mechanisms to unwind messenger RNA during translation. *Nature* 475:118-121
- Quan W, Liu X, Wang H, Chan Z (2016a) Comparative physiological and transcriptional analyses of two contrasting drought tolerant alfalfa varieties. *Front Plant Sci* 6:1256
- Quan W, Liu X, Wang H, Chan Z (2016b) Physiological and transcriptional responses of contrasting alfalfa (*Medicago sativa* L.) varieties to salt stress. *Plant Cell Tiss Org* 126:105-115
- Rajashekar CB, Panda M (2014) Water stress is a component of cold acclimation process essential for inducing full freezing tolerance in strawberry. *Sci Hortic-Amsterdam* 174:54-59
- Ramírez DA, Rolando JL, Yactayo W, Monneveux P, Mares V, Quiroz R (2015) Improving potato drought tolerance through the induction of long-term water stress memory. *Plant Sci* 238:26-32
- Rhodes D, Hanson AD (1993) Quaternary ammonium and tertiary sulfonium compounds in higher plants. *Annu Rev Plant Biol* 44:357-384
- Robinson BS, Yao Z, Baisted DJ, Vance DE (1989) Lysophosphatidylcholine metabolism and lipoprotein secretion by cultured rat hepatocytes deficient in choline. *Biochem J* 260:207-214
- Rodriguez MCS, Edsgård D, Hussain SS, Alquezar D, Rasmussen M, Gilbert T, Nielsen BH, Bartels D, Mundy J (2010) Transcriptomes of the desiccation-tolerant resurrection plant *Craterostigma plantagineum*. *Plant J* 63:212-228
- Rogers SO, Bendich AJ (1985) Extraction of DNA from milligram amounts of fresh, herbarium and mummified plant tissues. *Plant Mol Biol* 5:69-76
- Sato H, Takasaki H, Takahashi F et al (2018) *Arabidopsis thaliana* NGATHA1 transcription factor induces ABA biosynthesis by activating *NCED3* gene during dehydration stress. *Proc Natl Acad Sci USA* 115:E11178-E11187
- Sato N, Mori N, Hirashima T, Moriyama T (2016) Diverse pathways of phosphatidylcholine biosynthesis in algae as estimated by labeling studies and genomic sequence analysis. *Plant J* 87:281-292
- Savvides A, Ali S, Tester M, Fotopoulos V (2016) Chemical priming of plants against multiple abiotic stresses: mission possible?. *Trends Plant Sci* 21:329-340
- Serna A, Maitz M, O'Connell T et al (2001) Maize endosperm secretes a novel antifungal protein

REFERENCES

- into adjacent maternal tissue. *Plant J* 25:687-698
- Schwartz DC, Parker R (1999) Mutations in translation initiation factors lead to increased rates of deadenylation and decapping of mRNAs in *Saccharomyces cerevisiae*. *Mol Cell Biol* 19:5247-5256
- Sher A, Sarwar T, Nawaz A, Ijaz M, Sattar A, Ahmad S (2019) Methods of Seed Priming. In: Hasanuzzaman M, Fotopoulos V (ed) Priming and pretreatment of seeds and seedlings. Springer, Singapore, pp 1-10
- Sherwin HW, Farrant JM (1998) Protection mechanisms against excess light in the resurrection plants *Craterostigma wilmsii* and *Xerophyta viscosa*. *Plant Growth Regul* 24:203-210
- Shi H, Wang Y, Cheng Z, Ye T, Chan Z (2012) Analysis of natural variation in bermudagrass (*Cynodon dactylon*) reveals physiological responses underlying drought tolerance. *PLoS ONE* 7:e53422
- Shi H, Ye T, Chan Z (2014) Nitric oxide-activated hydrogen sulfide is essential for cadmium stress response in bermudagrass (*Cynodon dactylon* (L.) Pers.). *Plant Physiol Bioch* 74:99-107
- Shinozaki K, Yamaguchi-Shinozaki K (2000) Molecular responses to dehydration and low temperature: differences and cross-talk between two stress signaling pathways. *Curr Opin Plant Biol* 3:217-223
- Shukla N, Awasthi RP, Rawat L, Kumar J (2015) Seed biopriming with drought tolerant isolates of *Trichoderma harzianum* promote growth and drought tolerance in *Triticum aestivum*. *Ann Appl Biol* 166:171-182
- Siljak-Yakovlev S, Stevanovic V, Tomasevic M, Brown SC, Stevanovic B (2008) Genome size variation and polyploidy in the resurrection plant genus *Ramonda*: cytogeography of living fossils. *Environ Exp Bot* 62:101-112
- Sinclair BJ, Roberts SP (2005) Acclimation, shock and hardening in the cold. *J Therm Biol* 30:557-562
- Smit E, Caiment F, Piepers J, Kleijnans JC, van den Beucken T (2018) Translational regulation is a key determinant of the cellular response to benzo[a]pyrene. *Toxicol Lett* 295:144-152
- Stothard P (2000) The sequence manipulation suite: JavaScript programs for analyzing and formatting protein and DNA sequences. *Biotechniques* 28:1102-1104
- Sullivan CY (1972) Mechanisms of heat and drought resistance in grain sorghum and method of

REFERENCES

- measurements. In: Rao NGP, House LR (ed) Sorghum in the seventies. Oxford and IBH Publishing, New Delhi, pp 247-264
- Sun RZ, Lin CT, Zhang XF, Duan LX, Qi XQ, Gong YH, Deng X (2018) Acclimation-induced metabolic reprogramming contributes to rapid desiccation tolerance acquisition in *Boea hygrometrica*. *Environ Exp Bot* 148:70-84
- Sun M, Peng F, Xiao Y, Yu W, Zhang Y, Gao H (2020) Exogenous phosphatidylcholine treatment alleviates drought stress and maintains the integrity of root cell membranes in peach. *Sci Hortic-Amsterdam* 259:108821
- Sun Y, Sun Y, Wang M, Li X, Guo X, Hu R, Ma J (2010) Effects of seed priming on germination and seedling growth of rice under water stress. *Acta Agron Sin* 36:1931-1940
- Sundler R, Akesson B (1975) Regulation of phospholipid biosynthesis in isolated rat hepatocytes. Effect of different substrates. *J Biol Chem* 250:3359-3367
- Szklarczyk D, Morris JH, Cook H et al (2017) The STRING database in 2017: quality-controlled protein-protein association networks, made broadly accessible. *Nucleic Acids Res* 45:362-368
- Tasseva G, Richard L, Zachowski A (2004) Regulation of phosphatidylcholine biosynthesis under salt stress involves choline kinases in *Arabidopsis thaliana*. *FEBS Lett* 566:115-120
- Thomas J, Palusa SG, Prasad KVSK, Ali GS, Surabhi GK, Ben-Hur A, Abdel-Ghany SE, Reddy ASN (2012) Identification of an intronic splicing regulatory element involved in auto-regulation of alternative splicing of *SCL33* pre-mRNA. *Plant J* 72:935-946
- Thomashow MF (1999) Plant cold acclimation: freezing tolerance genes and regulatory mechanisms. *Annu Rev Plant Biol* 50:571-599
- Todaka D, Zhao Y, Yoshida T et al (2017) Temporal and spatial changes in gene expression, metabolite accumulation and phytohormone content in rice seedlings grown under drought stress conditions. *Plant J* 90:61-78
- Towbin H, Staehelin T, Gordon J (1979) Electrophoretic transfer of proteins from polyacrylamide gels to nitrocellulose sheets: procedure and some applications. *Proc Natl Acad Sci U S A* 76:4350-4354
- Uno Y, Furihata T, Abe H, Yoshida R, Shinozaki K, Yama-guchi-Shinozaki K (2000) Arabidopsis basic leucine zipper transcription factors involved in an abscisic acid-dependent signal

REFERENCES

- transduction pathway under drought and high-salinity conditions. *Proc Natl Acad Sci USA* 97:11632-11637
- Untergasser A, Cutcutache I, Koressaar T, Ye J, Faircloth BC, Remm M, Rozen SG (2012) Primer3—new capabilities and interfaces. *Nucleic Acids Res* 40:e115-e115
- Valenzuela-Avenidaño JP, Mota IA, Uc GL, Perera RS, Valenzuela-Soto EM, Aguilar JJ (2005) Use of a simple method to isolate intact RNA from partially hydrated *Selaginella lepidophylla* plants. *Plant Mol Biol Rep* 23:199-200
- Valleriani A, Zhang G, Nagar A, Ignatova Z, Lipowsky R (2011) Length-dependent translation of messenger RNA by ribosomes. *Phys Rev E* 83:042903
- Van den Dries N, Facchinelli F, Giarola V, Phillips JR, Bartels D (2011) Comparative analysis of *LEA-like 11-24* gene expression and regulation in related plant species within the Linderniaceae that differ in desiccation tolerance. *New Phytol* 190:75-88
- Vance JE, Vance DE (2004) Phospholipid biosynthesis in mammalian cells. *Biochem Cell Biol* 82:113-128
- Veitch DP, Cornell RB (1996) Substitution of serine for glycine-91 in the HXGH motif of CTP:phosphocholine cytidyltransferase implicates this motif in CTP binding. *Biochemistry* 35:10743-10750
- Veitch DP, Gilham D, Cornell RB (1998) The role of histidine residues in the HXGH site of CTP:phosphocholine cytidyltransferase in CTP binding and catalysis. *Eur J Biochem* 255:227-234
- Velikova V, Yordanov I, Edreva A (2000) Oxidative stress and some antioxidant systems in acid rain-treated bean plants: protective role of exogenous polyamines. *Plant Sci* 151:59-66
- Virlouvet L, Fromm M (2015) Physiological and transcriptional memory in guard cells during repetitive dehydration stress. *New Phytol* 205:596-607
- Vogel C, Marcotte EM (2012) Insights into the regulation of protein abundance from proteomic and transcriptomic analyses. *Nat Rev Genet* 13:227-232
- Walter J, Nagy L, Hein R, Rascher U, Beierkuhnlein C, Willner E, Jentsch A (2011) Do plants remember drought? Hints towards a drought-memory in grasses. *Environ Exp Bot* 71:34-40
- Walter J, Jentsch A, Beierkuhnlein C, Kreyling J (2013) Ecological stress memory and cross stress tolerance in plants in the face of climate extremes. *Environ Exp Bot* 94:3-8

REFERENCES

- Wang X, Vigjevic M, Liu F, Jacobsen S, Jiang D, Wollenweber B (2015) Drought priming at vegetative growth stages improves tolerance to drought and heat stresses during grain filling in spring wheat. *Plant Growth Regul* 75:677-687
- Wang X, Vignjevic M, Jiang D, Jacobsen S, Wollenweber B (2014) Improved tolerance to drought stress after anthesis due to priming before anthesis in wheat (*Triticum aestivum* L.) var. Vinjett. *J Exp Bot* 65:6441-6456
- Wang Y, MacDonald JJ, Kent C (1995) Identification of the nuclear localization signal of rat liver CTP: phosphocholine cytidyltransferase. *J Biol Chem* 270:354-360
- Wang Z, Zhu Y, Wang L, Liu X, Liu Y, Phillips J, Deng X (2009) A WRKY transcription factor participates in dehydration tolerance in *Boea hygrometrica* by binding to the W-box elements of the galactinol synthase (*BhGolSI*) promoter. *Planta* 230:1155
- Wang T, Cui Y, Jin J, Guo J, Wang G, Yin X, He Q, Zhang G (2013) Translating mRNAs strongly correlate to proteins in a multivariate manner and their translation ratios are phenotype specific. *Nucleic Acids Res* 41:4743-4754
- Whittaker A, Martinelli T, Farrant JM, Bochicchio A, Vazzana C (2007) Sucrose phosphate synthase activity and the co-ordination of carbon partitioning during sucrose and amino acid accumulation in desiccation-tolerant leaf material of the C4 resurrection plant *Sporobolus stapfianus* during dehydration. *J Exp Bot* 58:3775-3787
- Willige BC, Kutzer M, Tebartz F, Bartels D (2009) Subcellular localization and enzymatic properties of differentially expressed transketolase genes isolated from the desiccation tolerant resurrection plant *Craterostigma plantagineum*. *Planta* 229:659-666
- Willing RP, Leopold AC (1983) Cellular expansion at low temperature as a cause of membrane lesions. *Plant Physiol* 71:118-121
- Wood AJ, Oliver MJ (1999) Translational control in plant stress: The formation of messenger ribonucleoprotein particles (mRNPs) in response to desiccation of *Tortula ruralis* gametophytes. *Plant J* 18:359-370
- Yobi A, Schlauch KA, Tillett RL, Yim WC, Espinoza C, Wone BWM, Cushman JC, Oliver MJ (2017) *Sporobolus stapfianus*: Insights into desiccation tolerance in the resurrection grasses from linking transcriptomics to metabolomics. *BMC Plant Biol* 17:67
- Yoo CY, Pence HE, Jin JB, Miura K, Gosney MJ, Hasegawa PM, Mickelbart MV (2010) The

REFERENCES

- Arabidopsis GTL1 transcription factor regulates water use efficiency and drought tolerance by modulating stomatal density via transrepression of *SDD1*. *Plant Cell* 22:4128-4141
- Yunus IS, Liu YC, Nakamura Y (2016) The importance of SERINE DECARBOXYLASE 1 (SDC1) and ethanolamine biosynthesis during embryogenesis of *Arabidopsis thaliana*. *Plant J* 88:559-569
- Zhang Q, Linnemann TV, Schreiber L, Bartels D (2016) The role of transketolase and octulose in the resurrection plant *Craterostigma plantagineum*. *J Exp Bot* 67:3551-3559
- Zhao J, Missihoun TD, Bartels D (2017) The role of Arabidopsis aldehyde dehydrogenase genes in response to high temperature and stress combinations. *J Exp Bot* 68:4295-4308
- Zhao Y, Du H, Wang Z, Huang B (2011) Identification of proteins associated with water-deficit tolerance in C4 perennial grass species, *Cynodon dactylon* × *Cynodon transvaalensis* and *Cynodon dactylon*. *Physiol Plant* 141:40-55
- Zuker M (2003) Mfold web server for nucleic acid folding and hybridization prediction. *Nucleic Acids Res* 31:3406-3415

ACKNOWLEDGEMENTS

Here, I would like to express my deep gratitude to people who either directly or indirectly contributed to the accomplishment of this PhD thesis during these years.

Firstly, I thank greatly my supervisor Professor Dr. Dorothea Bartels for offering me the valuable opportunity to study in her group at University of Bonn. I indeed encountered many challenges during the process of research works in these years, which made me learn more scientific knowledge and research skills. I still clearly remembered she gave me such genuine concern and support with her patience and immense knowledge when I met the most difficult moments. I also want to thank Professor Bartels for the time she spent to read and revise the published paper and this PhD thesis. Her professional comments let me learn a lot.

Special thanks go to Dr. Dinakar Challabathula for his valuable advices and remarks of this research work. Special thanks should also be given to Dr. Valentio Giarola for his theoretical and technical support during my research work. Thanks go to Professor Gabriel Schaaf and his group for providing vector and yeast cells for the yeast complementation assay. I would like to thank Christiana Buchholz and Tobias Dieckmann for technical support and plant cultivation. Special thanks go to Christine Marikar and Ellen Schulz for the kind help and assistance to solve any office problem. I want to thank Xiaomin Song who helped me solve lots of problems when I first arrived in Bonn. I am grateful for the help from Ahmad Taghipour, Aishwarya Singh, Abdelaziz Nasr, Selvakumar Sukumaran, Niklas Jung, Bennet Rohan. I appreciate all the current and former group members who helped me during my PhD.

My deepest appreciation express to my parents and my close friend Dr. Wenli Quan for their support and constant encouragement during the hardest times in past years. It is very challenging to study abroad alone. I really cannot imagine how I can finish my

ACKNOWLEDGEMENTS

PhD study without their understanding, encouragement, and inspiration. Thanks for them, I can know myself and recognize the world in a better way, which makes me to be a better person.

I am grateful to the members of my dissertation committee, who have generously spent their time to review this thesis and gave expert suggestions to make my work better. I also thank the China scholarship council (CSC) for providing scholarship to me from 2016 to 2020.

DECLARATION

I hereby declare that the whole Ph.D. thesis is my own work, except where it is explicitly stated marked as citation in the text.

Bonn, 12.03.2020

Xun Liu

LIST OF PUBLICATIONS

This thesis contains parts from:

Liu X, Challabathula D, Quan W, Bartels D (2019) Transcriptional and metabolic changes in the desiccation tolerant plant *Craterostigma plantagineum* during recurrent exposures to dehydration. *Planta* 249:1017-1035

in **CHAPTER 2.**